To the Graduate Council:

I am submitting herewith a dissertation by Michael A. Blanchard entitled "Synthesis and Reactivity of Titanium Amido Complexes with Relevance to Olefin Polymerization." I have examined the final electronic copy of this dissertation for form and content and recommend that it be accepted in partial fulfillment of the requirements for the degree of Doctor of Philosophy, with a major in Chemistry.

John F. C. Turner

John F. C. Turner, Major Professor

We have read this dissertation
And recommend its acceptance:

David C. Baker

Z. Ben Xue

Frank (Ted) Barnes

Accepted for the Council:

Carolyn R. Hodges

Vice Provost and Dean of the
Graduate School

(Original signatures are on file with official student records.)

Synthesis and Reactivity of Titanium Amido Complexes with Relevance to Olefin Polymerization

A Dissertation
Presented for the
Doctor of Philosophy
Degree
The University of Tennessee, Knoxville

Michael A. Blanchard
August 2007

Acknowledgments

First and foremost, I would like to thank Prof. John Turner. Your drive and care for detail has guided my years at UT and pushed me to strive for perfection as well. I appreciate all that you have taught and given me over the past four years. Your humor and candor will be greatly missed.

I would also like to thank Dr. David C. Baker, Dr. Ben Xue, and Dr. Ted Barnes for serving on my committee and providing support throughout my graduate career.

A large thank you must be given to all of the members of the Turner group. Andy, you have provided more than a friendly ear to bounce ideas off of, you were an inspiration to all of us. Jamie, you truly were the glue that held us all together; I appreciate your smile and good heart. Sylvia and Cara, thank you for setting the bar high. You left a lot for us to aspire to be. Megan and to a greater extent Brad, your interest and knowledge of NMR made me appreciate it more than you ever imagine. Liz, your care and precision were a great help to me on many occasions, and more importantly, thank you for putting up with me. Rob, where do I begin? I guess that it is probably best said – thank you for being Rob. Michelle, thank you for befriending Laura and I throughout out years together. I do appreciate your stories, now that I don't have you to tell them anymore - ironic. Ben, your laughs and smiles made the first and last year of my time much more fun.

Great thanks must go to the Baker, Barnes and Xue groups, who aided me in countless ways over the years. Thank you for access to your chemicals, labs, instruments, and your expertise. Jeremiah and Dave, thank you for the friendship and fun

over the years. Jeremiah thank you for being a smiling face and warm heart to both Laura and me. A major thank you must go to Art Pratt in the glass shop. Without your expert skills, I would not have been able to conduct my research. I also appreciate the instruction you have given me over the years in developing my own glass-blowing skills.

Travis and Dana, you two mean more to Laura and I than words can ever impart to you. You have been our closest and dearest friends while here at UT. Thank you both for all of the dinners and conversations shared. Travis, I appreciate all of the lunches and beers we have shard for the last few years, you are a wonderful friend.

To all of my family, thank you for all of the support you have given over the years. I could not have made it, nor could Laura and I have weathered the Knoxville years without your love and care. Mom and Dad, thank you for the gentle pushes and guidance throughout life. Larry and Di, thank you for laughing at my horrible humor and lending us all of your love and support. Katy, Leeanna, Ryan and Connor, we appreciate all of your smiling faces and the support you have given.

My loving wife Laura, I would like to thank you most of all. Without your constant support and love, I would not have been able to complete my degree. Your determination and integrity pulled me through the hardest times of my degree. I thank you and Lily for reminding me that there is a life outside of school; I will never forget the sacrifices that you have made for me.

Abstract

Ziegler-Natta catalysts are well known in the chemical industry. They are responsible for the production of more than half of the HDPE and HDPP worldwide annually. Ziegler-Natta catalysts exist in many forms, both in homogeneous and heterogeneous types as well as both with early and late transition metal basis. While Ziegler-Natta catalysts can exist in various forms, all polymerize *via* the same general mechanism. Dissecting the known mechanism(s) results in three items that must be in place for polymerization to occur. First, the active metal center must be highly Lewis acidic, enough to allow coordination of approaching olefins. Second, a vacancy in the coordination sphere around the active metal center must exist to allow coordination of the approaching olefin. Thirdly, there must be a metal-alkyl bond, M-R, into which the coordinated olefin can insert.

The Lewis acidity and vacancy in the coordination sphere are obviously necessary for polymerization, but it is the third aspect that is questionable. In organic chemistry Lewis acids are often used to induce carbocationic character on olefinic carbons, which can in turn be utilized in a large variety of transformations. Among those transformations lies the ability to create carbon-to-carbon bonds. Transition metal mediated carbon-carbon bond formations are well documented, although they concentrate on sp^2-sp^2 bond formation.

Synthesis of highly Lewis acidic coordinatively unsaturated titanium-amido systems is reported. These systems include $(Ph_2N)_3TiCl$, $(Ph_2N)_3TiMe$, $(Ph_2N)_3TiCH_2PMe_2$, $[(Ph_2N)_3Ti{\bullet\bullet\bullet}Me{\bullet\bullet\bullet}BAr^F{}_3]$ and $[(Ph_2N)_3Ti][BAr^F{}_4]$. Polymerization

studies are reported including three systems: $(Ph_2N)_3TiCl$/ MAO, $[(Ph_2N)_3Ti{\bullet}{\bullet}{\bullet}Me{\bullet}{\bullet}{\bullet}BAr^F{}_3]$, and $[(Ph_2N)_3Ti][BAr^F{}_4]$.

Table of Contents:

Index of Figures:

Index of Tables:

List of abbreviations

Me	methyl
Et	ethyl
Ph	phenyl
R	alkyl
Flu	Fluorenyl
Ind	indenyl
Cp	cyclopentadienyl
BAr^F_3	*tris*(pentafluorophenyl)boron
$[BAr^F_4]^-$	*tetrakis*(pentafluorophenylborate anion
L	donor ligand
Pyr	pyridine
MAO	methylaluminoxane
THF	Tetrahydrofuran
HDPE	High Density Polyethylene
LLDPE	Linear Low Density Polyethylene
HDPP	High Density Polypropylene
Wt%	weight percent
Ar'	$[3,5\text{-}(CF_3)_2C_6H_3]$
^{t}Bu	tertiarybutyl
^{n}Bu	*n*-Buryl
ppm	parts per million
sec	second
min	minute
PDI	polydispersity index
D_1	delay time between pulses
Et_2O	diethyl ether

§ CHAPTER 1 Introduction

§ 1.1 Historical overview and introduction

Ziegler-Natta polymerizations are unique, highly specific methods for olefin polymerization. Classical anionic, cationic and free radical polymerization methods progress by an addition of monomers to the active end of a polymer that is separated from the initiator; Ziegler-Natta catalysts, on the other hand, progress with insertion of the monomer into the catalyst alkyl-chain bond. The difference in propagation imparts the versatility of Ziegler-Natta catalysts, which are able to polymerize α-olefins, dienes and cycloolefins into highly stereospecific polymers. Most importantly, these are the only industrial catalysts able to polymerize propylene, 1-butene or ethylene.

Industry employs Ziegler-Natta catalysts to produce both high-density and low-density polypropylene and polyethylene (HDPP, HHPE, LDPP and LDPE respectively), and the field has provided a major focus of academic organometallic chemistry. Ziegler-Natta catalysis owes its success to a long list of individuals over a period of 50 years; the next section provides a brief historical overview.

§ 1.1.1 Historical outline

1952 – G. Wilkinson identifies the first sandwich complexes.[1]

1953 – Wilkinson publishes the first syntheses of Cp_2ZrX_2 and Cp_2TiX_2 (X = halogen).[2]

1953 – K. Ziegler polymerizes propylene and ethylene into high-density polypropylene and polyethylene, respectively (HDPP and HDPE), at standard temperature and pressure using a $TiCl_4$-$AlEt_3$ catalyst.

1953 – Ziegler discloses his catalyst to G. Natta, who characterizes the semi-crystalline polypropylene catalyzed from the modified Ziegler catalyst: α-$TiCl_3$-$AlEt_3$.

1956 – J. Hogan and R. Banks of the Phillips Petroleum Company patent the Phillips process – heterogeneous, low-pressure polymerization of ethylene with CrO_3 supported on SiO_2/Al_2O_3 to produce HDPE.

1959 – D. Breslow and N. Newburg suggest that the first step in the $[Cp_2TiCl_2]$-$[AlClEt_2]$ system is alkylation then halide-bridged binuclear complex: $[Cp_2Ti(Et)$-Cl-$Al(Et)Cl_2]$.[3]

1961 – A. Shilov suggests $[Cp_2TiR]^+$ as the active species in the binary Cp_2TiCl_2-$AlClEt_2$.

1963 – The Nobel Prize in chemistry is awarded to Ziegler and Natta for their work with polymerization catalysis.

1964 – E. Arlman and P. Cossee propose their mechanism for the stereoregulation of the growing polymer chain with α-$TiCl_3$-$AlEt_3$.[4]

1973 - The Nobel Prize in chemistry is awarded to Wilkinson and Fischer for their seminal work with ferrocene and the newly emerging organometallic field.

1977 – W. Kaminsky discovers and characterizes the reactivity of methylaluminoxane (MAO).

1980 – Kaminsky demonstrates the usefulness and activity of MAO with metallocene catalysts in the production of polyethylene and polypropylene, birth of the term Kaminsky systems.

1982 – H. Brintzinger synthesizes the first chiral, bridged metallocenes.

1983 – M. Brookhart and M. L. H. Green propose their mechanism for chain propagation. They suggest that the insertion step is facilitated by α-agostic interactions of one C-H bond of the alkyl ligand with the Lewis acidic metal center.

1984 – J. Ewen at Exxon demonstrates with appropriate titanocenes render partially isotactic polypropylene *via* homogeneous conditions.[5]

1984 – Kaminsky uses zirconocenes analogous to Ewen's titanocenes to produce highly isotactic polymers.[6]

1986 – M. Bochmann synthesizes and characterizes the complex: $[Cp_2ZrMe(L)]^+$ $[BPh_4]^-$ with L = NH_3, NCR and Pyr, which cannot dissociate to the active species: $[Cp_2ZrMe]^+$.[7]

1986 – R. Jordan reports $[Cp_2ZrMe(L)]^+$ $[BPh_4]^-$ with L = THF which is able to dissociate to the active cationic and polymerize ethylene.[8]

1988 – Ewen obtains syndiotactic polypropylene using C_2-symmetric catalysts such as (flu)$CpZrCl_2$.[9]

1991 – T. Marks uses *tris*(pentafluorophenyl)boron as a Lewis acid to abstract an alkyl group from Cp_2ZrMe_2 to form the isolable complex $[Cp_2Zr(Me)\cdots Me\cdots B(C_6F_5)_3]$.

1991 Exxon utilizes metallocenes to produce linear low-density polypropylene (LLDPE) industrially for the first time.

1995 – Brookhart synthesizes extremely active, non-metallocene catalysts based on Pd and Ni.

1998 – Brookhart and V. Gibson synthesize extremely active, non-metallocene catalysts based on Fe with a tridentate *bis*-imine-pyridyl ligand, and demonstrates that its activity is similar to the original Ziegler-Natta systems.

§ 1.1.2 Origins of the Ziegler-Natta catalysts

The origins of Ziegler-Natta catalysis begin with Karl Ziegler and his interest in organoaluminum and organolithium chemistry. Friedrich and Marvel demonstrated the potential of alkyl lithium reagents as polymerization catalysts in the early 1930s.[10] Ziegler took interest with the mechanism by which these polymerizations occurred. With the onset of World War II, the German chemical industry turned to the country's wartime needs, leaving the original polymerization catalysts behind. Following the war, Ziegler reinitiated German interest in alkyl lithium and polymerization chemistry in hopes of finding a route to high molecular weight polymers. Friedrich and Marvel's work yielded only low molecular weight products, because of premature chain termination. As the chain grows, the lithium species becomes unstable and eliminates the chain as a primary olefin and precipitates lithium hydride, which is almost entirely inactive as a catalyst.[11] Ziegler's investigations of the mechanism showed that if an ether were added, the activity of lithium hydride and, to a lesser extent, lithium alkyls increased. He turned to the then recently discovered lithium aluminum hydride ($LiAlH_4$), which is soluble in

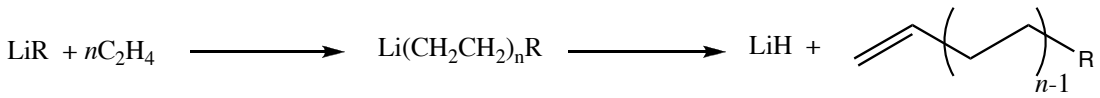

Figure 1.1: Polymerization of ethylene by alkyl lithium reagents.

diethylether and was thought to be able to serve as a source of alkyl lithium. $LiAlH_4$, known to convert into $LiAlEt_4$ in the initial reaction with ethylene, was believed to be a renewable source of ethyl lithium, which would polymerize the excess ethylene. $LiAlEt_4$ is in equilibrium with ethyl lithium and triethyl aluminum. Any elimination of lithium hydride would be reversed by reactivation to ethyl lithium *via* reaction with either triethylaluminum or tetraethylaluminate. The activity of these systems was much higher than with lithium alkyls, but Ziegler and Gilbert discovered that the aluminum species was responsible for the increase, not the extended life of lithium hydride.

Activity was increased with the use of triethylaluminum, but more importantly, so did the average molecular weight of the resulting chains. Hydride elimination of the growing chain deactivates the aluminum catalyst similarly to the lithium catalysts. Aluminum hydride (AlH_3) reacts with ethylene to form triethylaluminum ($AlEt_3$), which in turn reacts with more ethylene to produce longer alkyl chains. The cycle continues until the chain(s) reach approximately 200 carbons in length, when the chain terminates. Ziegler named this reaction the *aufbau* reaction because of the stepwise 'building up' of the alkyl chain. The *aufbau* reaction is discussed further in § 1.5.1. While elimination limits the length of the growing polymer, aluminum hydrides, $R_{2-x}AlH_x$, which are soluble in ether, are able to react with ethylene to produce the active catalyst again, in contrast to lithium hydride, which is insoluble.

The discovery of the binary catalytic system known today as Ziegler-Natta catalysts happened accidentally. In one experiment, Ziegler and Holzcamp noticed that instead of the polyethylene product expected 1-butene was recovered. The new product was a result from contamination of colloidal nickel, a remnant of a hydrogenation

reaction. The added nickel provided a method to modify the *aufbau* reaction. In subsequent reactions triethylaluminum was reacted with a large series of transition metal salts in order to find other displacement reactions. Most transition metal salts resulted in similar results to the nickel; zirconium acetylacetonate and $AlEt_3$ provided the most interesting reaction. Instead of 1-butene, long chain, high molecular weight polyethylene was produced.[12] Other Group IV complexes were tried, and titanium tetrachloride and triethylaluminum were found to be the most active all the binary systems tried. Ziegler designated this reaction the *Mülheim Atmospheric Polyethylene Process*.

Before announcing his discoveries at the International Symposium on Macromolecular Chemistry in Prague in 1957, Ziegler disclosed his process to the Montecantini Company in Italy and Goodrich-Gulf Chemical Company in the United States. Guido Natta, a consultant at the Montecantini Company and associate of Ziegler, undertook the Ziegler catalysts. His original work involved studying the kinetics of ethylene addition to alkyl aluminum species and the study and characterization of stereospecific, crystalline polymers. The $TiCl_4$-$AlEt_3$ catalyst produces mixtures of amorphous and crystalline polyethylenes and polypropylenes from ethylene and propylene respectively.[13] When Natta switched to other titanium chlorides, especially α-$TiCl_3$, the polyethylene polymers produced were more crystalline than before. Natta was also able to polymerize propylene, 1-butene and styrene into highly crystalline polymers, which had been previously unknown. Natta discovered that these crystalline polymers, namely polypropylene, produced from the α-$TiCl_3$/$TiCl_4$ catalysts were made up of

monomeric subunits with the side chains all in the same configurations; he named these polymers isotactic, from *iso* meaning same as and *tactic* meaning with order.[14]

Shortly after his determination of isotactic polypropylene, Natta disclosed that VCl_4-$AlEt_2Cl$ systems were able to produce syndiotactic polypropylene if kept below -78°C. Syndiotactic polymers have a regular alteration at alternating carbons.

For this work, Ziegler and Natta were awarded the Nobel Prize for chemistry in 1963. Traditionally, Ziegler catalysts are known to consist of transition metals in their highest oxidation state, i.e. $TiCl_4$-$AlEt_3$, and Natta catalysts consist of transition metal systems

with the metal in a lower oxidation state such as α-$TiCl_3$-$AlEt_3$. Collectively, binary systems comprised of metal alkyls (Groups I-III) and a transition metal salt (Groups IV and V) that polymerize α-olefins are known as Ziegler-Natta catalysts.[15]

§ 1.1.3 Metallocenes and their role in Ziegler-Natta catalysis

The original heterogeneous titanium/aluminum catalytic systems provide little in the way of tailoring or optimizing the catalyst for higher molecular weight and/or higher stereospecificity of the product(s). Homogeneous catalysts were sought to alleviate these problems, with metallocenes looking particularly favorable. As opposed to the surface-only active sites of bulk, heterogeneous catalysts, homogeneous analogues provide a more uniform active species as well as less deactivation because of polymer coatings on the catalytic surface, believed to be one of the mechanisms for deactivation of heterogeneous catalysis (see § 1.5 for more mechanistic information).[16] With a single-site

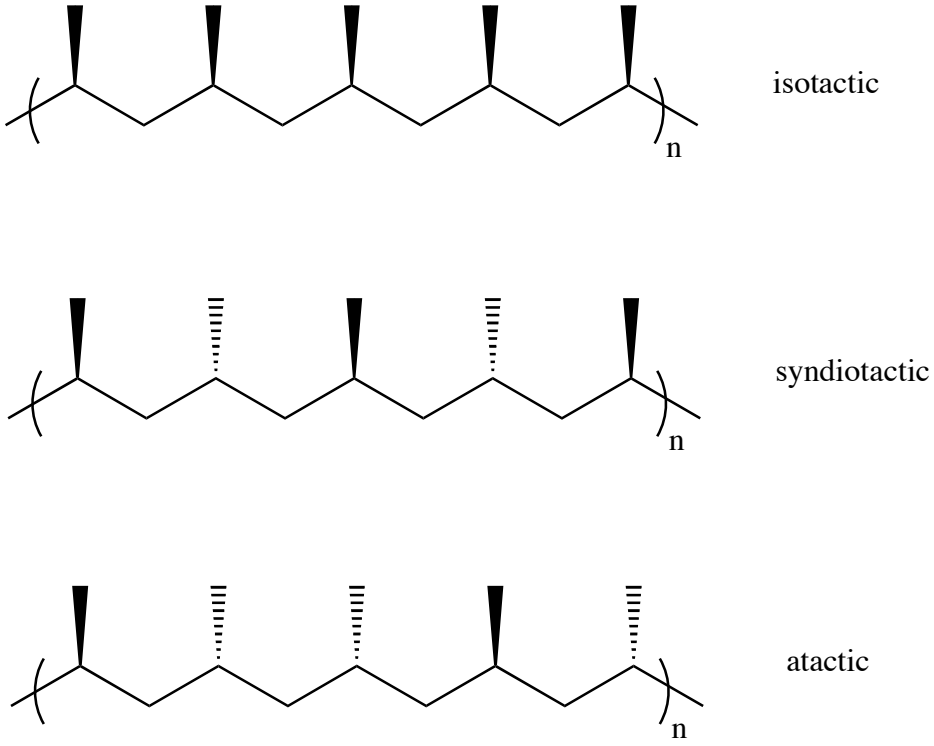

Figure 1.2: Isotactic polypropylene, syndiotactic polypropylene and atactic polypropylene.

active species responsible for all of the polymerizations, a narrower molecular weight range and higher stereospecificity of the product would be possible.

§ 1.2. General metallocene properties

Metallocenes provide a solution to the problems listed in the previous section. In general, metallocenes are soluble in hydrocarbons and are easily synthesized. Their structures can be manipulated relatively easily and their symmetry provides for a single type of active site. Wilkinson and Fischer identified the first known metallocene, ferrocene, in 1952. Shortly after, Wilkinson and Cotton demonstrated that it was possible to synthesize other metal sandwich complexes, both as homoleptic species and with other ligands bound.[2] By binding other ligands, the coordination of the cyclopentadienyl (Cp) rings changes, such that the Cp rings are no longer parallel but are tilted towards each other. The high symmetry of the metallocene complexes is reduced with the 'bent' metallocenes.

Substitution of one or more hydrogens on the cyclopentadienyl rings can have a dramatic effect on the angle between the two rings. Depending on the substituting group, electron-releasing properties can be altered[17] and/ or introduce chirality onto the metallocene.[18] By bridging the Cp rings to one another in a bent complex, the coordination of the Cp rings is locked into one configuration, which can again affect the chirality of the complex.[19] The most significant bridging groups are $–CMe_2$-, $-SiMe_2$- and $–CH_2$-, of which the $–CH_2$- is the smallest.

Bridging the Cp ligands to one another also creates a chelating effect making Cp slippage unlikely; in general Cp slippage is rare. The Cp ligands on a bent metallocene provide an extremely rigid coordination sphere around most of the metal, leaving only a single vacant well for reactivity on the metal. The size of the well depends on the positions of the Cp ligands and the angle created between them.

Typical Cp-metal-Cp angles (γ) for the bent metallocene are between 115° and 150° with the vast majority of the complexes exhibiting an angle between 128° and 134° (Figure 1.4). The angle (γ) varies depending on the metal and substituents on each Cp ring. The bulkier the substituents on the ring, the larger γ becomes, conversely the shorter the bridge between the Cp rings, the smaller γ becomes. As γ becomes larger, the vacant coordination site on the metal, opposite to the Cp rings is enlarged making the metal center much more electrophilic and therefore more Lewis acidic in principle. The Lewis acidity of the vacant coordination site is crucial to the activity of the catalyst.[19]

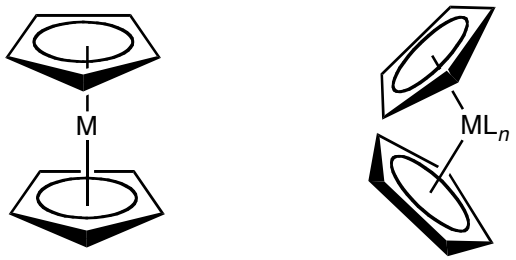

Figure 1.3: Linear metallocene and bent metallocene.

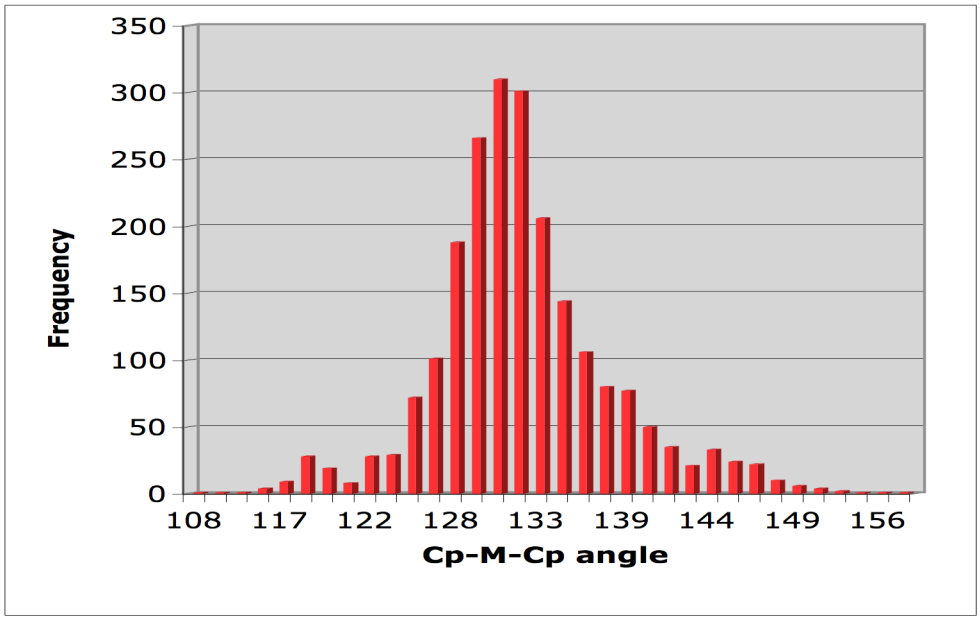

Figure 1.4: Histogram illustrating the relative amount of (γ) for bent metallocenes.

Table 1.1.1: Various Metallocenes showing Cp-M-Cp angle, (γ)

	Name	Structure	Molecular formula	γ
1	titanocene dichloride	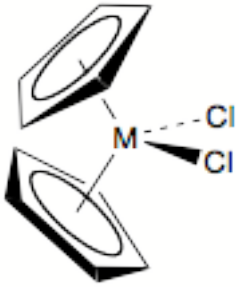	$C_{10}H_{10}TiCl_2$	131°
2	zirconocene dichloride		$C_{10}H_{10}ZrCl_2$	129.3°
3	hafnocene dichloride		$C_{10}H_{10}HfCl_2$	127.1°
4	*ansa*-$SiMe_2$titanocene dichloride	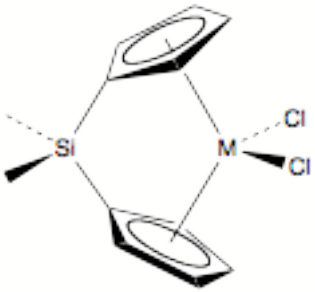	$C_{12}H_{14}SiTiCl_2$	128.7°
5	*ansa*-$SiMe_2$zirconocene dichloride		$C_{12}H_{14}SiZrCl_2$	125.4°
6	*ansa*-$SiMe_2$hafnocene dichloride		$C_{12}H_{14}SiHfCl_2$	126.8°
7	*ansa*-$CiMe_2$titanocene dichloride	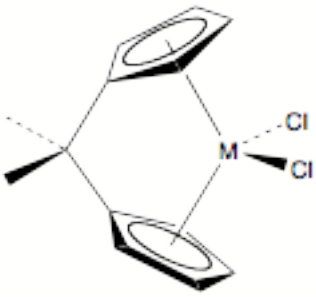	$C_{13}H_{14}TiCl_2$	121.5°
8	*ansa*-CMe_2zirconocene dichloride		$C_{13}H_{14}ZrCl_2$	116.6°
9	*ansa*-CMe_2hafnocene dichloride		$C_{13}H_{14}HfCl_2$	117.1°

Chirality can be conferred to the complex in three general ways: first, the complex's chirality stems from the asymmetric arrangement of achiral ligands around a metal center; this type of asymmetry is termed metal-centered chirality. A second type of chirality, termed ligand-derived chirality, stems from a chiral ligand that is bound to the achiral metal center. The third type of chirality is a combination of types one and two. The effects of chirality on Ziegler-Natta polymerization are discussed in § 1.2.4.

For chiral Ziegler-Natta catalysts, the most crucial aspect is that every incoming olefin inserts in the same orientation with respect to the growing polymer. To ensure that the incoming olefin will insert properly, the ligands are arranged so that only a single orientation is possible, most often Cp or modified Cp rings are used to accomplish this. § 1.5 discusses the possible mechanisms for olefin insertion and chain propagation.

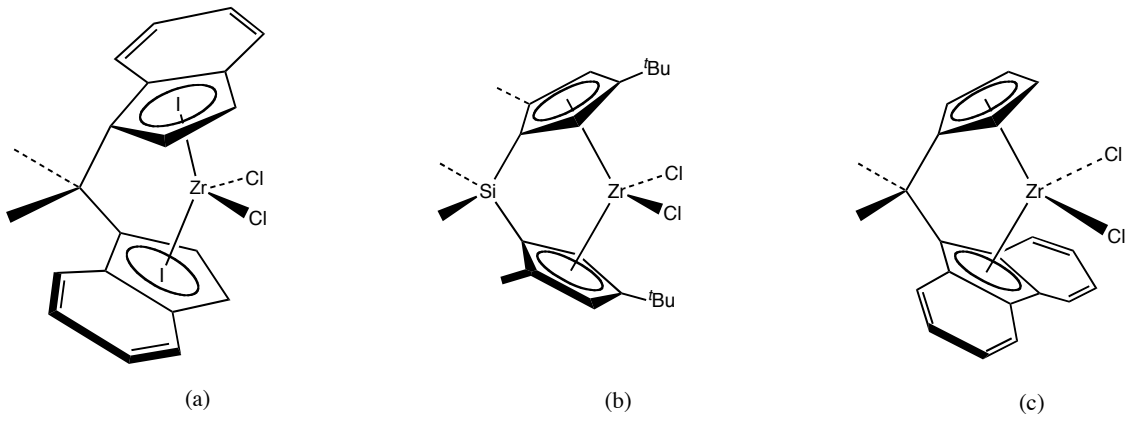

Figure 1.5: Chiral Zirconocenes.

(a) –CMe_2-ansa- indenyl ligands, (b) –$SiMe_2$-ansa-alkyl-substituted cyclopentadienyl ligands and (c) –CMe_2-ansa-fluorenyl-cyclopentadienyl ligands.

§ 1.2.1 Original metallocene containing Ziegler-Natta catalysts

Breslow[16] and Natta independently used binary mixtures of Cp_2TiCl_2 and $AlClEt_2$ to demonstrate that Ziegler-Natta polymerizations can be achieved in homogeneous conditions. Initial studies showed only medium activity with respect to ethylene; propylene was not polymerized at this time.[13] In 1975, Breslow and Long[20] announced that the partial hydrolysis of alkyl aluminum species yields a species (MAO) able with activities 1000 times that of R_2AlCl. Two years later, Kaminsky used MAO to activate Cp_2TiCl_2 and polymerizes ethylene at extremely high rates and produce polymers with a small range of molecular weights. Sinn *et al.* used the analogous zirconocene system to polymerize propylene.[21]

The activity and mechanistic understanding of Ziegler-Natta systems plateaued, until Bochmann *et al.* demonstrated similar activities to the Cp_2TiCl_2/MAO system with a method for activation, covered in more detail in § 1.4. While Bochmann's $[Cp_2TiMe][BPh_4]$ system showed high activity, its use was extremely limited due to sensitivity to water. In attempts to halt the hydrolysis and stabilize the systems, strong donor ligands such as NH_3, NCR, and Pyr were added. The addition of the donors did stabilize the system, however the new complexes were unable to polymerize.[7, 22] The use of more labile donors such as THF aided in stability but also yielded viable polymerization catalysts, with lower activities than their non-stabilized analogues.[8] Under similar conditions other precatalysts were attempted to find species that were stable enough to be studied as well as active enough to be comparable to the original Cp_2TiCl_2/MAO systems. Of the precatalysts tried, only $[Cp_2Zr(CH_2Ph)(THF)][BPh_4]$ showed potential, although it was only able to polymerize ethylene.[23]

$[BPh_4]^-$ is not the ideal candidate for a counter ion in the Ziegler-Natta systems. The perfluoro analogue, $[BAr^F{}_4]^-$, is far more effective (see § 1.4.4 for a discussion of anions and activators). Replacing $[BPh_4]^-$ with $[BAr^F{}_4]^-$ increases the activity of the metallocene system used by roughly 300 times, and can be as high as 3500 for $[Cp^*{}_2ThMe][BAr^F{}_4]$.[24] Many transition metal cation/$[BAr^F{}_4]^-$ systems capable of Ziegler-Natta catalysis have since been synthesized and studied. Figure 1.6 lists several of the more active systems. Another route to the cationic metallocene species was adopted by Marks *et al*, in which alkyl groups were abstracted from the metallocene with a Lewis acid. The first example of alkyl abstraction to yield the active species was $[Cp_2ZrMe\cdots Me\cdots BAr^F{}_3]$.[25] Mark's 'cation-like' zirconocene system was the first example of a stable, isolable, active catalyst, and more importantly it provided a method for characterizing the corresponding anion. § 1.4 discusses types and methods of activation.

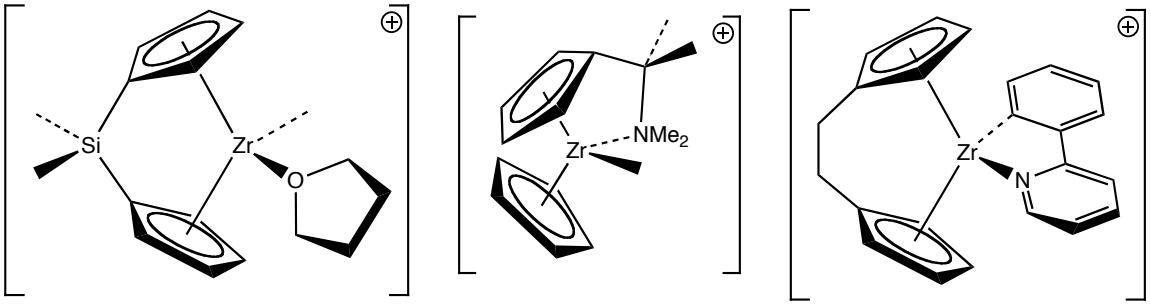

(a) (b) (c)

Figure 1.6: [Zirconocene][$BAr^F{}_4$]
(a) Marks' –$SiMe_2$-zirconocene cation,[26] (b) Erker's amine tethered zirconocene cation[27] and (c) Jordan's phenyl-pyridine stabilized zirconocene cation.[28]

In the crystal structure, the bridging methyl is asymmetrically bound tightly to the *tris*(pentafluorophenyl)boron moiety and only weakly to the zirconocene cation. All three hydrogens on the bridging methyl group are bent away from the boron, towards the zirconocene and two of the hydrogens are 'agostic' in nature, at a distance of 2.16 Å. The bridging methyl provides enough stability for the zirconocene cation to be isolated, while it is labile enough to be displaced. The activity level for $[Cp_2ZrMe\bullet\bullet\bullet Me\bullet\bullet\bullet BAr^F{}_3]$ complex is roughly comparable to the original Cp_2ZrCl_2/MAO system.

The ^1H NMR shifts of the $[Cp_2ZrMe]^+$ correspond with the valves for the methyl in the Cp_2ZrCl_2 activated with MAO, and the bridging methyl was assigned to 0.10 ppm (up-field from the methyls on Cp_2ZrMe_2). The ^{13}C NMR spectrum matches the assignments for the Cp_2ZrCl_2 activated with MAO as well.

§ 1.2.2Modified metallocene catalysts

While metallocenes provide homogeneous Ziegler-Natta catalysts with activities similar to their heterogeneous analogues, the product polymer was not improved. Optimization of the polymer produced was still sought after: increased average molecular weight and more stereospecificity of the polymer. Because of their highly rigid nature and favorable steric bulk, bridged metallocenes replaced the original bent metallocenes in hope of reducing premature chain termination. The rigid, steric bulk was thought to be able to control the orientation of the incoming olefin leading to hopes of producing a polymer with very precise stereoregularity.

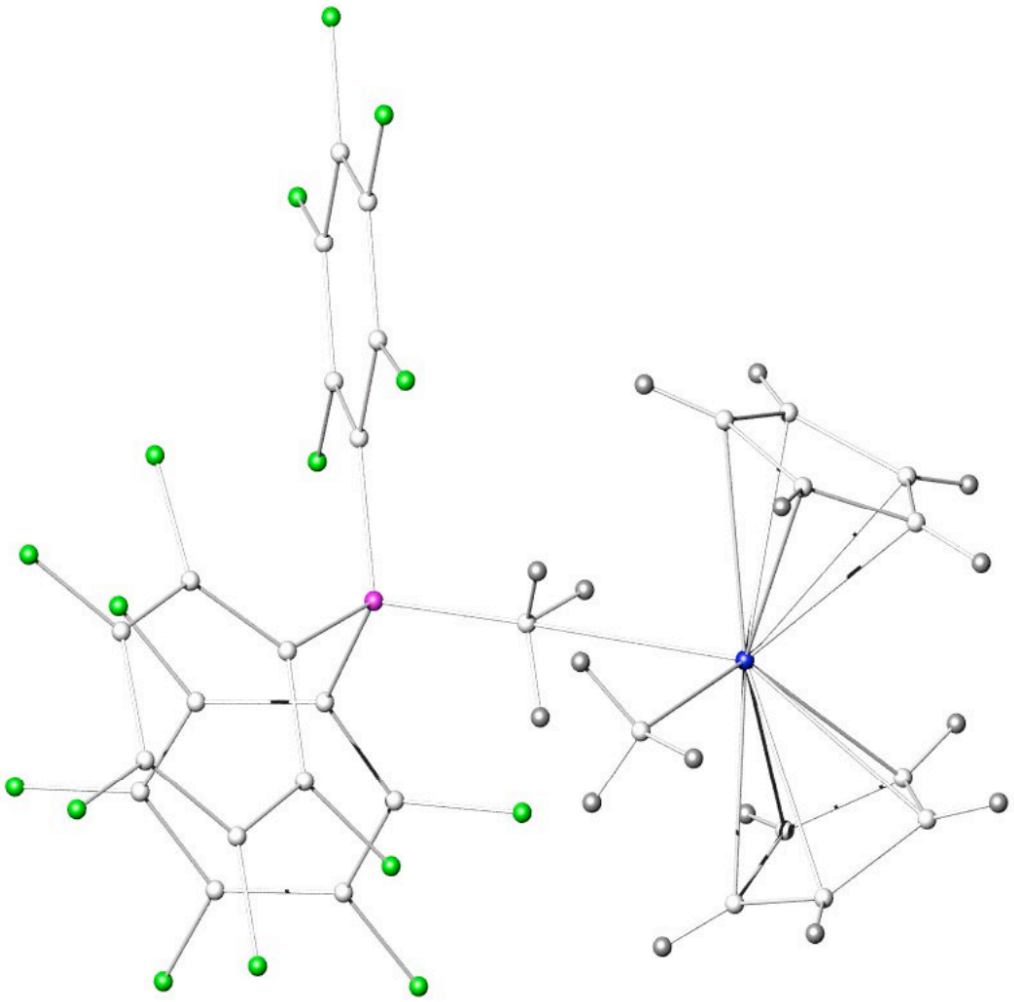

Figure 1.7: Structure of [$Cp_2ZrMe\bullet\bullet\bullet Me\bullet\bullet\bullet BAr^F{}_3$] with the hydrogens of the bridging methyl canted towards the zirconocene moiety

Ewen, while at the Exxon Chemical Company, in 1984 used *bis*indenyltitanium dichloride, $(Ind)_2TiCl_2$, activated with MAO to produce 63% isotactic and 37% atactic polypropylene at low temperatures.[5] At elevated temperatures, the polymer produced lost any stereospecificity. Ewen reasoned that the stereochemistry of the insertion step is regulated by the chiral β-carbon of the growing chain, and the hindered rotation of the indenyl rings provided the chiral bias for the β-carbon. If the catalyst is modified by bridging the rings to one another, *ansa*-C_2H_4-$(1\text{-}Ind)_2TiCl_2$ the stereoregulation of the polymer increases dramatically. Because the bridged catalyst has C_2 symmetry, any error in the stereochemistry is corrected, leaving only single sites with incorrect stereochemistry (figure 1.8). When the non-bridged analogue of the indenyl catalyst is used, the stereoerror is propagated. The difference in stereoregulation stems from the growing chain of the polymer being held in one particular orientation with respect to the bridged catalyst, with the β-carbon controlling the stereochemistry.

One year later, Kaminsky used the chiral ethylene *bis*(4,5,6,7-tetrahydro-1-indenyl)zirconium dichloride with MAO to produce highly isotactic polypropylene, which is almost entirely insoluble in toluene (0.2% solublility).[6] The reduced C_6 on the 4,5,6,7-tetrahydro-1-indenyl systems provides more steric bulk than the fully aromatic 1-indenyl systems; this extra bulk further regulates the stereochemistry of the growing chain. The rigidity that a bridging ring system imparts is not totally necessary for stereoregulation at low temperatures, but is essential for stereoregulation at elevated temperatures (above -50º C). Interestingly, $[(C_5H_4Pr^i)_2\ Ti\ Ph_2/\ MAO]$ produces isotactic

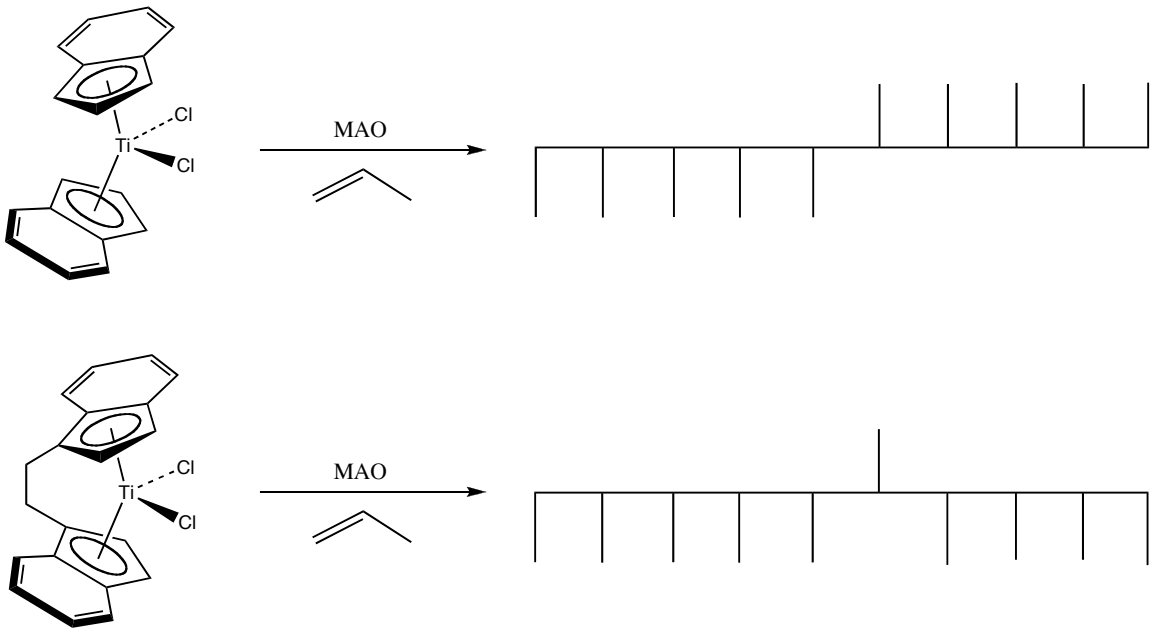

Figure 1.8: Stereoerror propagation and regulation with Ind_2TiCl_2 and ansa-$C_2H_4(Ind)_2TiCl_2$ respectively

polypropylene at -50º C, atactic propylene at –10º C, and semi-syndiotactic polypropylene at 10º C.

Other active chiral Ziegler-Natta systems have also been investigated, the -Me_2C- and -Me_2Si- systems are among the most studied systems. Both the –Me_2C- and –Me_2Si- systems are more sterically rigid than their ethylene-bridged analogues, ergo their stereoregulation is greater. Both of the single-membered bridges also have a smaller γ, so their activity is much higher than the ethylene-bridged catalysts.[29]

The indenyl systems provide another useful system. The ligand itself is considered to be non-innocent, meaning that the ligand-to-metal electron donation, the metal's oxidation state and the electronic structure of the ligand can exist in a variety of possibilities.[30] The indenyl ligand is traditionally thought to bind to the metal center, as a standard η^5-Cp ligand with other ring as acting like a diene, but if the indenyl ring slips to an η^3-ring, aromaticity is restored on the secondary ring. With the change from η^5 to η^3 coordination, electron donation from the ligand to the metal changes from 5 to 3 as well. This change in electron density can provide some versatility to the catalyst. However, since the indenyl ligand is not a traditional non-innocent ligand such as the dithiolenes, pyrocatechols and other ligands capable of multiple stable resonance structures, the change in stability granted to the complex is fairly small.

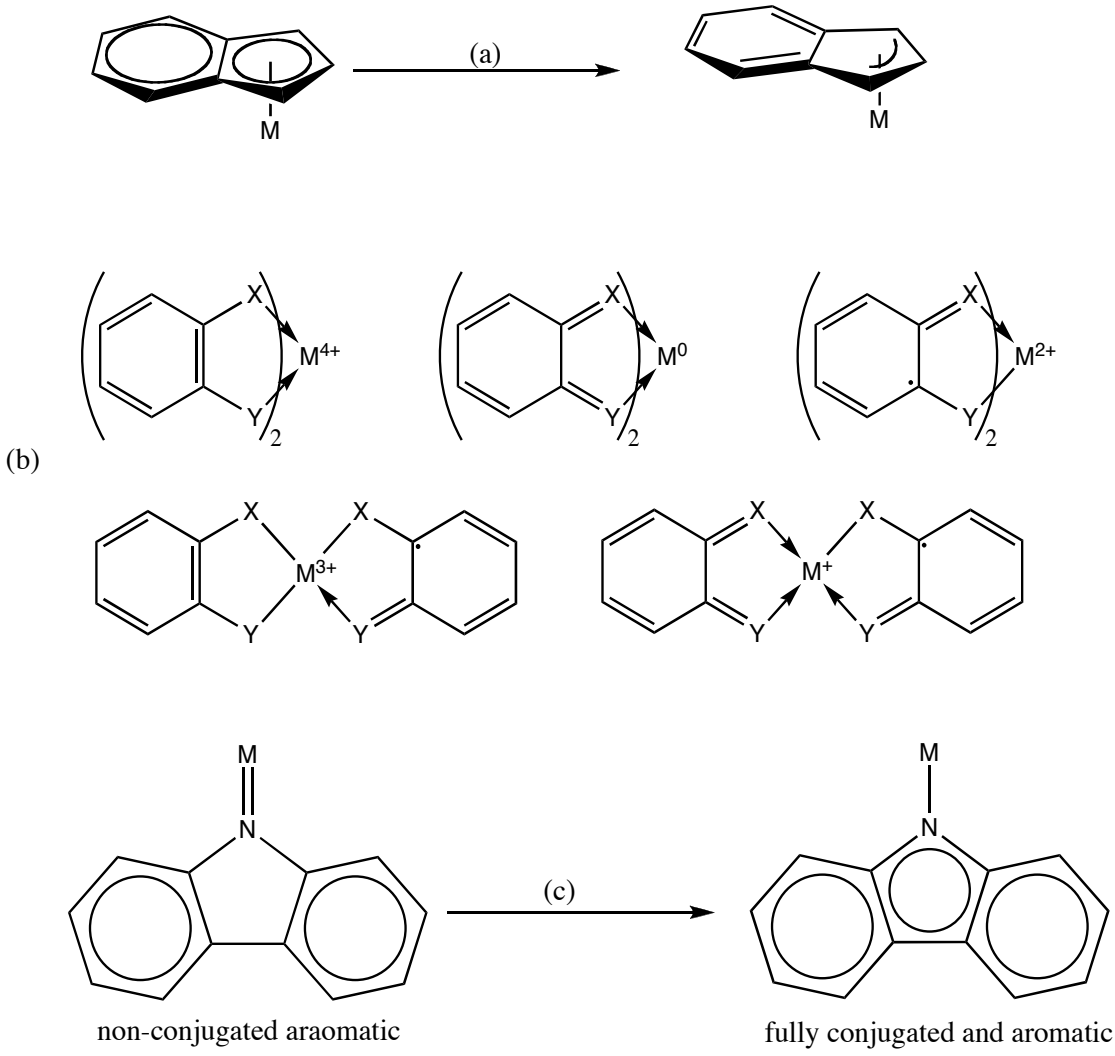

Figure 1.9: Non-innocent ligands.

(a) Indeninyl ligands, movement from η^5 to η^3. (b) Pyrocatechol and derivates, exhibiting change the electronic structure of the ligand and the various oxidation states of the metal center that it can stabilize; x, y = O, NH, S and M are typically group 10 metals. (c) Carbazolyl ligand, movement from two independent aromatic rings to a fully conjugated aromatic system.

The steric bulk and rigidity that Cp ligands convey to an active catalyst are robust. They are tunable to a certain degree, but they do have limitations; tedious steps must be taken to separate the diastereomers formed in the synthesis of chiral-bridged metallocenes. The easiest method for resolving the *ansa-bis(*1-indenyl) zirconium dichloride isomers involves selective hydrogenation and fractional crystallization to separate *dl* from the *meso* isomers. Next, coordination of the meso components to a chiral ligand (such as 1,1'-bi-2-naphthol) in order to create diastereomers allows a separation *via* chromatography. Quenching the complex with anhydrous HCl yields the resolved chiral complexes.[31]

Removing one of the Cp ligands from a metallocene opens more coordination sites on the metal center. In order to be utilized as an active polymerization catalyst, these piano-stool complexes are often paired with multi-dentate heteroatom ligands such as a phosphinimide or phosphinimine. Piers *et al* have used the $Cp^*/(^tBu)_3P{=}N$- ligand set to isolate a cationic titanium (IV) hydride. This piano-stool complex shows extremely high activity towards ethylene polymerization.

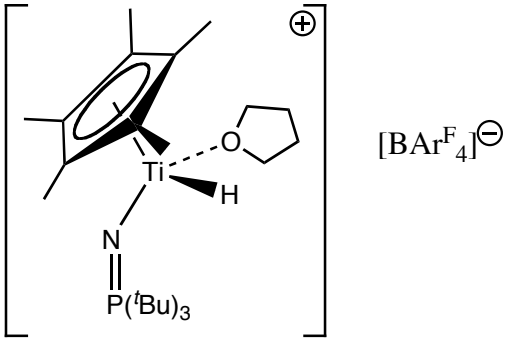

Figure 1.10: Piers' piano-stool complex, utilizing the phosphinimide ligand for stability.

Non-metallocene Ziegler-Natta systems

The origins of homogeneous Ziegler-Natta catalysis rest with the Group IV metallocenes and derivatives based on those systems. Not all homogeneous Ziegler-Natta systems involve ligand sets based on cyclopentadienyl ligands though. Major breakthroughs have occurred with heterogeneous and homogeneous chromium systems, homogeneous iron systems as well as other metal-based systems.

§ 1.2.3 Phillips Catalyst and other Chromium systems

Shortly after Ziegler and Natta reported their discoveries, Hogan and Banks of the Phillips Petroleum Company discovered and patented their heterogeneous, low-pressure polymerization catalyst. Banks and Hogan used CrO_3 on a calcined solid support such as silica. The Phillips catalyst does what traditional Group IV Ziegler-Natta catalysts cannot do; it is able to produce linear low-density polyethylene (LLDPE). It is for this reason that chromium-based catalysts are the second most commonly used catalysts in the industry following the Group IV systems.

The original Phillips catalyst maybe synthesized by impregnating silica supports with aqueous CrO_3 solutions. Once the correct amount of chromium has been added (>5 wt%), the solid catalyst system is dried thoroughly. During calcination at lower temperatures, at around 200 °C, the CrO_3 undergoes esterification with the hydroxyl groups on the solid support; it is during high temperature calcination at around 800 °C that the catalyst is activated. During the second calcination excess water (from surface hydroxyl groups) is removed, and the bound chromates are then free of coordination from those surface hydroxyl groups.[32]

There is much debate over the oxidation state of the active sites in all chromium-based catalysts. Miesserov suggests that there must be mixed oxidation states,[33] while Clark and Hogan maintain that chromium(IV) is vital for catalysis. Krauss and coworkers believe that divalent chromium, synthesized by reducing the bound chromate under an atmosphere of CO, is the most important.[34] Theopold hypothosized that chromium(III) is vital.[35, 36] The problem lies in the fact that very little of the chromium impregnated on the support surface is active, so that characterization techniques are almost useless.

The Phillips catalyst is typically slurried in solution, in contrast Union Carbide developed the Unipol process, in which polymerization on a supported chromocene catalyst takes place in a fluid-bed reactor. In these reactors, gaseous olefins react at low pressures with solid supports, eliminating the need for a solvent. While this method is extremely economical, it does have its limitations; in comparison with the original Phillips catalyst, the Unipol catalysts have lower activities, lower polymerization rates, and produce less product per unit of catalyst.[37]

Theopold began synthesizing organochromium and homogeneous analogues of the Phillips catalysts. Using the Unipol catalyst as the basis for his studies, he rationalized that the major catalytic component consisted of a chromium complex with a Cp ligand, an alkyl group for insertion and an oxygen donor from the solid support. Theopold *et al* demonstrated the ability of a complex of that type to polymerize ethylene, and at room temperature and ambient pressures. Structures such as $[Cp^{*}Cr(THF)_2CH_3][BPh_4]$ do not prove that the active species of the Unipol catalyst, although they do suggest what the possible active species might be.[35]

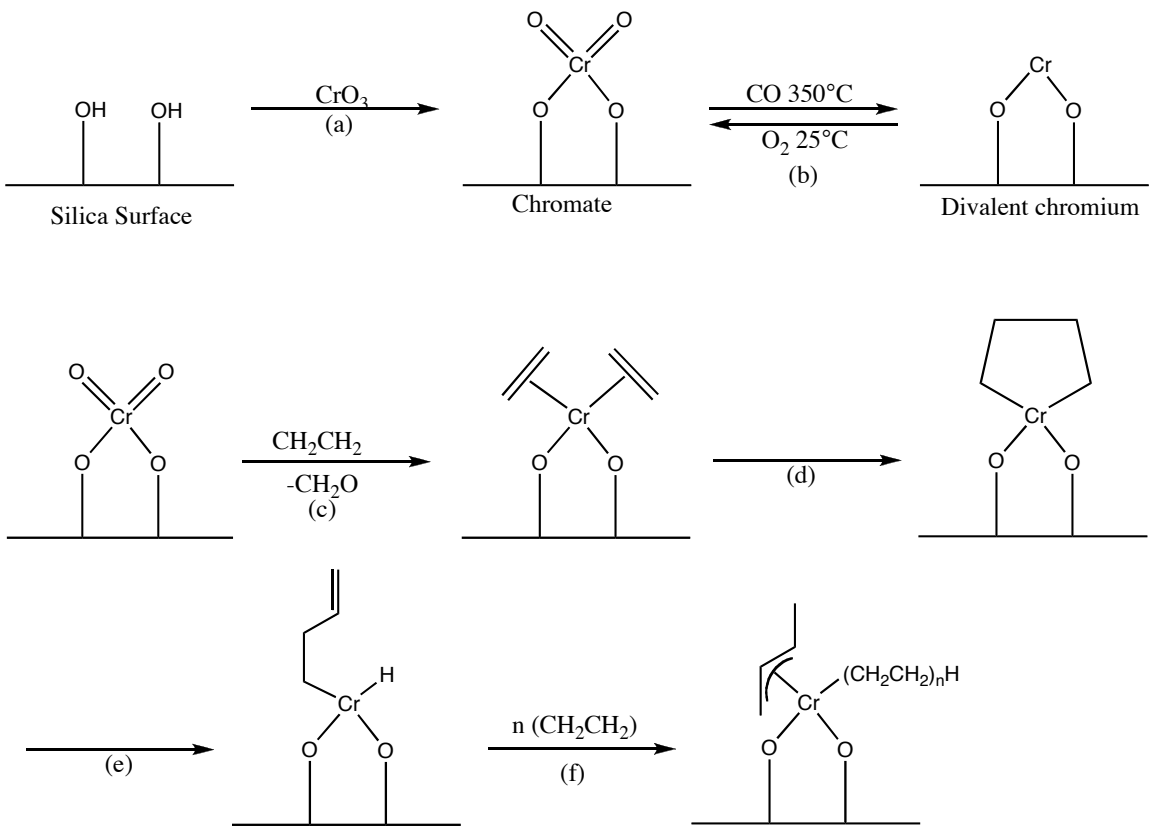

Figure 1.11: Formation of chromium based catalysts.

(a) Impregnation of CrO_3 on to silica surface. (b) Calcination under CO to give divalent chromium species. (c) Replacement of oxide for π-bonded olefin. (d) Insertion to metallocyclopentane. (e) β-Hydride elimination to give alkyl hydride. (f) Insertion of olefin into hydride, complex is stabilized by allyl ligand.

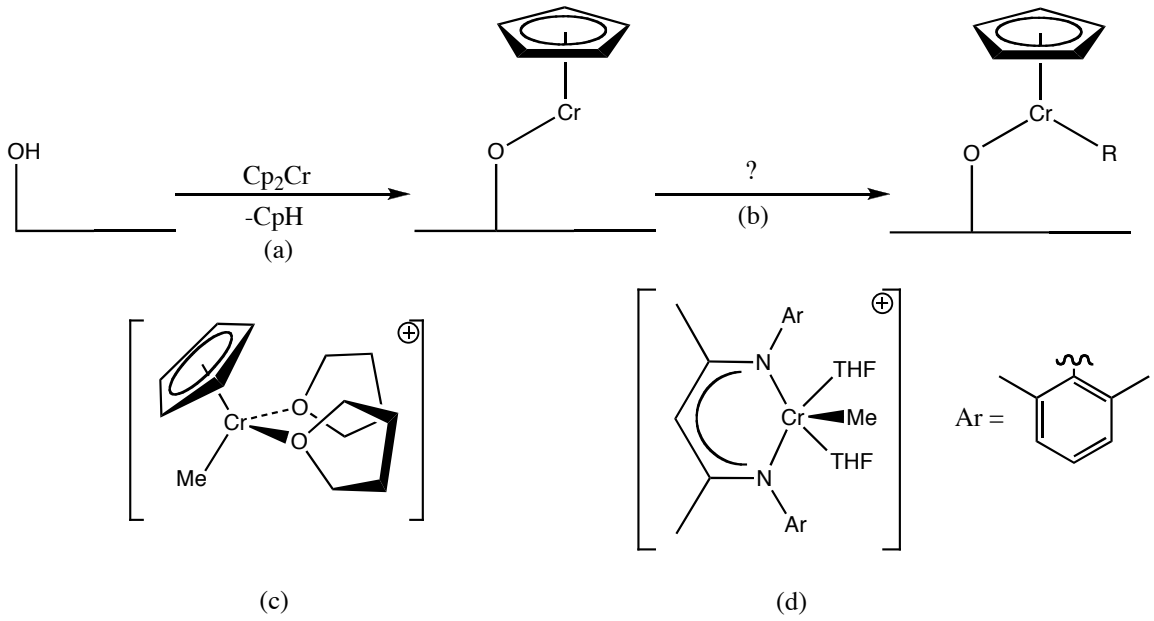

Figure 1.12: Structure of chromium based heterogeneous and homogeneous catalysts (a) impregnation of chromocene onto a solid silica support. (c) [CpCr(THF)$_2$Me][BPh$_4$], anion not shown. (d) [(2,6-Me$_2$Ph)$_2$nacnacCr(III)][BAr$_4^F$], anion not shown.

§ 1.2.4 Brookhart's systems

Group IV systems and chromium-based catalysts were known to catalyze the polymerization of α-olefins since the early 1950s. While a few examples of late transition metal-based Ziegler-Natta catalysts existed, the field remained almost entirely dormant until the 1990s. In the 1990s, Brookhart *et al* sought to find Ziegler-Natta catalysts able to copolymerize polar monomers, which was impossible to do with traditional early transition metal-based catalysts. Because of the oxophilicity of the Group IV metals, polar monomers often lead to early catalyst deactivation.

Most of the known late transition metal-based catalysts were only able to polymerize ethylene; higher α-olefins could only be dimerized or oligomerized. Partially due to lower steric encumbrance these systems terminated prematurely, with high rates of β-hydride elimination.[38, 39] The Shell Higher Olefin Process (SHOP) is based on this principle; the SHOP utilizes a nickel-based catalyst to oligomerize ethylene to alkenes with chain length of C_8 to C_{18}.[40] Brookhart reasoned that increasing steric bulk around these metals, especially nickel and palladium, should decrease the β-hydride elimination and increase the ability to polymerize α-olefins. In 1995, Brookhart *et al.* published their findings on the Group X complexes containing the diimine ligand (figure 1.14 (a)).[41] These complexes can be activated *via* MAO or $[BAr^F_4]^-$ and exhibit high activities. The Ni and Pd based catalysts yield linear to moderately branched polyethylene; the degree of the branching is a function of temperature and pressure. At higher pressures, the polymer product is linear and at higher temperatures, branching increases. At lower temperatures,

the substituted aryl rings sit almost perpendicular to the N-M-N plane. This arrangement blocks the axial approach to the metal center, leaving only a co-planar approach which yields a linear polymer. At elevated temperatures, the aryl rings lose their bias and branching of the polymer occurs.

Grubbs, three years later, used nickel(II) with a salicylaldimine ligand and demonstrated their ability to polymerize ethylene and other olefins (Figure 1.14 (b)). Grubb's Ni^{II} salicylaldiminato catalysts activate differently than most other Ziegler-Natta catalysts. The addition of strong Lewis acids such as BAr^{F}_{3} or $Ni(COD)_2$ acts to bind the phosphine, yielding a neutral, coordinatively unsaturated metal center. This type of catalyst yields mainly linear polymers, but the activity is not as high as the traditional Ziegler-Natta systems. Concurrently with Grubbs, Brookhart used a bulky *bis*(imino)pyridine iron(II) system to demonstrate the ability of late transition metal catalysts to have extremely high activities as well be able to produce linear olefins (Figure 1.14 (c)). Brookhart's systems[43] depend on the extremely bulky tridentate ligands to limit possible coordination to the metal center. Typically the larger the substituted aryl ring, the higher the linearity of the polymer produced.

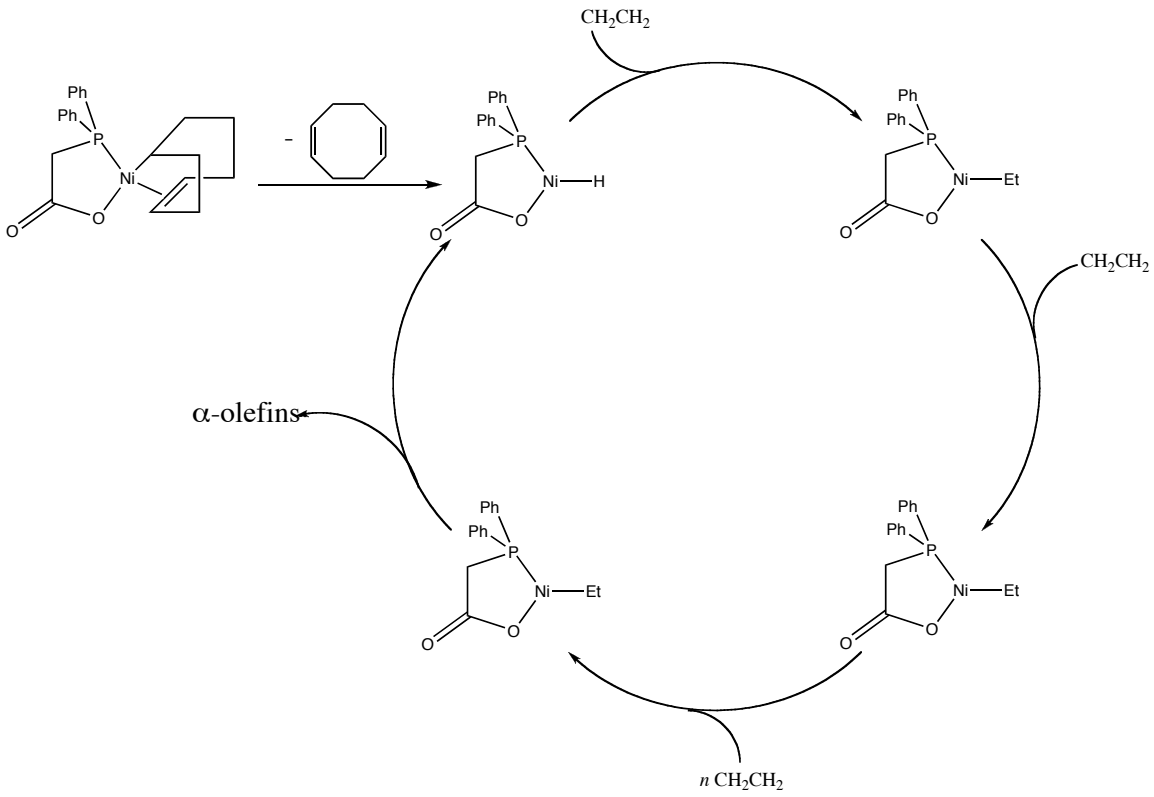

Figure 1.13: The Shell Higher Olefin Process; ethylene is oligomerized into α-olefins with chain lengths C_8-C_{18}.

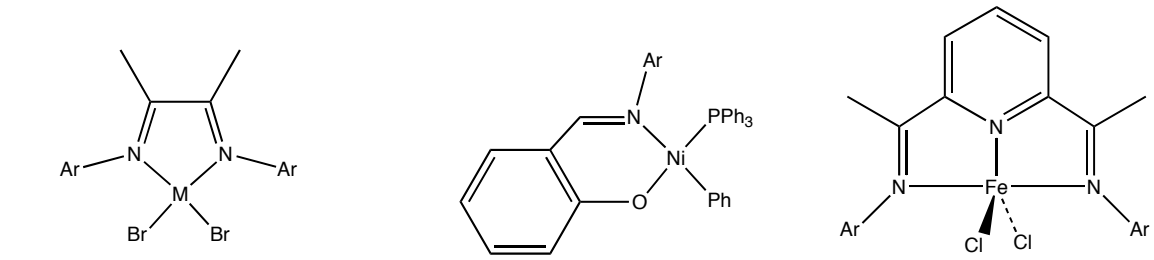

M = Ni, Pd Ar = 2,6-diisopropylphenyl (a)

Ar = 2,6-diisoproylphenyl (b)

Ar = 2,6 -dimethylphenyl (c)

Figure 1.14: Late transition metal Ziegler-Natta systems.

(a) Brookhart's substituted diimine complexes with Ni and Pd.[41] (b) Grubbs' substituted salicylaldimine Ni complex.[42] (c) Brookhart's 2,6-bis (imino)pyridine iron complex[43].

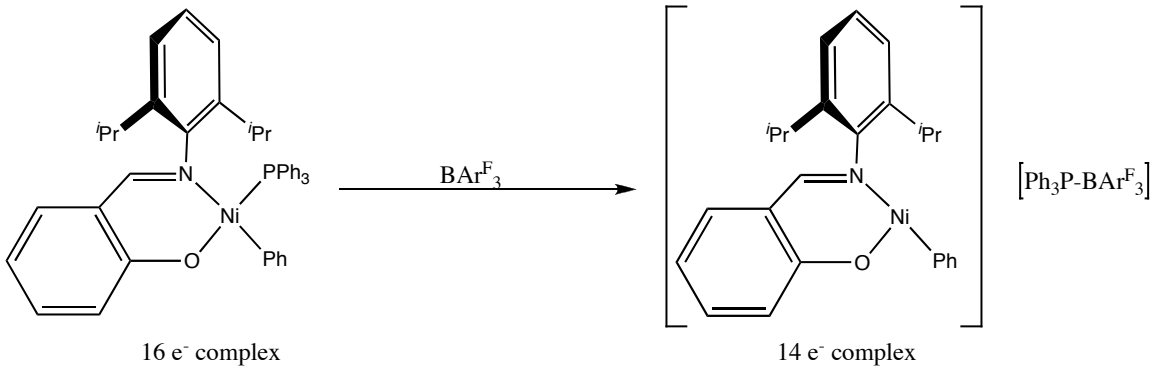

Figure 1.15: Grubbs Ni salicylaldimine catalyst.

The catalyst is activated by removing of and the trapping of the phosphine moiety with a stronger Lewis acid such as BAr^F_3. The precatalyst is a neutral 16 electron species that is activated to a 14 electron catalyst.

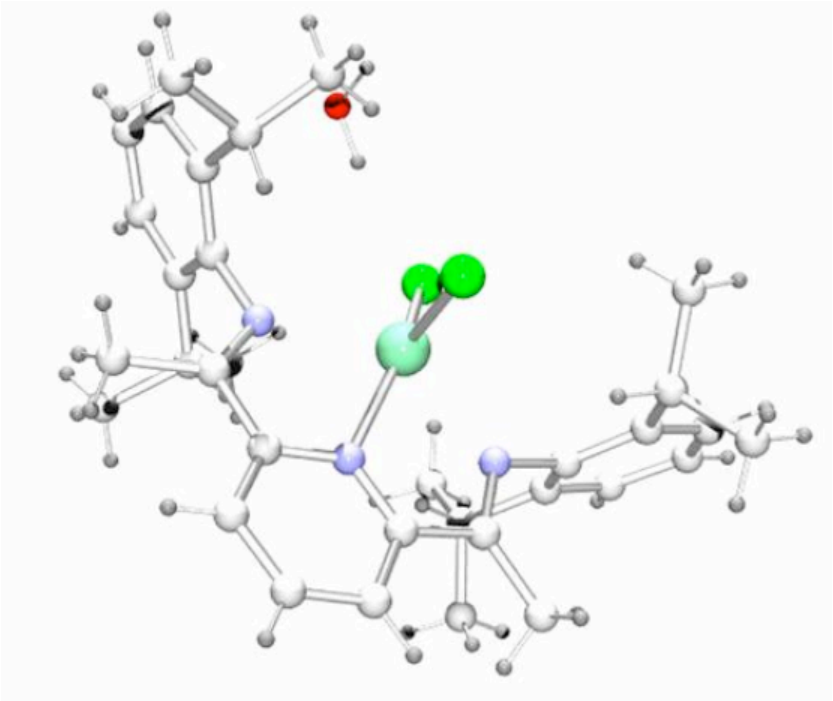

Figure 1.16: Brookhart's iron-based catalyst.

§ 1.3 General aspects of activation

All Zeigler-Natta binary systems must be activated prior to catalysis. For most of these systems, reacting the individual components together produces the active species. Some systems can then be stored in their active forms while others require several additional steps to isolate the active catalyst. There have been a large number of recent reviews and articles that discuss such activators.[31, 44-47]

§ 1.3.1 Activation of original systems

Ziegler's discovery and use of LiR, $LiAlH_4$ and AlR_3 in the production of linear α-olefins and introduction of the Ziegler direct process, demonstrated the ability of these alkylating reagents.[12,48] In the Ziegler direct process aluminum, hydrogen and an olefin are combined in a two-step process to produce the alkyl aluminum species. Alloying the aluminum with a variety of metals (in low amounts, less than 5%) increases the reactivity of the aluminum; when alloyed with titanium in low amounts (less than 2%), the activity is maximized. In the *aufbau* reaction, an alkyl aluminum species is reacted with an olefin to produce a series of long extended alkyl chains on the aluminum center. Displacement occurs with another incoming olefin to terminate the chain grown and produces a long chain primary olefin (up to 200 carbons in length). Ziegler noticed while using the titanium\ aluminum mixtures at high temperatures and pressures that the alkyl aluminum direct process and *aufbau* reactions took place simultaneously, the reaction that did not occur to the same degree without the titanium present.

Ziegler then used binary mixtures of transition metals and alkylating agents in hopes of finding a highly active polymerization catalyst. Mixtures of $TiCl_4$ or $TiCl_3$

reacted with Et_2AlCl or Et_3Al produced extremely active catalysts that polymerized ethylene at ambient pressures. The ratio of Al:Ti needed to be large in order to reach the high activities, at least 15:1 (Al:Ti). The original $TiCl_4$-Et_3Al systems produced a polymer with low mean molecular weights and an extremely wide molecular weight distribution; using the heterogeneous mixture of α-$TiCl_3$ and Et_2AlCl, Ziegler demonstrated that high activity and formation of large molecular weight polymers coul be achieved[11, 49].

§ 1.3.2 Trimethylaluminum and Methylaluminoxane

Breslow and Newburg were the first to demonstrate the ability of Cp_2TiCl_2 activated by diethylaluminum chloride to polymerize ethylene under 'mild' conditions.[16] This, the first example of an activated metallocene polymerization catalyst, demonstrated a ligand exchange between the Cp_2TiCl_2 and the dialkylaluminum chloride (R_2AlCl) to form the complex $Cp_2Ti(R)$-Cl•••AlR_2Cl (figure 1.17 step a).[50, 51] This adduct weakens the bond between the titanium and chloride thus making the titanium center more electropositive. Shilov suggested, as was later supported by electrochemical evidence[52] that the actual catalytically active species is the separated ion pair $[Cp_2TiR]^+$ $[RAlCl_3]^-$ (figure 1.17 step b).[53]

Coincidentally, Breslow and Long found that the addition of trace amounts of water to the Me_2AlCl Cp_2TiCl_2 system resulted in higher activity.[20] In some systems the addition of water activates previously inactive systems. The stoichiometric addition of

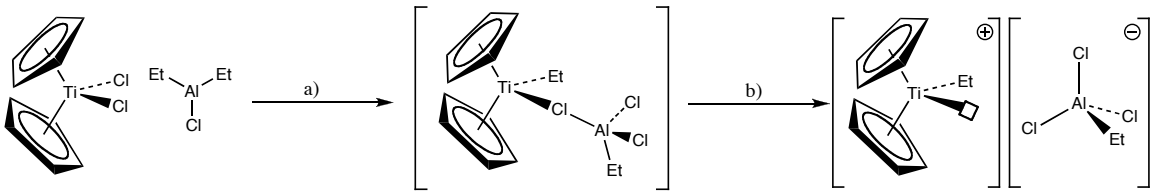

Figure 1.17: Activation of Cp_2TiCl_2 with Et_2AlCl.
(a) Activation to the bimetallic adduct. (b) Separation of the adduct into ion pairs.

water to Me_2AlCl results in the oxo-bridging dimer Cl(Me)Al-O-Al(Me)Cl + 2 CH_4; the dimer is a stronger activator than Me_2AlCl. The dimer is a stronger activator because the resulting anion stabilizes $[Cp_2TiCl]^+$ more than the $[MeAlCl_3]^-$; most likely it is the donation from the oxygen that makes the largest difference. Other systems without halides were investigated including trimethylaluminum (Me_3Al) and triethylaluminum (Et_3Al). Sinn and Kaminsky noticed a surprisingly high activation of Cp_2MCl_2 systems with Me_3Al and water,[21] much greater than that of Cp_2MCl_2 with Me_3Al alone.

Partial hydrolysis of trimethylaluminum yields a polymeric oxo-bridging aluminum species, methylaluminoxane (MAO), which is a much stronger activator than its precursor. The structure of MAO is unclear, although it is typically referred to as a linear oligomer with formula $[\text{-MeAl(O)-}]_n$[54, 55] also exists as cyclic planar structures with three-coordinate aluminum centers as well larger 3-dimensional clusters.[56] Typical methods for hydrolysis of Me_3Al to MAO leave residual amounts of Me_3Al within the MAO matrix, which can alter the effectiveness of the MAO.[57] Hydrolysis takes place with a hydrocarbon solution of a hydrated salt such as $Na_2SO_4 \bullet 7H_2O$ or $CuSO_4 \bullet 6H_2O$ and the controlled addition of Me_3Al to the solution.

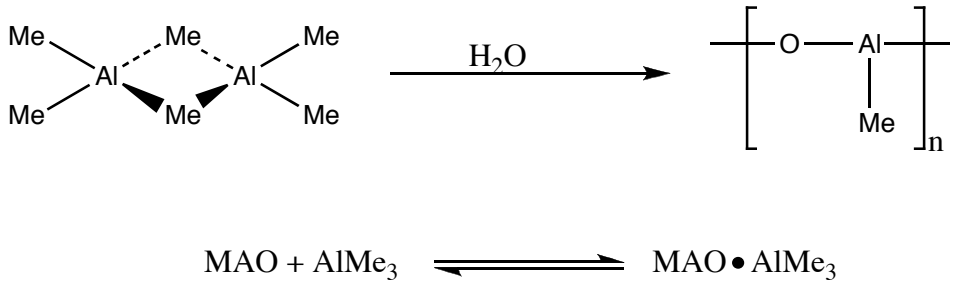

Figure 1.18: Partial hydrolysis of trimethylaluminum into methylaluminoxane.

Me_3Al is found within the MAO, both free and bound. Complete removal of the volatile Me_3Al from the MAO is impossible, and characterization of MAO content, while difficult, is not impossible. Me_3Al in the MAO is typically titrated with a Lewis base (typically pyridine) and analyzed as the complex *via* a change in the chemical shift and integrals in the ^1H NMR. These types of analysis do not reveal the true compositions of the Me_3Al /MAO mixtures because Lewis bases can often react with sites within the MAO matrix.[58]

MAO has at least three identifiable uses in the activation of the catalyst. First, MAO methylates the metallocene dichloride, replacing either one or both of the chlorides. Second, it can abstract one of those methyls (or chlorides) to form the cationic 14-electron complex, with a very complex aluminoxane anion. The third role that MAO can play is to reactivate any catalytic species that has become inactive, either from excess water or from termination due to β-hydride elimination of the polymer.[45] Polymerization reactions are run with a large excess of alkylaluminum activator (typically Al:M at least 300:1), to ensure that the catalyst stays active. Excess MAO will react with water in the

reaction mixture before it can react with the catalyst. To reactivate the catalyst, excess MAO exchanges the hydride with a methyl, and the reactivation process begins again.

§ 1.3.3 Conventional weakly coordinated anions

The active site of the original heterogeneous α-$TiCl_3$-Et_2AlCl catalyst and similar systems is not well understood. Understanding the activity of a heterogeneous, bulk catalyst is very difficult, often because more than one catalytic center is possible and maybe involved in the process. In the case of Ziegler-Natta catalysts, the active sites of the original systems were thought to be metal centers with a low-electron count and vacancies in the coordination sphere, but not much else was known. In order to develop a deeper understanding of Ziegler-Natta catalysts, homogeneous single-site catalysts were adopted for characterization. Metallocene-based catalysts possess the qualities necessary: 1) a single active site, 2) a simple binary systems composed of precatalyst and activator and 3) an easily characterized system.

Wilkinson's synthesis of the Group IV metallocenes in the early 1950s[2] provided robust, well-understood precatalysts for polymerization catalysis. Kaminski's use of Cp_2MCl_2-MAO (M = Ti and Zr) systems to polymerize olefins demonstrated a homogeneous, single-site catalyst, with an activity similar to the original heterogeneous systems. The use of MAO may promote the activity of the catalyst, but it is too complex for difficult mechanistic states to be observed. Kaminsky synthesized the first cationic Group IV metallocenes with simple anions.[7] Anions such as $[BF_4]^-$, $[PF_6]^-$, and $[BPh_4]^-$ are traditionally considered 'non-coordinating,' or weakly coordinating,[59] in contrast to

coordinating anions such as halides. To be considered a weakly-coordinating anion, the negative charge must be delocalized over the entire non-nucleophilic anion.[47, 60] Besides the delocalization of the negative charge, the anion must be both kinetically stable as well as stable with respect to oxidation.[45] Small anions such as $[BF_4]^-$ and $[PF_6]^-$ are known to exhibit decomposition *via* fluoride atom abstraction.[8, 61] Abstraction of small electronegative moieties such as a fluoride ion are extremely common in the literature;[22, 62, 63] if abstraction occurs, the catalyst is deactivated. Addition of a Lewis base such as pyridine or trialkylamines can be used to trap the electron-poor cation, which halts the abstraction but suppresses the catalytic activity. Addition of a less labile Lewis base such as tetrahydrofuran also halts the activity, but stabilizes the cation/ anion pair well enough to be characterized, as exemplified by the work of Jordan *et al* who isolated the complex $[Cp_2TiMe(THF)][BPh_4]$[8].

§ 1.3.4Perfluoroborates

Once the catalytic center was identified as a cationic 14 electron species, new synthetic routes were developed to achieve this. Two of the most significant routes developed from similar chemistry are: 1) abstraction of a ligand from a transition metal with a non-coordinating Lewis acid, and 2) metathesis of a halide for a larger non-coordinating anion. According to the Hard-Soft acid base principle (HSAB)[64] hard acids such as BF_3 are small, highly electropositive, and do not have low polarizability, and hard bases such as $[F]^-$, $[Cl]^-$ and $[Br]^-$ are relatively small donor atoms with high electronegativity. On the other hand, soft acids (such as most metals cations and BAr_3) have large acceptor

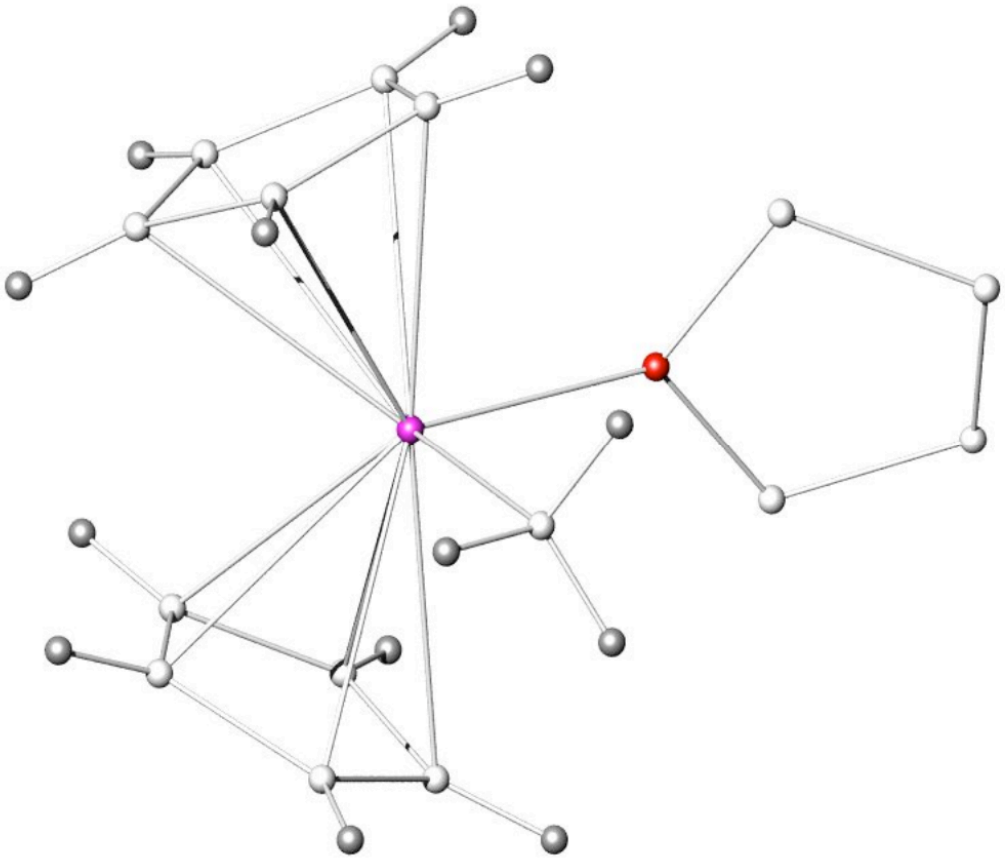

Figure 1.19: Ortep diagram of the structure of $[Cp_2ZrMe(THF)]^+$ observed in $[Cp_2ZrMe(THF)][BPh_4]$.

atoms with low electropositive nature and have high polarizability, while soft bases (such as H^- or R^-) have donor atoms with low electronegativity and are easily polarized.[65] The HSAB principle does not consider the strength of the acid or base, only that the Lewis acid-base complex will have extra stability if both the Lewis acid and Base are both considered hard or both soft. Scaling the strength of Lewis acids (and bases) is difficult due to the HSAB principle, although a representative scale (the pF^- scale) has been developed by Christe based on $[F]^-$ affinity for hard Lewis acids.[66]

Besides being inconvenient to work with, BF_3 is a hard acid and is therefore useful for abstractions with hard bases such as $[F]^-$ and $[Cl]^-$, but it does not abstract softer bases such as alkyl groups. Better abstraction occurs with the use of a softer acid than BF_3; triphenylboron is a soft acid, but its Lewis acidity is much less than BF_3.[67] *Tris*(pentafluorophenyl) boron on the other hand is a soft acid and has a similar Lewis acidity to BF_3. Other alkyl and aryl boranes have been used with limited success. Alkyl borans such as $B(CF_3)_3$ are good candidates, but because $B(CF_3)_3$ is extremely thermally unstable, its use is extremely limited. $B(CF_3)_3$ decomposes violently above -78°C, with the migration of a $[F]^-$ from the CF_3 moiety to the boron eliminating a highly stabilized CF_2 carbene. This migration/elimination happens so quickly, that they cannot be observed unless bound to π-bonding ligands such as: $B(CF_3)(NMe_2)_2$.[68] Although the π-donation stabilizes the borane, it is detrimental to the Lewis acidity of these systems, and is therefore useless in the abstraction process.

Tris(pentafluorophenyl)boron (BAr^F_3) is an ideal candidate for use as a Lewis acid. B-C bonds are less susceptible to hydrolysis than B-X bonds,[65] and the phenyl rings provide the polarizability of the acid. The offset rings limit the amount of π-donation from the aromatic rings because the overlap between the *p*-orbitals in the B-C_{Ar} bond is reduced.[69, 70] Massey and Park first synthesized and characterized *tris*(pentafluorophenyl)boron (BAr^F_3) in 1964,[69] and demonstrated its potential as a Lewis acid. Because of the steric bulk from the pentafluorophenyl rings the rings on BAr^F_3 are tilted out of plane, giving the borane a propeller-like structure.

BAr^F_3 was originally synthesized by the addition of pentafluorophenyllithium to a solution of BBr_3 at -80°C in a hydrocarbon solution. Filtration and removal of volatiles yield the crude tricoordinate borane. Subsequent sublimations yielded pure BAr^F_3.[71, 72] Pentafluorophenyllithium is known to be thermally unstable above -78°C, decomposing explosively into lithium fluoride and tetrafluorobenzyne. It was for that reason that the Grignard, traditionally much more stable their lithium counterparts, were investigated to replace the lithium reagent.

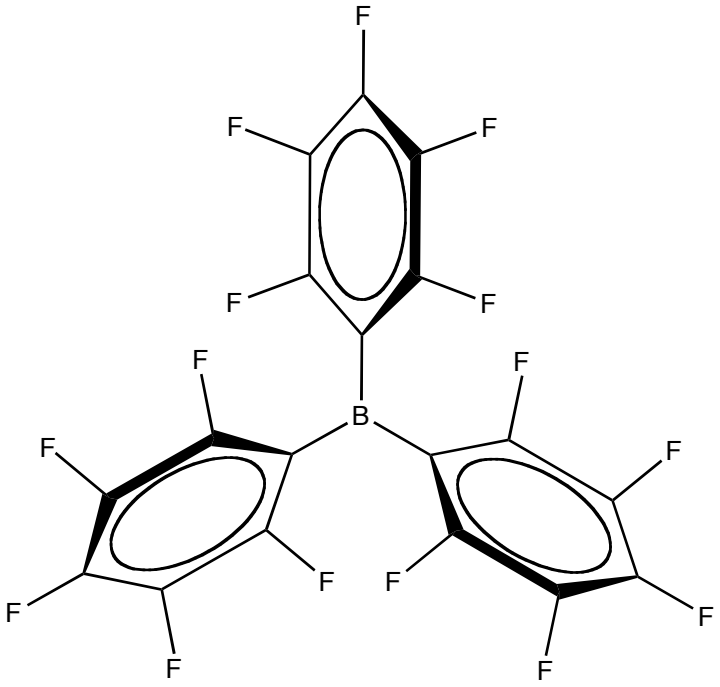

Figure 1.20: Tris(pentafluorophenyl)borane, drawn to illustrate the propeller like structure.

BAr^F_3 saw little use as a Lewis acid until the early 1990s when Marks *et al.* discovered its ability to abstract an alkyl group from a group IV metallocene,[25] and subsequently promote the polymerization of ethylene. Methyl*tris*(pentafluorophenyl) borate is easy to analyze as a counter anion, because the complex is stabilized by a bridging methyl group between the zirconocene and boron moieties. The bridging methyl can be displaced by a Lewis base such as THF, and the activity does not decrease, alluding to the fact that methyl-BAr^F_3 anion competes with the Lewis base for the zirconocene cation, which is not the case if the anion is BPh_4 or BAr^F_4.[68] Marks demonstrated the ability to produce a single site olefin polymerization catalyst that can be fully characterized along with its counter anion.

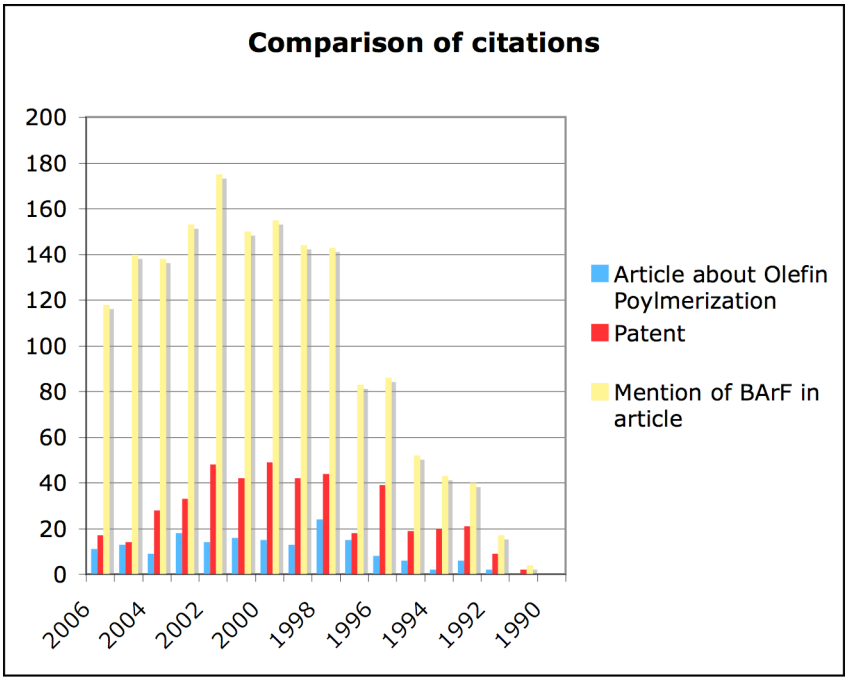

Figure 1.21: Citations regarding and use of BAr^F_3 in olefin polymerization in the chemical literature

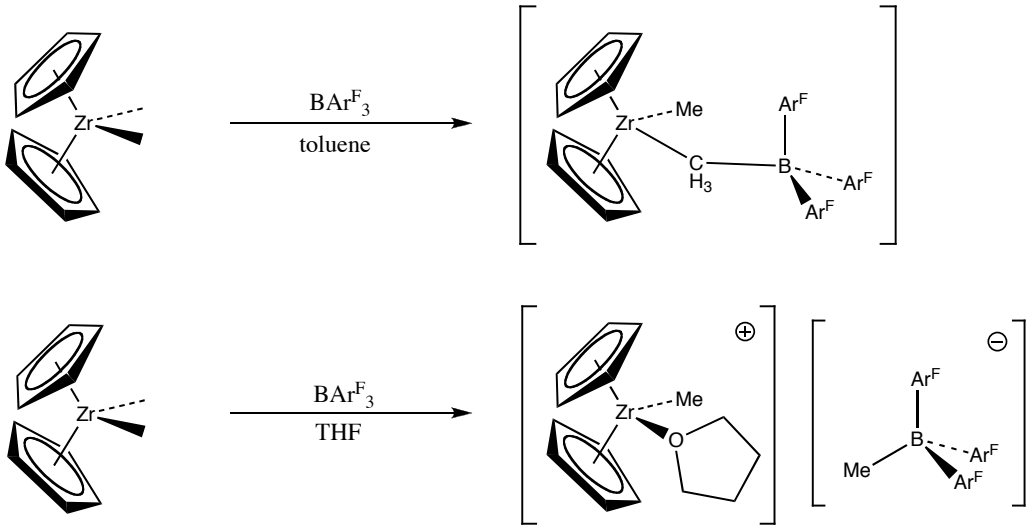

Figure 1.22: Alkyl abstraction in the presence of a donating solvent and without the donating solvent.

Metathesis of a halide for a larger non-coordinating anion is another way of producing a characterizable counter ion. The use of traditional non-coordinating anions such as $[PF_6]^-$ or even the bulkier $[BPh_4]^-$ created problems, since the metallocene cations are too electrophilic and will abstract $[F]^-$ or $[Ph]^-$, respectively. Highly electrophilic metallocene cations often do not tolerate these types of anions, as the anions are too Lewis basic.[8, 61] Exchanging the $[BPh_4]^-$ for a *tetrakis*(pentafluorophenyl) borate (BAr^F_4) does however yield a strongly activated catalyst, roughly 3500 times more active than their $[BPh_4]^-$ analogue.[24] The $[BAr^F_4]^-$ complexes are typically made by either metathesis of a coordinating halide with $KBAr^F_4$ (or other similar anion precursors) or metathesis of an alkyl group with $[HNMe_3][BAr^F_4]$ to produce CH_4, NMe_3, and the resulting cation BAr^F_4 complex.[24, 44]

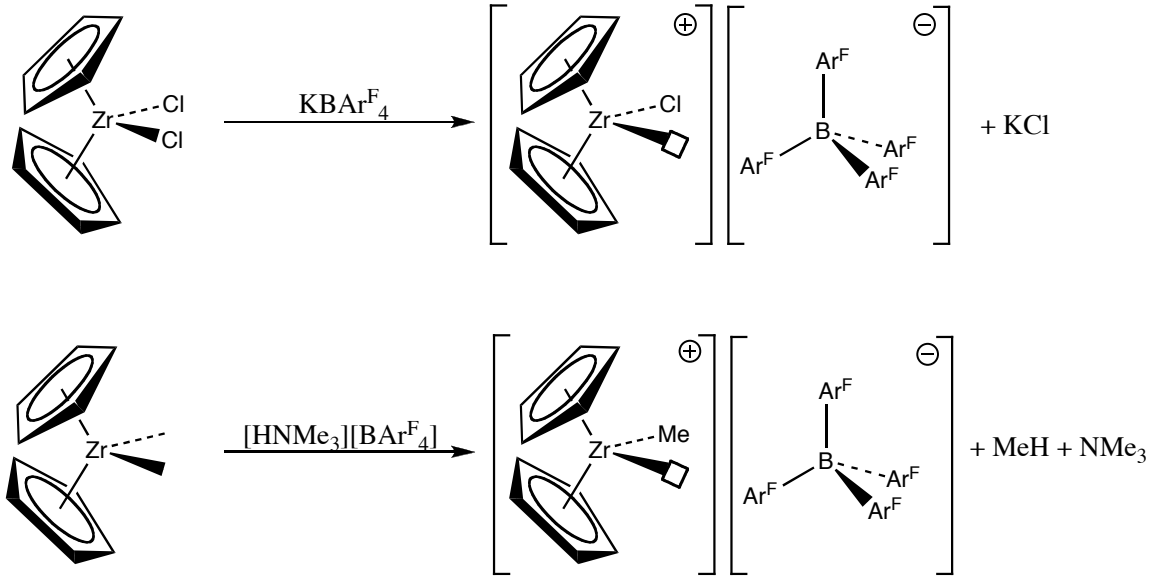

Figure 1.23: Formation of active cationic species via metathesis of a halide for a non-coordinating anion and the abstraction of an alkyl group.

Other fluorinated bulky, non-coordinating anions have been synthesized to probe the reactivity of the $[BAr^F_4]^-$ anions.[47] Most notable is the $[(3,5\text{-}(CF_3)_2C_6H_3)_4B]^-$ anion, which is often referred to as Brookhart's anion[73] due to its abundant use in his polymerization systems. Originally synthesized and characterized by Kobayashi[74] a decade prior to Brookhart's use, the $[BAr'_4]^-$ anion is used far less than the original $[BAr^F_4]^-$.

§ 1.4Mechanistic Aspects

The value of Ziegler-Natta catalysis lies in the stereoregularity of the polymer chain; the precise stereochemical outcome of the polymerization process leads naturally to the desirable properties of the syndio- or isotacticity, and great effort has been expended on determining the mechanism for this process. Understanding the rationale behind polymer chain propagation as well as the stereoregulation of the growing polymer has been one the most difficult issues in Ziegler-Natta catalysis. Although several proposals have been suggested, current models of Ziegler-Natta catalysis center on two major mechanistic proposals: the Arlman-Cossee mechanism, and the modified Green-Rooney mechanism. Recently, several reviews have appeared in the literature that detail many of these mechanistic proposals.[31, 75, 76]

§ 1.4.1 Arlman-Cossee Mechanism

After Ziegler and Natta's initial and independent discoveries[49, 77] that a transition metal alkyl polymerized propylene at low pressure and ambient temperature, several speculations arose attempting to provide a stereochemically accurate mechanism.[78-80] All

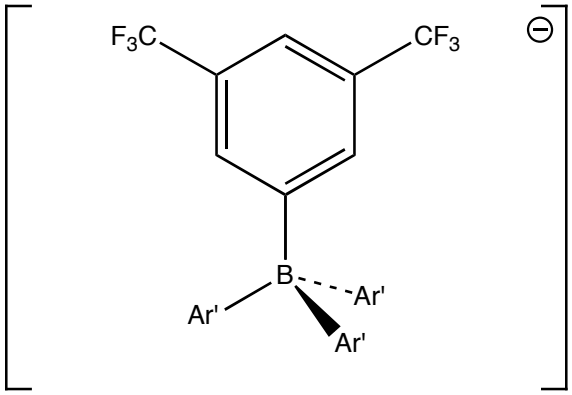

Ar' = [3,5-$(CF_3)_2C_6H_3$]

Figure 1.24: Brookhart's anion, typically paired with the [$H(OEt_2)_2$] cation

.

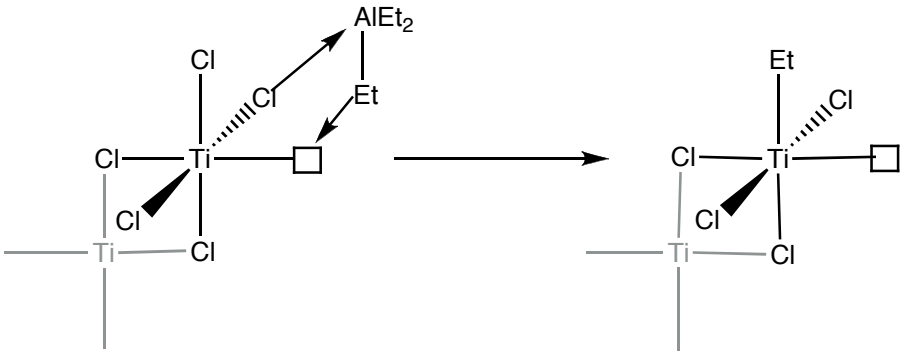

Figure 1.25: Activation of a Titanium center in the Arlman-Cossee mechanism.

of these suggested mechanisms infer that the incoming olefin aligns with one metal center and the growing polymer chain is coordinated with another metal center in the solid state.[81] Cossee uses a molecular orbital approach to determine the chain propagation. Beginning with Arlman's description of coordination vacancies,[4] Cossee rationalized that the active sites were formed in the reaction of the alkyl aluminum species with those vacancies in coordination[82] (Figure 1.25). The newly formed vacant site on the titanium is *cis* to a titanium alkyl bond.

It is that vacant site *cis* to the alkyl chain on a single metal center that is crucial to Cossee's argument.[83] After the incoming olefin is coordinated to the vacant coordination site, the olefin inserts into the titanium alkyl bond *via* a metallocyclobutane intermediate. The alkyl chain then migrates and opens a new vacancy in the coordination sphere. Cossee rationalizes that the insertion and alkyl migration is a result of the availability of the *d*-orbitals (namely the d_{z2}, d_{yz}, and the p_z orbitals for the alkyl migration).[82]

A series of 'head to tail' insertions lengthens the growing polymer chain; after each insertion, a new vacancy in the coordination sphere is created. Each new vacancy is then occupied with a new incoming olefin. Only those metal centers with an unsaturated coordination sphere that occurs on the outer layer of the heterogeneous catalyst are accessible for reaction; the surface vacancies also provide for a catalyst that is asymmetric through differentiation between the faces of the incoming α-olefin. The alkyl chain on the incoming olefin needs to be *anti* to the growing polymer chain. As the chain continues to grow the incoming alkyl group is always *anti* to the chain, resulting in the isotacticity of the polymer chain.[84]

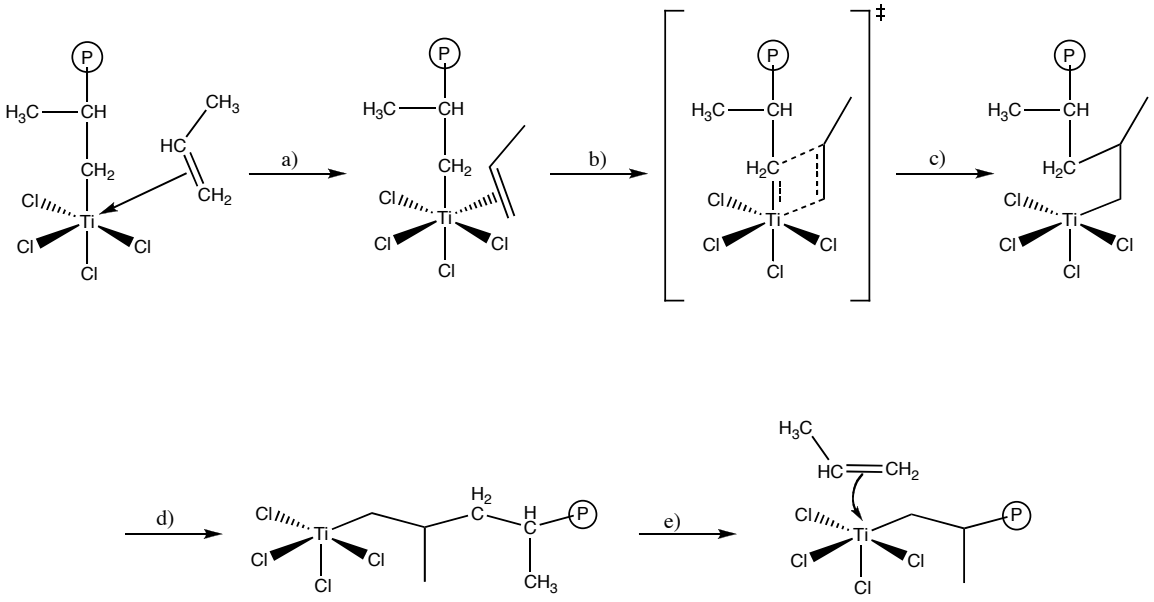

Figure 1.26: Cossee Mechanism.

a) coordination of the olefin b) formation of the transition state c) chain propagation d) rearrangement of the polymer chain e) coordination of the olefin (cycle starts over again)

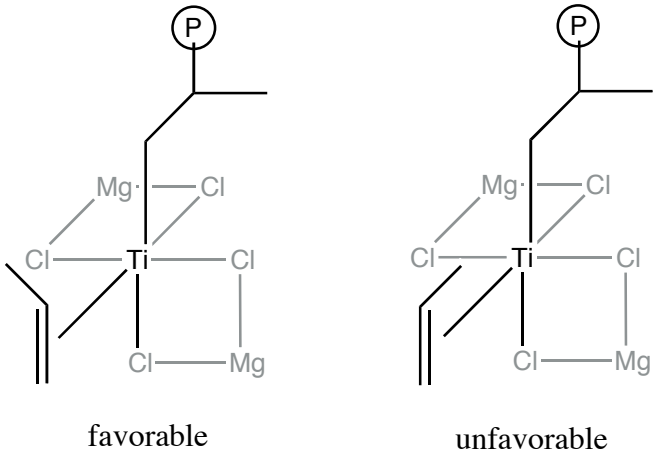

Figure 1.27: Sobotta's representation of the chiral face of a Ziegler-Natta catalyst supported in $MgCl_2$.

The favorable interaction places the incoming methyl group on the α-olefin anti to the growing polymer chain.[84]

§ 1.4.2 Modified Green-Rooney mechanism

An important part of any mechanism is the retention of the configuration of the polymer chain with respect to the vacant site. The original Cossee-Arlman mechanism provides no explicit reason for why this should be so, unless the number density of monomers is so high that coordination and reaction takes place so fast that there is no possibility that the chain can rearrange between additions, which is inherently unlikely. In addition, the Arlman-Cossee mechanism stems from heterogeneous conditions and makes little sense in homogenous ones. The Green-Rooney mechanism however can be invoked in either hetero- or homogeneous conditions.

The second mechanism derives from Green and Rooney's explanation of agostic interactions from the a nearby C-H bond.[85, 86] An agostic interaction is described as a 3-center-2-electron (3c-2e) bond between a C-H and metal center, exemplified by Green's titanium ethyl species $[(Me_2PCH_2CH_2PMe_2)TiEtCl_3]$.[87, 88] One hydrogen on the ethyl moiety is held close to the titanium center (2.29Å), with a Ti-C-C bond angle of 85.9(6)°. Traditional M-C-C bond angles for transition metal ethyl complexes range from 108-123°.[89-91] The smaller angle and short distance indicates an interaction between the titanium and the C-H on the methyl demonstrates this agostic interaction. Agostic interactions are only seen in metal complexes with a low electron count; the donation of the C-H bond to the electropositive metal center helps to alleviate the low electron density. The agostic interaction can be classified as an 'L' type ligand according to the MLX classification system.[92] With the agostic interaction, the electron count for the complex is effectively increased by two. Ignoring the β-agostic interaction the $[(Me_2PCH_2CH_2PMe_2)TiEtCl_3]$ can be classified as a ML_2X_4 system, which is a 12

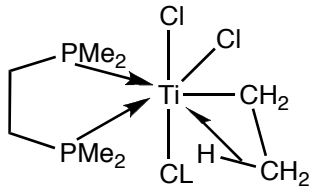

Figure 1.28: Green's [$(Me_2PCH_2CH_2PMe_2)TiEtCl_3$].

electron complex. Including the β-agostic interaction, the complex becomes a ML_3X_4 and has 14 valence electrons.

In dealing with agostic interactions, concerns about isotope effects arise.[75] C-H bonds differ from C-D bonds, the largest of the differences being the zero point energy in the transition state. The zero point energy of the C-D bond is lower than that of the C-H bond.[65] Because neither the C-D nor C-H bond is being made or broken, the isotope effect is considered as 'secondary.' With respect to agostic interactions, Shapley describes the M-H-C bond as having a larger interaction than that of M-D-C due to the gap between zero point energies.[93, 94] The Shapley effect is often only noticed when the isotopic alterations occur within the ground-state, and are witnessed by NMR or IR. This effect employs thermodynamic considerations, and involves the ground-state stability of the resting complex; if the agostic interaction is evolved in a transition state, kinetic considerations may be employed, but the Shapley effect cannot.

Green and Rooney's original mechanism stems from similarities between polymerization of olefins and olefin metathesis[85] and invokes carbene intermediates and olefin insertion into M=C bonds to yield the metallocyclobutane intermediate, and the

reductive elimination to produce the polymer. Two major problems identified with this mechanism are:

1. Reductive elimination requires a gain in oxidation state of two, which these d^0 complexes cannot accommodate
2. The metallocycle created can eliminate to the other M-C bond, giving a branched polymer (this is typically not observed).

These two inconsistencies led Green and Rooney to modify their original mechanism and replaced the alkylidene hydride with an agostic C-H interaction.[95]

The modified mechanism utilizes the agostic hydrogen in several ways: 1) The 3c-2e bond decreases electron density on the α carbon, increasing the propensity of olefin insertion, 2) the bridging hydrogen of the alkyl chain would reduce the steric 'inhibition of the carbon-carbon bond forming step,' and 3) the 'Ti-H-C interaction could provide a means for controlling the stereochemistry of the alkyl chain with respect to the incoming olefin.'

§ 1.5Overview for Dissertation

As demonstrated by various examples of Ziegler-Natta systems, all Ziegler-Natta catalysts depend on their Lewis acidity. Increasing the Lewis acidity of the active metal center should increase the activity the complex shows towards polymerization. Looking at the specific example of Cp_2ZrMe_2, the system can be considered an L_4X_4 system with coordinately saturated zirconium(IV) metal center. On abstraction of one of the methyl groups from the zirconium moieties with a Lewis acid, the system becomes L_4X_4Z or L_5X_3; the zirconium moiety becomes coordinately unsaturated and more Lewis acidic as

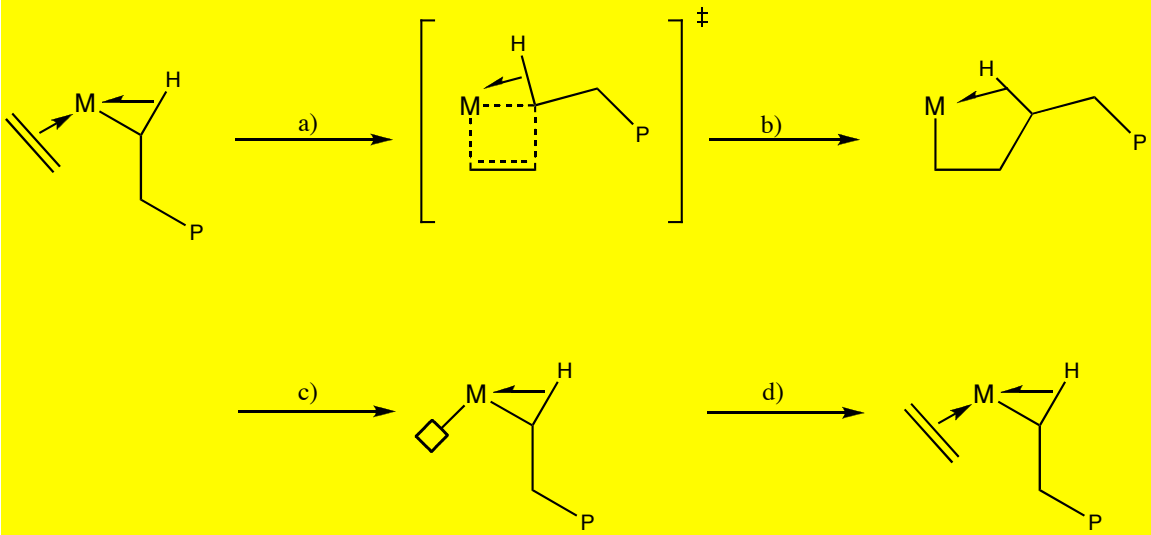

Figure 1.29: Modified Green-Rooney mechanism to describe the stereoselective polymer-chain grown in Ziegler-Natta Catalysis.

a) Insertion of the olefin monomer into the polymer chain that is held in place by an α-agostic hydrogen. b) Interchange to the γ-agostic hydrogen. c) Migration of the polymer chain and interchange a new α-agostic hydrogen. d) Addition of an olefin to renew the cycle.

the bound Me-Lewis acid becomes less bound. In solution, with loss of the Me-Lewis acid moiety the active catalytic species is thought to be an L_4X_3 system. Synthesis of a highly Lewis acidic metal center with enough steric bulk for sufficient complex stabilization should afford an extremely active Ziegler-Natta catalyst.

Arylamido ligands are ideal for this application due to their relative large size and ability to delocalize their π-electrons through the nitrogen to stabilize the metal center that they are bonded to. Group IV metals have proven themselves as ideal metals for Ziegler-Natta catalysis. Synthesis of a *tris*(arylamido)titanium(IV) species should provide a system with these considerations in place. If each arylamido ligand represents an LX moiety, then the cationic complex, analogous to the cationic zirconocene species

$[Cp_2ZrMe]^+$, exists as an L_3X_3 system. The arylamido-titanium cation contains 2 fewer electrons than its zirconocene analogue. The synthesis and reactivity of *tris*(arylamido)titanium(IV) species is discussed in great detail in the following chapters.

§ CHAPTER 2 Synthesis and reactivity studies of *tris*(diphenylamido)titanium (IV) complexes.

§ 2.1 Introduction

§ 2.1.1 Overview

The amido ligand has been known since the late 1920s. Amido ligands have since been employed in a myriad of complex types. Amido ligands are utilized in a large variety of chemical applications; the first industrial application using these systems was olefin polymerization. Homoleptic transition metal complexes with ligand sets consisting of $-NR_2$, with R = alkyl and/or aryl, were used in the late 1950s and 60s to polymerize ethylene and other short chain α-olefins. These systems were heterogeneous and bound to supports such as $MgCl_2$. Most of the these systems were based on the Group IV and V metals in the 3^+ or 4^+ oxidation state; all of the early catalysts were heterogeneous in nature.[96-101]

In the last decade there has been a resurgence of interest in amido transition metal chemistry, most notably regarding their usage in Chatt-type nitrogen cycle reactions. Cummins *et al.* first demonstrated cleavage of dinitrogen on a single three-coordinate molybdenum center. The system utilizes molybdenum's ability to span the oxidation states necessary and tolerate the six-electron reduction. While this cycle was not catalytic, Cummins also used this same cycle as a method to deliver N-atom transfer to organic reagents. The only ligands used to stabilize the molybdenum center were three bulky amido ligands.[102-104] A few years later, Schrock *et al*. used bulkier amido analogues to demonstrate the ability of [$(HIPTN_3)$]Mo] to catalytically reduce dinitrogen to

ammonia.[105, 106]

Group IV amido complexes have seen a wide variety of applications, including aspolymerization catalysts, hydroamination catalysts, and reagents for small molecule activation. Odom *et al.* has demonstrated the activity of [(dpma)Ti(NMe_2)$_2$] in hydroamination, (where dpma is *N*, *N*-di(pyrrolyl-a-methyl)-*N*-methylamine); traditional early transition metal hydroamination catalysts utilize metallocene complexes. Odom has also demonstrated the use of homoleptic M(NR_2)$_4$ complexes (M=Ti and Zr) as highly active hydroamination catalysts.[107] In the late 1980s Wolczanski *et al.* demonstrated the ability of Zr amido complexes to activate both methane and benzene. His [HNSi(^{t}Bu)$_3$]$_3$ZrMe complex undergoes reversible thermal RH elimination to give a three coordinate *bis*amido,-imido species.[108, 109]

§ 2.1.2Introduction to Diphenylamido systems

Arylamido ligands provide a more complex electronic environment than their simple alkylamido analogues. Alkylamido systems can decompose due to β-hydride elimination, as with standard alkyl ligands. With a lack of β-hydrogens, aryl systems do not have this problem. With the ability to delocalize one or both pairs of electrons into the aromatic rings, arylamido ligands can also provide various amounts of electron donation to the metal center. Diphenylamido is the most fundamental of the set of arylamido ligands. As a starting material, Ph_2NH is an inexpensive, easily handled solid; purification is possible by recrystallization and/or sublimation. The amine is extremely soluble in polar aprotic solvents, as well as in hydrocarbons. Alterations can be made to the phenyl rings easily, and synthesis of isotopically labeled analogues is also possible.

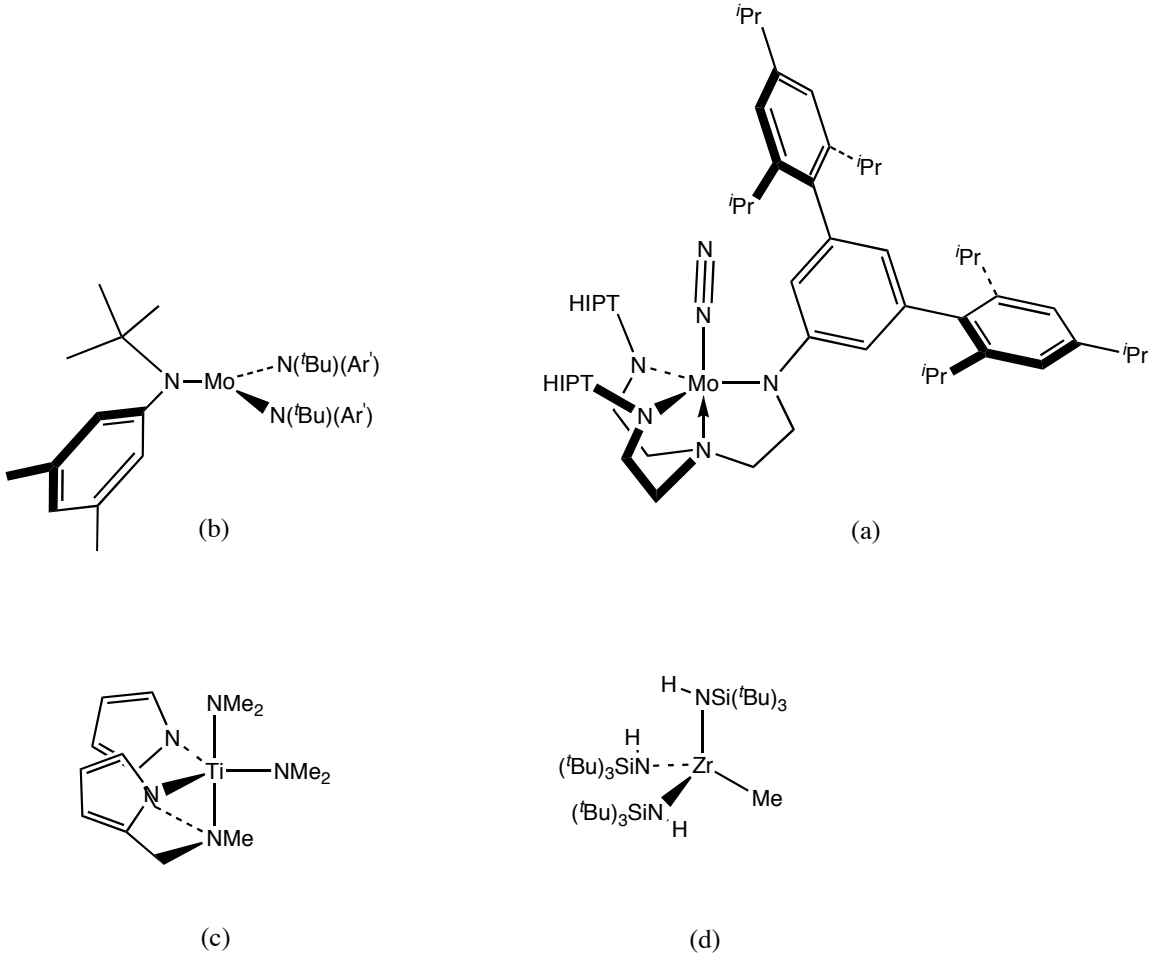

Figure 2.1: Transition metal amido complexes

(a) Schrock's [HIPTN$_3$N]Mo(N$_2$) catalyst with dinitrogen bound, (b) Cummins' [^{t}BuNAr']$_3$Mo catalyst without L donor such as dinitrogen, (c) Odom's (dpma)Ti(NMe$_2$)$_2$ hydroamination catalyst, (d) Wolczanski's [HNSi(^{t}Bu)$_3$]$_3$ZrMe complex which shows activation for methane.

While exploring *bis*arylamido ligands, other similar ligands have been examined in this laboratory. The dihydrodibenzoazepinyl and carbazolyl ligands contain the diphenylamido motif, but in both cases the phenyl rings are tethered together at the ortho carbons. In the case of dihydrodibenzoazepinyl system, an ethyl bridge limits torsion around the C_{Ar}-N bond. The carbazolyl system is a fused 6-5-6 ring framework; the carbazolyl rings can be considered non-innocent ligands, based on their ability to change their aromaticity based on bonding to the metal center. The diphenylamido is the simplest of the three systems, because it contains no restrictions on electronic donation or steric demand for the metal center.

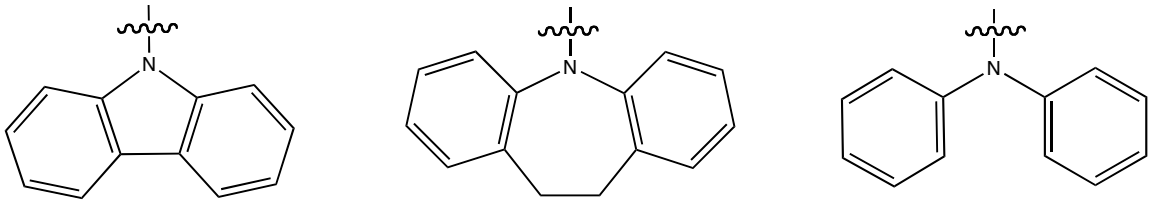

carbazolyl dihydrodibenzoazepinyl diphenylamido

Figure 2.2: Arylamido ligands.

§ 2.2 Synthesis of Complexes

§ 2.2.1 Synthesis of $LiNPh_2$ (1)

Synthesis of the diphenylamido ligand is accomplished in one step; treatment of 1 equivalent of diphenylamine (Ph_2NH) with 1.2 equivalents of ^{t}Bu-Li in a hydrocarbon solvent yields the lithium amide salt **(1)** in ~95% yield. Diphenylamine is soluble in hexane, but its lithium salt is not, providing for simple work up. Filtration and drying of the product under reduced pressure affords a very fine, white powder. Compound **(1)** is an extremely water and oxygen sensitive solid. At concentrations above 25 ppm of oxygen, the white solid turns a light green; the addition of any amount of oxygen turns the solid a deep forest green. **(1)** is insoluble in hydrocarbon solvents, extremely soluble in ethereal solvents, and slightly soluble in toluene and benzene.

The aromatic region of the ^{1}H NMR of **(1)** is almost identical to that of $HNPh_2$. The presence of a broad singlet near 5.8 ppm represents the N-H peak from any residual $HNPh_2$. This N-H resonance provides an easy method to assess complex decomposition. The peaks in the ^{13}C NMR of $LiNPh_2$ are shifted downfield to related $HNPh_2$ peaks.

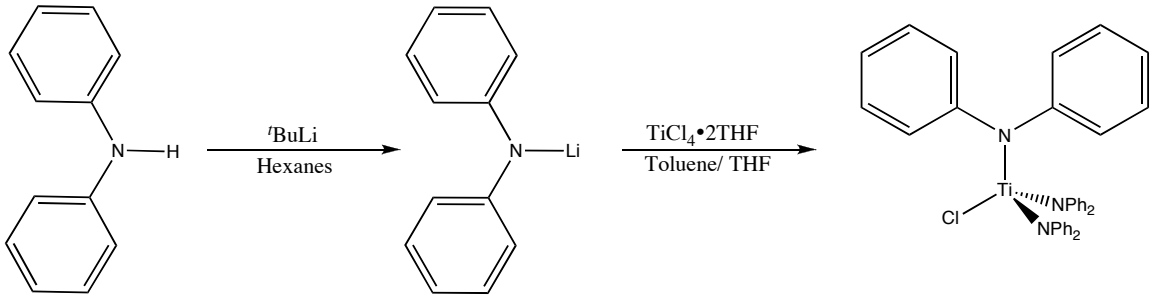

Figure 2.3: Synthetic scheme for the production of compounds (1) and (2).

§ 2.2.2Synthesis of $(Ph_2N)_3TiCl$ (2)

The reaction of three molar equivalents of **(1)** with one equivalent of $TiCl_4$•2THF yields $(Ph_2N)_3TiCl$ **(2)** in 88% yield. The reaction is conducted in toluene in dilute solution; the addition of small amounts of THF improved the solubility markedly. Upon addition the reaction mixture turns blood-red, and the reaction is essentially complete after twelve hours. Filtration, recrystallization from pentane and drying under reduced pressure yields a red powder. If the complex is not fully recrystallized and dried properly, a single THF molecule is bound. This THF is weakly bound, and removal is possible through further recrystallization and drying. The fact that a donor ligand such as THF can still be bound to the metal center implies two things: 1) The coordination sphere around the metal is not saturated, and 2) The metal center is sufficiently Lewis acidic to bind the extra ligand. If the THF is left bound to the complex, further reactions do not proceed.

The stability of **(2)** is surprising; after three days in dry oxygen, no decomposition is detected. Hydrolysis on the other hand begins at water concentrations near 4 ppm. Just as the ligand decomposes to green upon hydrolysis, the red hue of **(2)** turns to brown and then to green with higher water concentrations. The fact that complex is oxygen tolerant is remarkable; most high valent and low coordinate early transition metal complexes are extremely oxophilic. Nearly all Group IV based Ziegler-Natta catalysts are poisoned by low amounts of oxygen and trace amounts of water.[45]

The ^1H spectrum of **(2)** consists of resonances in the conventional aromatic region, with 3 sets of peaks, each with extensive coupling to neighboring protons.

Integration of the peak area gives a perfect 2:1:2 ratio when the delay time $D_1 \geq 30$ sec. Coupling between the *ortho-meta*, *ortho-para* and *meta-para*, confirm that the peaks are *meta* at 7.114 ppm, *ortho* at 6.817 ppm and *para* at 6.978 ppm. Figure 2.4 illustrates the splitting and a tabulation of the coupling constants. The degree of coupling between the protons on the individual rings can also be seen in the DQ-COSY spectrum of **(2),** which can be found in Appendix I. Because of the relative simplicity of the spectrum of **(2)**, it may be inferred that **(2**) is highly symmetric, most likely due to a C_3 axis along the Ti-Cl bond. When d_8-THF is used as the solvent, two sets of THF peaks are seen, one corresponding to the free solvent and one corresponding to the bound THF in a ratio of 1:1 **(2)**:THF. The bound solvent exhibits extreme amounts of coupling due to its loss of symmetry and the free solvent is very broad.

Assigning the ^{13}C spectrum is easily accomplished from the gHSQC spectrum. The three carbons with protons exhibit cross peaks in the gHSQC spectrum, leaving the *ipso* carbon as the only carbon without a cross peak, and because the 3 individual C-H peaks are assigned in the proton, direct correlation can be made. The resonance for the *ortho* carbon is located at 123.91 ppm, the *para* carbon at 126.10 ppm, the *meta* carbon at 129.90 ppm, leaving the *ipso* carbon at 150.65 ppm. $(Ph_2N)_3TiCl$ is soluble in Et_2O, THF, toluene, pentane, hexane, benzene, TMS_2O, methylcylohexane, dioxane, CH_2Cl_2, bromobenzene and pyridine. Recrystallizations have been attempted in every solvent and combinations of each solvent in attempts to obtain single crystal for X-ray diffraction. All of the recrystallizations have produced extremely clean powder, but no single

.

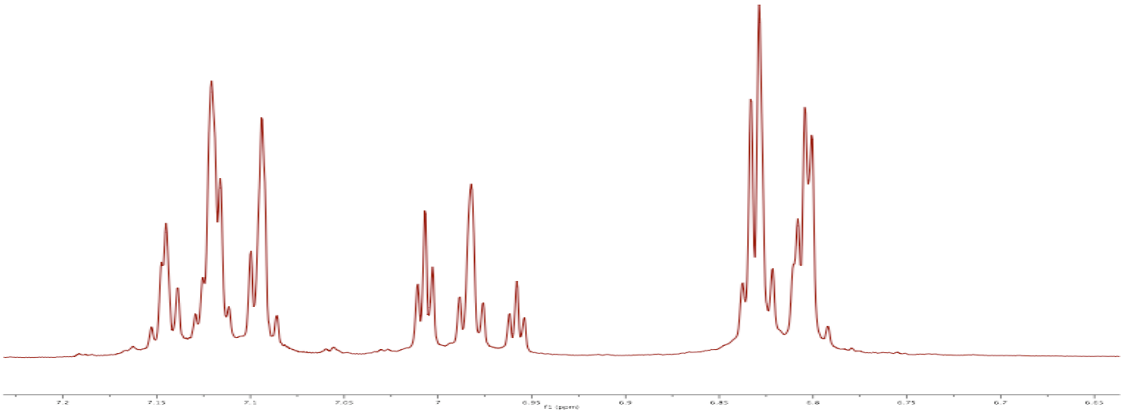

$(Ph_2N)_3TiCl$ in d_8-THF				
Proton	δ /ppm)	Coupling Pattern	H-H Coupling	Value (/Hz)
ortho	6.82	doublet of triplets	$^3J_{o\text{-}m}$	6.00
meta	7.11	triple of triplets	$^3J_{m\text{-}p}$	5.40
para	6.98	triple of triplets	$^4J_{o\text{-}p}$	1.20

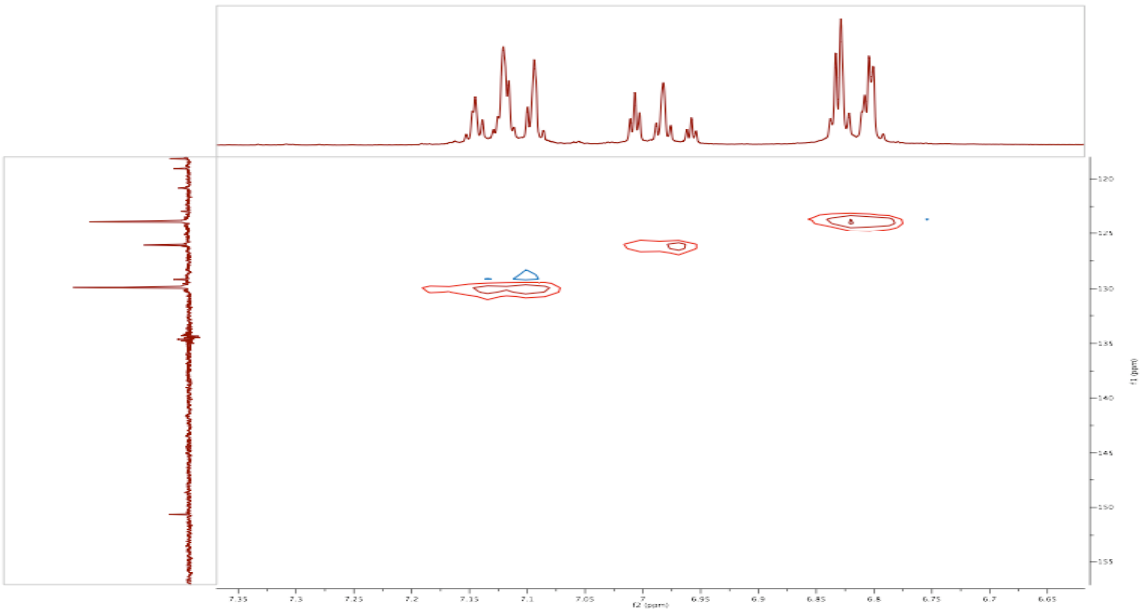

Figure 2.4: Spectra of $(Ph_2N)_3TiCl$ in d_8-THF.

(top) Aromatic region of the ^1H spectrum. (middle) table listing peaks and coupling constants. (bottom) gHSQC $(Ph_2N)_3TiCl$ in d_8-THF of spectrum.

crystals. Sublimation of **(2)** above 95 ºC leads to decomposition; thermal decomposition results in white/green free amine and black metal waste

§ 2.2.3 Synthesis of $(Ph_2N)_3TiI$ (3)

In hopes of solving the solubility situation of **(2)**, the chloride was replaced with an iodide. The iodo complex was rationalized to be less soluble in hydrocarbon solvents and it would therefore be much easier to obtain a single crystal for X-ray diffraction. **(3)** can be synthesized *via* two routes. First, three equivalents of the lithium salt **(1)** and one equivalent of TiI_4 in toluene yields complex **(3)** in moderate yields, 63%. Separating the product from the LiI side product is difficult, and it is difficult to obtain a powdery product. The product remains oily and sticky after several recrystallizations. Using ethereal solvents is impossible due to the Lewis acidity of the TiI_4.

The second route produces cleaner product and uses less solvent than the TiI_4 method. One equivalent of **(2)** is stirred with a large excess of KI (at least 10 equivalents) and a small amount of LiI (less than .5 equivalent) in THF for a week in a sealed ampoule. After a week, pentane is added to precipitate all of the dissolved KI, and the solution is filtered and stripped. After a couple of recrystallizations, dry red-orange powdered **(3)** is obtained in 89% yield.

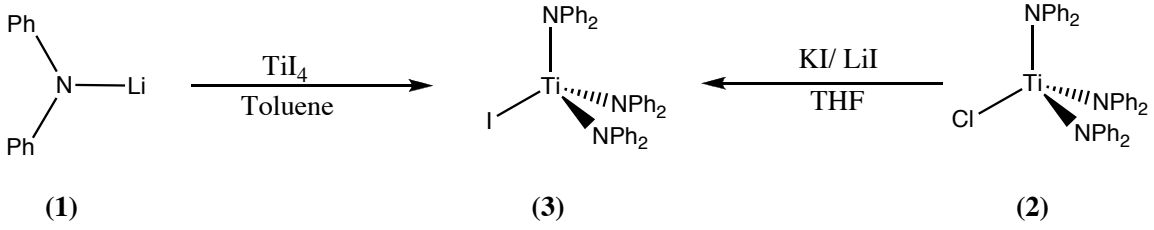

(1) **(3)** **(2)**

Figure 2.5: Two synthetic pathways to complex (3)

Again, sublimation decomposes the complex, although **(3)** decomposes about four degrees higher than **(2)** does (just under 100 ºC). While the iodide is less soluble than the chloride in pentane and hexane, all recrystallization attempts yield similar powder products to its chloride analogue. Replacing **(3)** for **(2)** in other reactions provides no benefit; reaction times are longer and yields are lower than when run with the **(2)**.

The ^{1}H and ^{13}C NMR spectra of **(3)** are similar to **(2)**; in the ^{1}H spectra, the differences between two compounds must be made from the coupling constants, the chemical shifts hardly change. The differences in the ^{13}C spectra of both complexes are minute, but because of the lack of coupling in the spectrum, the chemical shifts of **(3)** easier to distinguish.

§ 2.2.4Synthesis of $(Ph_2N)_3TiMe$ (4)

Isolation of the methyl-substituted complex was difficult. Using one equivalent of LiMe as an alkylating agent proved to partially successful. Total conversion was not achieved, and due to solubility issues, isolating **(4)** proved fruitless. In the ^{1}H NMR, both

Table 2.1: Comparison of the ^{13}C NMR chemical shifts for complexes **(2)** and **(3)** in d_8-THF

Carbon	$(Ph_2N)_3TiCl$ **(2)**	$(Ph_2N)_3TiI$ **(3)**
meta	129.9 ppm	129.79 ppm
para	126.1 ppm	123.5 ppm
ortho	123.9 ppm	120.67 ppm
ipso	118.2 ppm	118.1 ppm

the Ti-Me and the Li-Me can be identified. The same reaction was attempted, using an excess of LiMe and similar results occurred. Because of the problems that alkylating with LiMe caused a second route was investigated in order to alkylate complex **(2)**. Other experiments in this lab explored the use of Grignard reagents with Mg trapping agents such as 1,4-dioxane. The addition of 1,4-dioxane shifts the Schlenk equilibrium completely to the to one side by complexation with $MgCl_2$ and produces the M-Alkyl species. Freshly prepared MgMeI in Et_2O was added to a toluene solution of $(Ph_2N)_3TiCl$ in a drop-wise manner. After one hour, a solution of 1,4-dioxane in Et_2O was added slowly over a period of 20 minutes. The reaction mixture was allowed to settle and the solution was filtered from the $MgCl_2$•2dioxane precipitate. The filtered solution was cooled to -80 ºC for 12 hours to precipitate $(Ph_2N)_3TiMe$. The mother solution was again filtered while at -80 ºC leaving clean **(4)** behind; the room-temperature mother solution's volume was then reduced to half and cooled to -80 ºC again to collect more product.

Complex **(4)** is bright orange and extremely oxygen and moisture sensitive; concentrations ≥ 3 ppm of either cause decomposition. While **(4)** exhibits lower

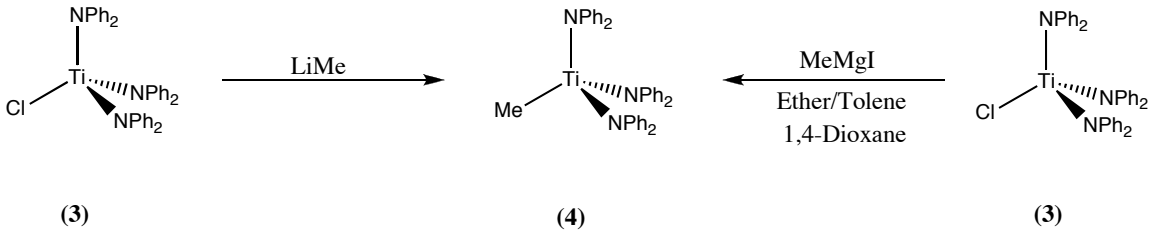

Figure 2.6: Two synthetic pathways to complex (4).

solubility than chloride starting material, it is still soluble in the same solvents. Separation of the two complexes can be achieved thermally. Sublimation attempts yield decomposition above 65 ºC. While recrystallization from toluene/ Et_2O mixtures at -80 ºC does produce large single crystals, the crystals decompose instantaneously upon solvent removal.

The ^1H spectra of **(4)** is comprised of four signals: three in the aromatic region each with a high degree of coupling and a singlet at ~0.424 ppm. The coupling constants and splitting simplify the assigning the peaks. In benzene the *ortho* protons are at 7.166 ppm, the *meta* protons are at 7.043 ppm and the *para* protons are at 6.843 ppm, leaving the methyl to be assigned at 0.424 ppm. Integration of the upfield shift indicates three protons. Other Group IV metal-methyl complexes have methyl signals assigned to peaks from 0.4-1.8 depending on solvent.[110-112]

There is also small amount of toluene that is always present in the ^1H NMR spectrum. Spectra from the 300 MHz NMR displays only the small singlet consistent with the methyl of toluene at 2.11 ppm; all of the aromatic peaks from the residual toluene are lost in the base of peaks from the diphenylamido peaks, figure 2.7. displays the singlet at 2.11 ppm. The same sample run on the 600 MHz resolves the separation of the diphenylamido peak enough to see the three characteristic peaks from the residual toluene. Figure 2.8 displays the small peaks in between the larger diphenylamido peaks. The **(4)**: toluene ratio is roughly 10:1, based the ratio of integrals of the two species both methyl: methyl integrations and *para* hydrogen: *para* hydrogen. This small amount of toluene does not affect the reactivity of the complex; but it seems to be responsible for its stabilization, when recrystallized to remove the toluene, the complex decomposes.

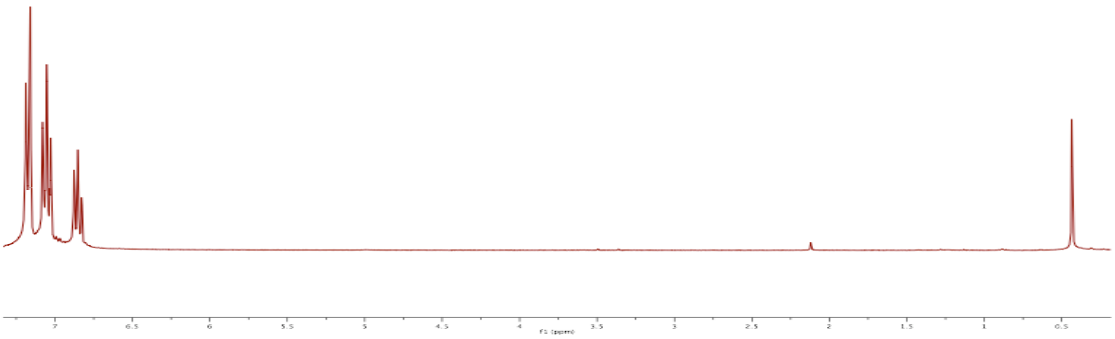

$(Ph_2N)_3TiMe$ in d_6-Benzene				
Proton	δ (/ppm)	Coupling Pattern	H-H Coupling	Value (/Hz)
ortho	7.17	doublet of triplets	$^3J_{o\text{-}m}$	7.44
meta	7.04	triple of triplets	$^3J_{m\text{-}p}$	7.90
para	6.84	triple of triplets	$^4J_{o\text{-}p}$	1.20

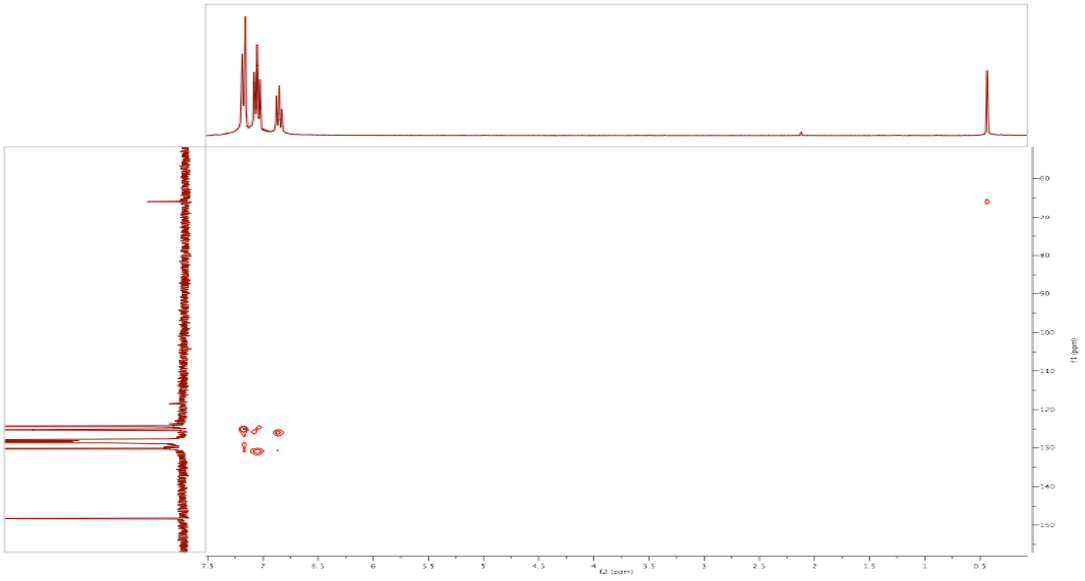

Figure 2.7: Spectra for $(Ph_2N)_3TiMe$ in d_8-THF.

(top) ^1H NMR spectrum, (middle) table of coupling constants and chemical shifts and (bottom) gHSQC spectrum.

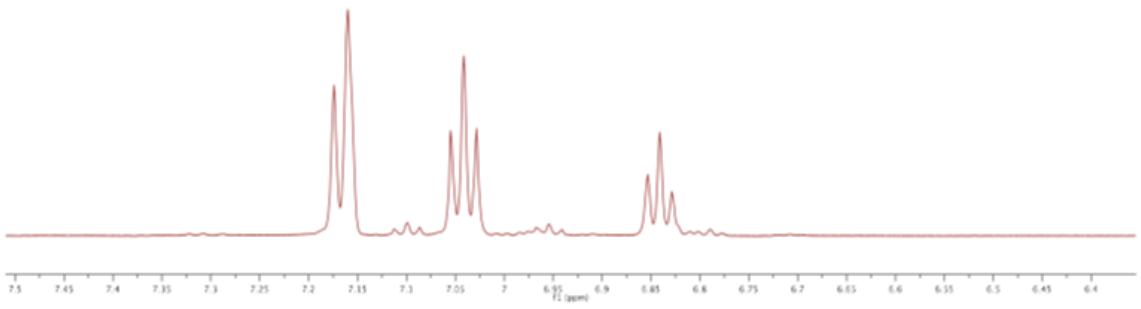

Figure 2.8: ^{1}H NMR $(Ph_2N)_3TiMe$ on the 600 MHz,

Assigning the carbon spectra of **(4)** is not as easy. The four aromatic carbons of the complex have standard relaxation times and therefore are easily detected; the methyl on the other hand has a considerably longer delay time. Relaxation time of the methyl is approximately 73 sec and is at 65.509 ppm. The $^{1}J_{C\text{-}H}$ constant for the methyl was determined to be 131.8 Hz, from the coupled ^{13}C NMR spectrum. Relaxation time was determined by trial and error rather than standard T_1 detection methods. Standard methods looking at T_1 longer than 30 secs require several days to a week for detection. Because of the intense signal in the ^{1}H spectrum, detection of the methyl peak through proton correlation was also attempted. The gHSQC spectrum did in fact show correlation from the ^{1}H signal at 0.424 ppm to the ^{13}C signal at 65.509 ppm. This assignment falls just inside the range for other Group IV metal-methyl complexes 110- 60 ppm.[111, 112]

The NOESY spectrum provides further information about complex **(4)**. The methyl protons show correlation to the ortho protons on the phenyl rings. NOESY

provides through space and intermolecular proton-to-proton distance information. An intense peak would infer a shorter bond distance than a weaker signal; the methyl-to-*ortho* proton coupling is fairly weak, indicating a distance of 3-5 Å between the protons.[113]

Complex **(4)** demonstrates interesting reactivity. Transition metal alkyl species can act as synthons for transition metal hydrides. The addition of molecular hydrogen to a coordinatively unsaturated electron deficient metal center is often difficult or impossible in the case of d^0 systems. If the complex contains an alkyl ligand, the addition of molecular hydrogen can add across the M-R bond and produce M-H and H-R. $(Ph_2N)_3TiMe$ dissolved in pentane was sealed in an ampoule with ~ 1 atm of dry hydrogen and allowed to react for 1 week, upon which time no color change occurred. A sample was taken for ^1H NMR analysis, and the spectrum was identical to the starting $(Ph_2N)_3TiMe$ complex. The methyl signal remained and no Ti-H bond could be detected. The reaction ampoule was refilled prepared again and allowed to react for a week again, this time while under reflux. After the reaction, another ^1H NMR was taken and resulted in the same analysis as before.

Insertion into the Ti-Me bond was also attempted with CO, in hopes of synthesizing the Ti-acetyl. Complex **(4)** was loaded into a J-Young's valved NMR Tube and dry ^{13}CO was condensed into the tube, roughly 4 equivalents. The ^1H MR spectrum was identical to the starting material and the ^{13}C NMR spectrum showed only free CO as the only new peak. Insertion into the Ti-Me bond proved to be unsuccessful.

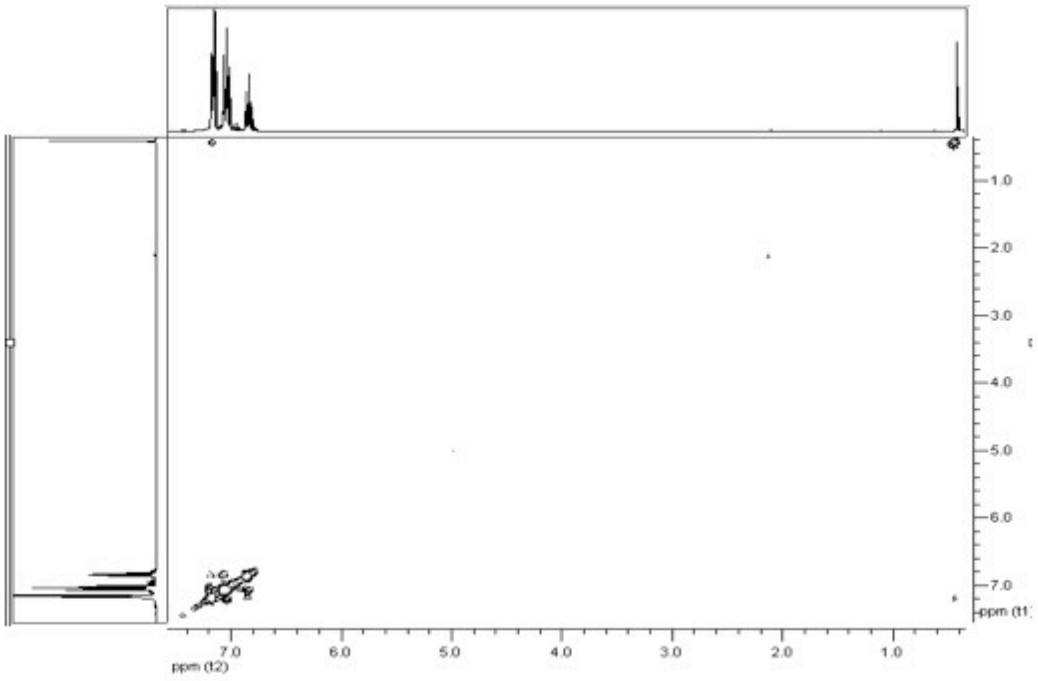

Figure 2.9: NOESY of complex (4) in d_6-benzene.

§ 2.2.5 Synthesis and Reactivity of [(Ph2N)3Ti•••Me•••BArF3] (5)

Abstraction of the methyl from complex **(4)** also seemed probable. Marks *et al*. demonstrated the ability of strong Lewis acids such as *tris*(pentafluorophenyl)boron to abstract an alkyl group from dialkyl zirconocenes (Yang JACS JACS Cation-like). BAr^F_3 has been extensively used to abstract alkyl from a variety of early transition metal complexes. Zirconocene dichloride is a 16 electron L_4X_4 system; with on equivalent of BAr^F_3 added, the complex shifts to a L_5X_3 system. The abstraction weakens the Zr-Me bond sufficiently enough that insertion of Lewis bases may occur, especially π-bases such as olefins. $(Ph_2N)_3TiMe$ is a 14 electron L_3X_4 complex, after abstraction of the methyl, the complex would then be L_4X_3 and should show activity for olefin polymerization.

One other possibility could exist for the reaction of BAr^F_3 with complex **(4)**, one of the diphenylamido ligands could donate the nitrogen's lone pair to the boron instead of the titanium, while this would change diphenylamido moiety from LX to X with respect to the titanium center. Figure 2.10 displays both structural possibilities for complex **(5)**. Of the two possible structures, possibility (a) is more likely; each diphenylamido ligand can act as an LX with great Ti=N double bond character. The Ti-Me can only act as an X ligand and is therefore has only σ-bond character. The Ti-N bond strength is also greater than the bond strength of Ti-C. Possible structure (a) is also the more likely of the two due to the fact that large phenyl rings should also provide enough steric bulk to block the formation of the N-B bond.

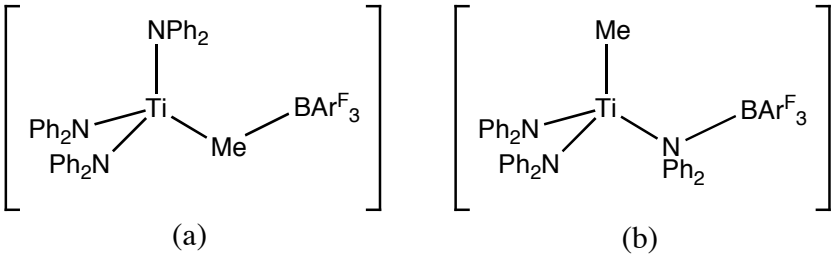

Figure 2.10: Two structural possibilities for [$(Ph_2N)_3TiMe$][BAr^F_3].
(a) Ti-C-B and (b) Ti-N-B bonding possibilities

When one molar equivalent of BAr^F_3 is reacted with **(4)**, the solution darkens immediately and solubility increases drastically. While, isolation of adduct **(5)** is possible, the dry product degrades extremely quickly in under 2 ppm concentrations of water or oxygen. Adduct **(5)** is easy to synthesize *in situ* and because there are no side product, this is the preferred method for handling it. The ^1H NMR shows the methyl peak shifting downfield from 0.4356 ppm to 1.1983 ppm, $\Delta\delta = 0.7627$. This downfield shift is indicative for alkyl abstraction (possible structure (a) from figure 2.10). [$Cp_2Zr(Me)$•••**Me**•••BAr^F_3] has a downfield shift of 0.1 ppm.[111] Adduct **(5)** is air-sensitive, exposure to any concentration of water or water causes decomposition and the color changes from deep-red to green and slowly to gray.

§ 2.2.6Synthesis and Reactivity of $(Ph_2N)_3TiCH_2PMe_2$ (6)

With successful synthesis of methyl complex **(4),** other alkyl groups were attempted. The Et-, ^{t}bu-, ^{i}Pr- and ^{n}Bu were all attempted, but all resulted in either no reaction for the butyl species or complex decomposition with the ethyl and isopropyl complexes.

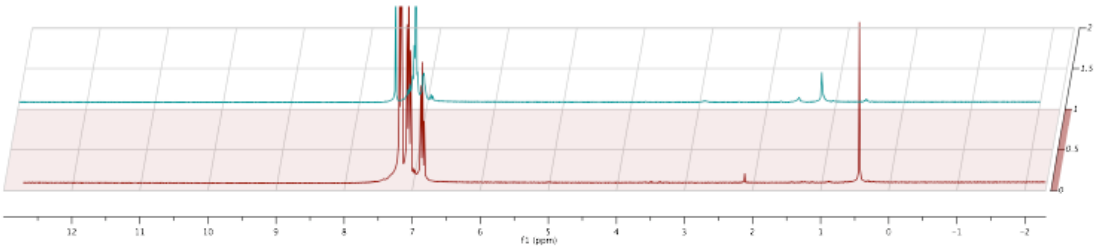

Figure 2.11: Stacked plot of 1H spectra of $(Ph_2N)_3TiMe$ (front) vs $[(Ph_2N)_3Ti•••Me•••BAr^F{}_3]$ (back) in d_6-benzene

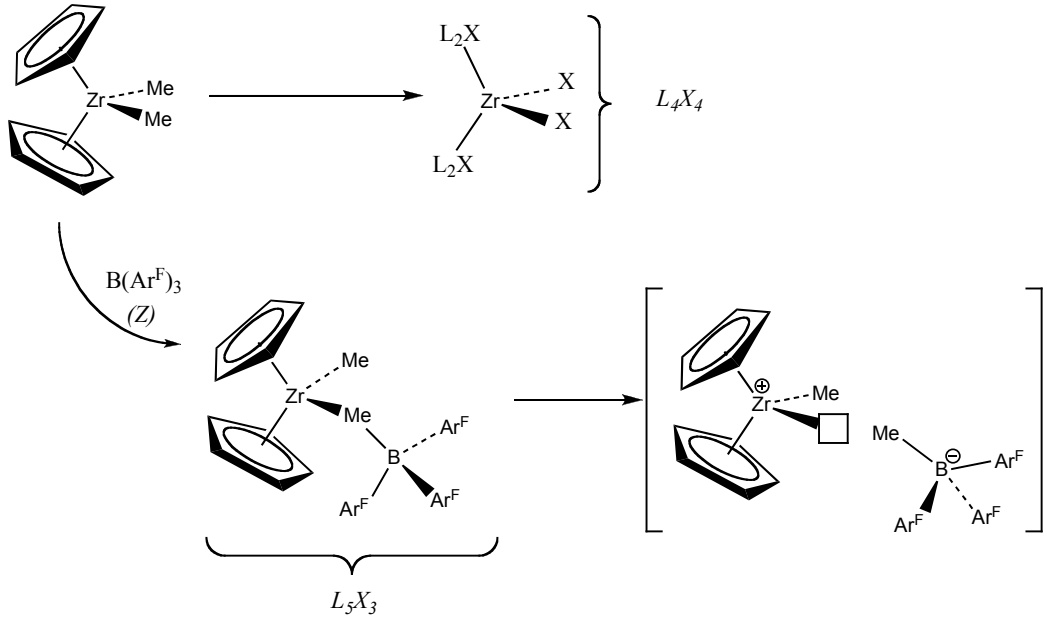

Figure 2.10: Abstraction of a methyl group from Cp_2ZrMe_2 to form a bridging methyl species which acts like the fully separated analogue.

However, prior experiments in this laboratory have demonstrated the potential of $-CH_2PMe_2$ as ligand.[114] With the ability to act as both an X and L ligand, the $-CH_2PMe_2$ complex was reasoned to be more easily synthesized due to the extra electron density donated to the Ti center. One equivalent of $LiCH_2PMe_2$ dissolved in toluene was added to a toluene solution of **(2)** drop wise over a period of twenty minutes. The color darkened to a purple/red solution upon addition of the phosphinomethanide. Filtration and removal of the solvent yielded **(6)** in 83.6%. Decomposition occurs with low concentrations of oxygen and water; upon decomposition the stench of PMe_3 is noticed immediately and the color changes to green and eventually to gray.

Complex **(6)** could have three different structures. The first of which is where the phosphinomethaide ligand acts only as an X ligand, where the lone pair on the phosphorus is not involved in any bonding. The second structure possibility uses the phosphinomethanide ligand as both an X and L ligand; the lone pair on the phosphorus donates to the Ti center making a three membered ring containing the Ti, P and CH_2 between them. The third structure motif that can exist is a dimer (or oligomer) with bonding similar to the second type, but instead of the lone pair donating to the Ti that the σ bond is made, the lone pair is bonded to another Ti center. Of the three types, the first is the least likely; if the structure existed as defined, the metal center is a highly Lewis acidic 14 electron metal center, with a Lewis basic phosphorus adjacent to it. More probable are the other two possibilities, both of which are 16 electron species.

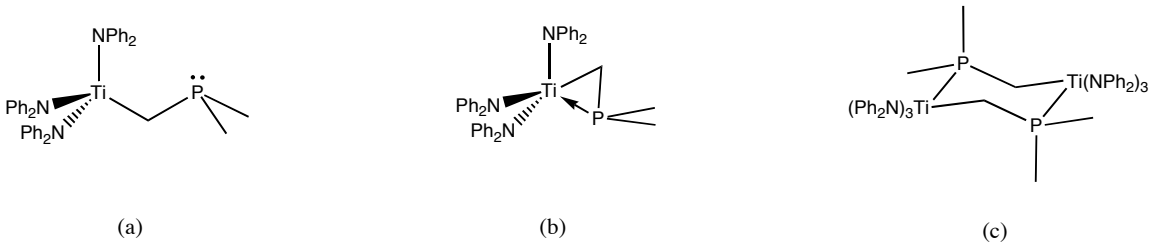

Figure 2.11: The three structural possibilities for $(Ph_2N)_3TiCH_2PMe_2$.

(a) 14 electron monomer, (b) 16 electron monomer and (c) 16 electron dimer.

Spectroscopic analysis of complex **(6)** is easier to monitor than the chloride **(2)** due to the phosphorus moiety. The ^{31}P NMR of complex **(6)** shows single resonance at -39.18 ppm (referenced to D_3PO_4), which is 1.12 ppm downfield from the $LiCH_2PMe_2$ starting material. The ^{1}H NMR is much more complicated than complexes **(2)**, **(3)** or **(4)**. The aromatic region contains at least two separate systems and is extremely complex. Integration is uninformative, as although individual resonances are identifiable, they are not sufficiently well resolved for definitive integration. The two identifiable spin systems are intertwined within each other, one consists of broad featureless peaks, while the other has tangible coupling patterns. Both sets seem to have no coupling between one another, as observed from the gCOSY spectrum. In the aliphatic region of the aromatic, the CH_2 protons are distinguished from the methyl protons.

The hydrogens on the CH_2 are diastereotopic in nature, and their ^{2}J-coupling is easily identified in the gCOSY (figure 2.14). The CH_2 coupling constant is 7.5 Hz, which is lower than traditional geminal ^{1}H-^{1}H coupling of 12-15 Hz for non-cyclic molecules. Cyclopropyl derivatives have ^{2}J coupling of 4-9 Hz and ^{2}J coupling for

cyclohexyl derivatives are between 11 and 14.[115] While both the three and six-membered rings are possible structures, the coupling data suggests that the three-membered ring is more likely. However, when considering the fact that this ring is not made up entirely of carbon atoms, but rather the ring consists of two sets of C-P-Ti, the six-membered ring becomes possible again. Increasing electronegativity increases the relative ^{2}J, and increasing the electropositivity decreases ^{2}J; both titanium and phosphorus are lower than carbon on the Pauling electronegativity scale, 1.4 (Ti), 2.1 (P) and 2.5 (C). Also ring constraints with the added size differences between titanium, phosphorus and carbon, a geminal ^{1}H-^{1}H coupling constant of 7.5Hz is probable for a six-membered ring.

In the ^{13}C spectra of complexes **(2)**, **(3)**, **(4)** and **(5)** there are only four resonances which correspond to each of the four unique carbons; free rotation of the amido ligands makes both of the phenyl rings equivalent to one another. There are eight resonances in the ^{13}C NMR of complex **(6)**, corresponding to the 8 unique carbons for the complex. In dimer form (or LX ligand monomer) free rotation of the amido ligands is hindered, and because of this hindrance, both of the phenyl rings possess 4 unique carbons. This is reinforced by the complexity of the aromatic region of the ^{1}H NMR spectrum; the two coupling systems represent each of the individual rings.

Figure 2.12: ^{1}H NMR of $(Ph_2N)_3TiCH_2PMe_2$ in d_6-benzene.

(top), zoom of the aromatic region of the gCOSY spectrum of $(Ph_2N)_3TiCH_2PMe_2$ in d_6-benzene on 300 MHz (middle) and zoom of the aliphatic region of the gCOSY spectrum of $(Ph_2N)_3TiCH_2PMe_2$ in d_6-benzene on 300 MHz (bottom).

Assigning the ^{13}C NMR spectrum is more difficult; the gHSQC displays correlations between the ^{1}H and ^{13}C spectra, but definitive assignments cannot be made. One of the two spin systems from the ^{1}H spectrum correlated to the three carbons visible in the ^{13}C spectrum, the other system correlates to non-existing signals in the ^{13}C spectra.

X-ray analysis of $LiCH_2PMe_2$ reveals that the structure exists as a dimer in the solid state. The difference in ^{31}P chemical shifts between the $LiCH_2PMe_2$ and complex **(6)** is very small. The dihydrodibenzoazepinyl analogue of **(6)** has a ^{31}P NMR chemical shift of -33.1 ppm, which is 7.2 ppm downfield from $LiCH_2PMe_2$ and 6.98 ppm downfield from **(6)**. The chemical shift difference is much smaller between **(6)** and the $LiCH_2PMe_2$ than the difference between $(dda)_3TiCH_2PMe_2$ and the lithium dimethylphosphinomethanide, signifying that **(6)** exists most likely as a dimer. Complex **(6)** was also envisioned to be a possible synthon for $(Ph_2N)_3TiH$. Because **(5)** did not react with H_2, **(6)** was thought to be a better route to the hydride. If **(6)** would react, it should provide the ligand environment as the original complex (both complexes would be L_4X_4) either $TiCH_2PMe_2$ or $Ti(PMe_3)H$. Complex **(6)** was dissolved in pentane in an ampoule and approximately 1 atm of dry H_2 was expanded into the ampoule. The ampoule was sealed and allowed to react for one week. After one week, an aliquot was taken for ^{1}H NMR analysis and displayed no changes from the original spectrum for **(6)**. The ampoule was sealed again, placed in an oil bath and heated to reflux for another week. ^{1}H NMR analysis again revealed no changes to the original

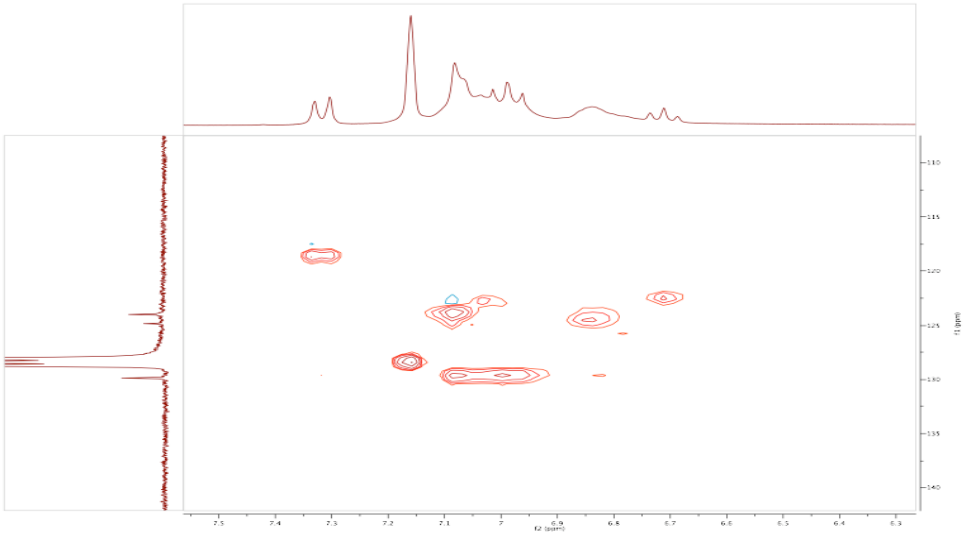

Figure 2.13: gHSQC spectrum of $(Ph_2N)_3TiCH_2PMe_2$ in d_6-benzene on 300 MHz.

spectrum for **(6)**. The lack of reactivity with molecular hydrogen implies that the dimethylphosphinomethanide moiety is tightly bound and the coordination sphere around the titanium center is saturated.

§ 2.2.7 Synthesis and Reactivity of $[(Ph_2N)_3TiCH_2P(Me)_2BAr^F_3]$ (7) and $[(Ph_2N)_3Ti][^FAr_3BCH_2P(Me)_2BAr^F_3]$ (8)

Abstraction of the alkyl group from complex **(6)** was also envisioned. Addition of one equivalent of BAr^F_3 should bind to the lone pair on the phosphorus, creating a zwitterionic adduct. While this adduct should be as active as the similar CH_3 species **(4)**, a second equivalent of BAr^F_3 would be necessary to abstract the $–CH_2PMe_2$ moiety completely from the titanium center. Prior experiments in the laboratory have demonstrated this same principle; the complex $Cp_2Zr(CH_2PMe_2)•2BAr^F_3$ does not show polymerization activity, but when a third equivalent was added, polymerization

occurred.[114]

In two separate J-Youngs valved NMR tubes, one equivalent of $(Ph_2N)_3TiCH_2PMe_2$ was combined with one and two equivalents of BAr^F_3 respectively. Dry d_6-benzene was vacuum distilled into each tube and each were allowed to react for at least twenty minutes before analysis were taken. The ^1H spectrum of **(6)** does not change with the addition of one or two molar equivalents of BAr^F_3. The ^{13}C and ^{31}P NMR spectra also show no change to complex **(6)**. Both tubes were allowed to stand for twenty-four hours and analysis was taken again. After 24 hours, no change was detected. Figure 2.16 depicts the lack of change in the complex **(6)** and its two BAr^F_3 adducts. The noticeable differences are due to concentration of he samples. The chemical shifts and relative intensities are identical to one another.

The fact that even two molar equivalents of BAr^F_3 cannot abstract the

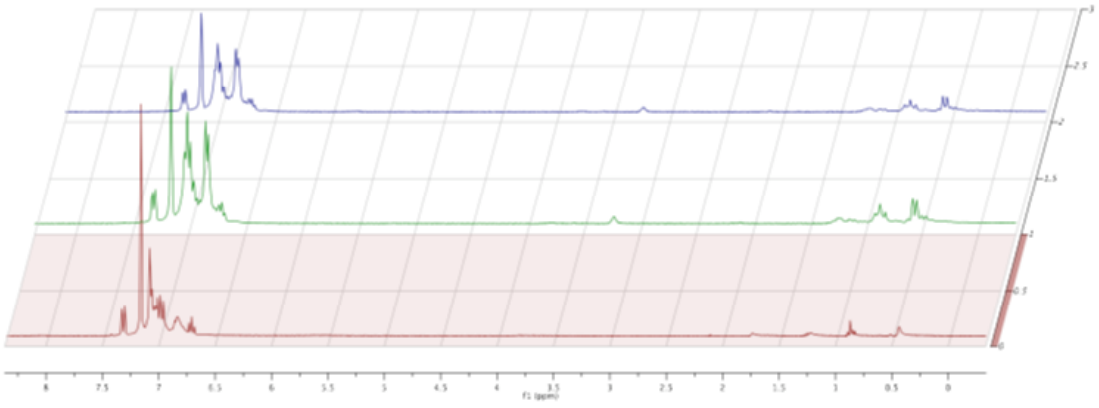

Figure 2.14: Stacked plot of ^1H NMR spectra of complex (6) and adducts. (front): $(Ph_2N)_3TiCH_2PMe_2$ in d_6-benzene, (middle) $(Ph_2N)_3TiCH_2PMe_2$ and one equivalent of BAr^F_3, and (back): $(Ph_2N)_3TiCH_2PMe_2$ ad two equivalents of BAr^F_3.

dimethylphosphinomethanide from the Ti center, the dimethylphosphinomethanide moiety must be bound extremely tightly. If this ligand is bound so tightly, it is likely that complex **(6)** does exist as either structure type (b) or (c) from figure 2.16, with the dimethylphosphinomethanide acting as a LX ligand. The fact that the BAr^F_3 does not induce a change in complex **(6)** also implies that each of the diphenylamido ligands are bound tightly as LX ligands, and the nitrogen's lone pairs are unavailable to complex with the Lewis acid, which in turn supports the alkyl abstraction in complex **(5)** and not a N-B abstraction.

§ 2.2.8 Synthesis and Reactivity of $[(Ph_2N)_3Ti][BAr^F_4]$ (9)

With the successful abstraction of the methyl moiety from complex **(4)**, attempts to form a formally fully cationic system were pursued. Metathesis of the chloride from **(2)** with a non-coordinating anion was attempted first. A small amount, 500 mg, of potassium *tetrakis*(pentafluorophenyl)borate ($KBAr^F_4$) was dissolved in 50 mL of benzene. This solution was added slowly to a solution of 430 mg of **(2)** in 200 mL of benzene. After a few hours, hexane was added to force the KCl out of solution. The solution was filtered and solvent was removed under reduced pressure. The resulting purple/ red solid is extremely unstable; complex **(9)** decomposes in low concentrations, under 2.0 ppm, of oxygen and water.

Complex **(9)** consists of a tricoordinate titanium cation and the BAr^F_4 anion. Its sensitivity to oxygen and water along with its reactivity data supports the ion pair conclusion. Remarkably, complex **(9)** is capable of olefin polymerization, discussed in

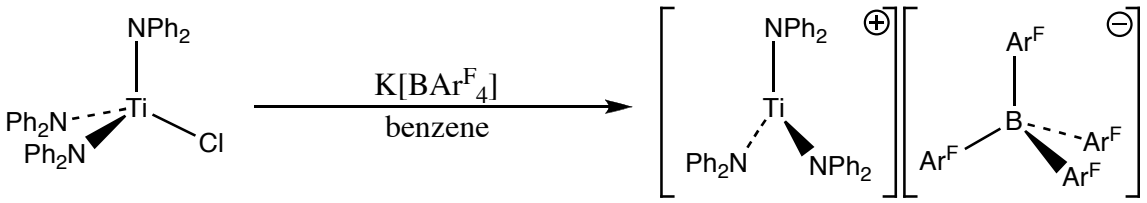

Figure 2.15: Synthesis of [(Ph$_2$N)$_3$Ti][BAr$^F_4$]

the next chapter. When exposed to π-donor ligands such as a phosphine, binding of one-two phosphines is possible, discussed in the next chapter.

The ^{1}H NMR spectrum of **(9)** displaces a few unusual peaks. There are no traditional aliphatic components in the complex, therefore no signals should be present in the traditional aliphatic region of the ^{1}H NMR. However, the ^{1}H spectrum displaces several peaks in the aliphatic region. The aromatic region consists five signals consisting of three triplets and two doublets. Unlike complexes **(2)** and **(4)**, the coupling constants do not aid in the assignment of the peaks. Also different from complexes **(2)** and **(4)** is the range of the aromatic region, the aromatic range of complex **(9)** is nearly twice of the other complexes. Integration of these peaks provides little information, as four of the signals overlap in the baseline.

The ^{13}C NMR of complex **(9)** displays six peaks in the aromatic region corresponding to the six carbons of the phenyl rings. All carbons of the phenyl rings are nonequivalent, meaning that free rotation of the ring around the N-Ph bind is hindered. This hindrance is most likely cause by the extremely electropositive nature of the titanium cation. The tricoordinate titanium moiety of **(9)** should be considered trigonal

planar with respect to the Ti-N bonds and each of the phenyl rings run perpendicular to the Ti-N_3 plane. There are therefore six unique carbons and five unique hydrogens (supported by both ^{1}H and ^{13}C NMR spectra). This could only be true if something large were bound in the 'pocket' created by the rings. Benzene has the potential to donate its π-electrons to the titanium center; this can be used to explain the extra aliphatic peaks. If benzene was to donate it's π-electrons to the titanium center, electron density is removed from the aromatic system and would shift the C_{ring}-H resonance downfield, possibly into the aliphatic region. This donation would have to be liable and would cause the resonances for those protons to be broad. If the benzene moiety were loosely bound, the carbon resonances would not show up in the ^{13}C NMR spectrum, but would show in the ^{1}H NMR spectrum.

Due to the lability of the benzene ring, substitution can occur if a better donor

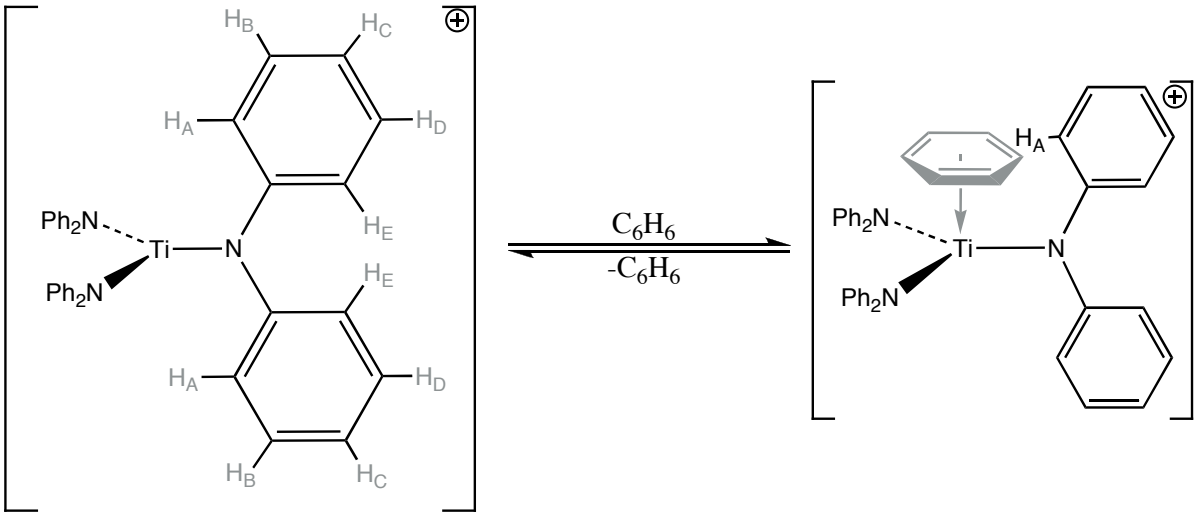

Figure 2.16: Nonequivalence of the hydrogens on the phenyl rings and benzene bound.

ligand is present. On equivalent of propylene was added to complex (**9)** in benzene and coordination occurs, this reaction is discussed further in chapter 4. After olefin coordination was successful, polymerization techniques were attempted and proved successful; this reaction is discussed further in chapter 3.

§ 2.2.9Synthesis and Reactivity of $[(Ph_2N)_3Ti(PMe_3)_2][BAr^F_4]$ (10)

Complex **(9)** is extremely sensitive to both water and oxygen. The titanium center is a tricoordinate 12 electron species and will bind any electron density available. With that in mind, it was reasoned that binding strong donor ligands, easier spectroscopic characterization would be possible. Two donor ligands examined as possibilities were THF and PMe_3. THF posed a large problem; powerful Lewis acids are capable of ring opening the ether and subsequently polymerizing it. When reacted with THF, the complex did indeed oligomerize the ether into a non-characterizable tar.

Binding the phosphine ligand does not pose the same problems. For the PMe_3 addition, a small amount of complex **(9**) was added to a J-Youngs valved NMR tube, d_6-benzene was vacuum distilled into the tube and exactly two equivalents of PMe_3 were condensed into the tube. The tube was thawed and allowed react for one hour before analysis.

The ^{13}C NMR spectrum of complex **(10)** displays 5 peaks, as expected. Four signals appear in the aromatic region, 150.3, 129.7, 125.89 and 123.72, and a singlet resonance at 67.4 ppm, which corresponds to the methyls on the phosphine. The ^{13}C resonance for free trimethylphosphine in d_6-benzene is found at 13.4 ppm. This 54 ppm downfield shift is characteristic of a bound phosphine.[115]

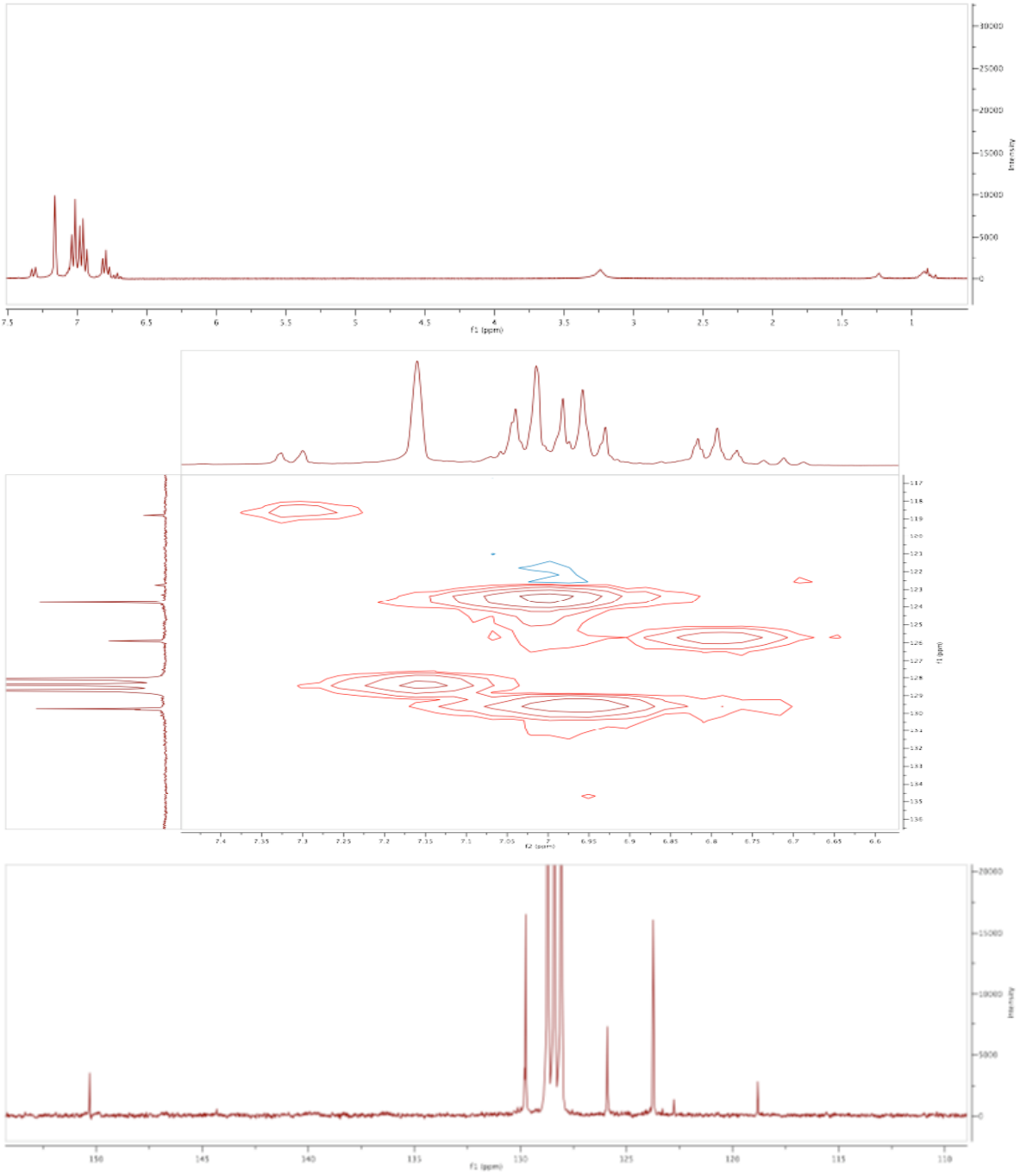

Figure 2.17: (top) ^{1}H NMR of (9), (middle) gHSQC of (9) and ^{13}C NMR of (9)

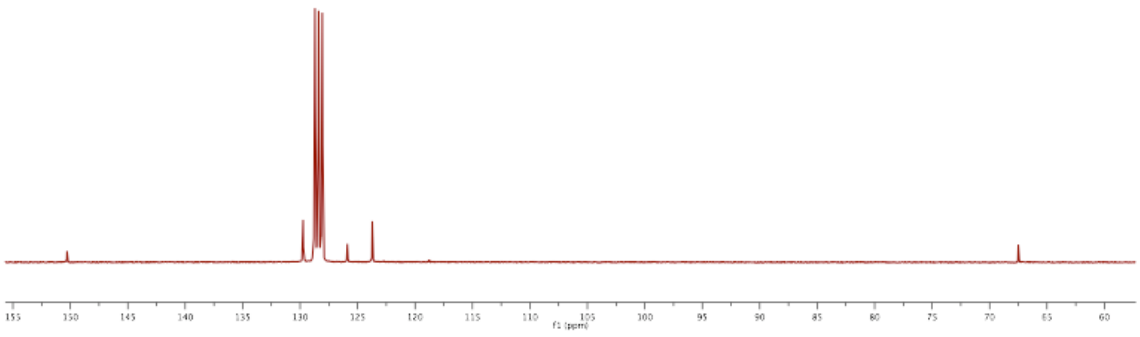

Figure 2.18: $[(Ph_2N)_3Ti(PMe_3)_2][BAr^F{}_4]$ in d_6-benzene

If exactly two equivalents of phosphine were added the cation, the ^{1}H NMR is difficult to understand, very similar to complex **(9)**. The ^{1}H NMR spectrum of complex **(10)** is the same as spectrum of complex (**10)**, but **(10)** contains two additional signals, a singlet at 3.35 ppm and a singlet at 0.8 ppm. The resonance at 0.8 ppm is assigned to free PMe_3 and the other new resonance is assigned to the bound phosphine. The integration of the phospines is 1.3: 0.7, bound: free. It is apparent that on the ^{1}H NMR time scale, the phosphine is exchanging between being bound and free. That is to say, one phosphine is bound and the other is equilibrium being bound and unbound. On the ^{13}C NMR time scale, this averages out to give only one resonance for the phosphine.

If an excess of phosphine is added to the NMR tube, approximately 5 equivalents extra, the ^{1}H NMR simplifies. With excess phosphine the only signals upfield of the aromatic region are the bond and free phosphine with integrations equal to 2:5, bound:

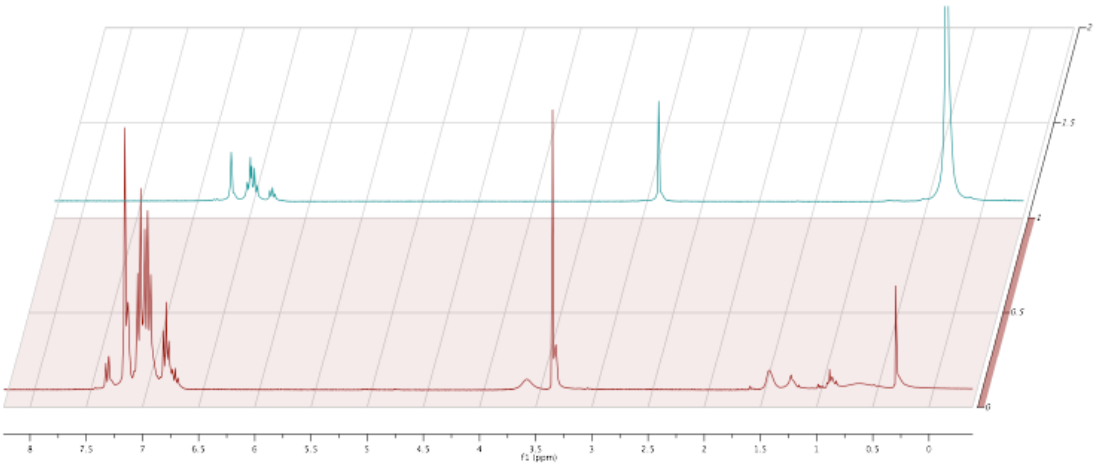

Figure 2.19: Comparison of [(Ph$_2$N)$_3$Ti(PMe$_3$)$_2$][BAr$^F{}_4$] spectra in d$_6$*-benzene (front) exactly 2 equivalents of PMe$_3$ (back) same sample with 5 more equivalents of PMe$_3$*

free. The ^{13}C NMR spectrum shows only one new peak, free trimethylphosphine at 13.4 ppm. The addition of excess phosphine shift the equilibrium to bind two PMe_3 moieties to the titanium cation.

The ^{31}P NMR for complex **(9)** with 2 equivalents of trimethylphosphine shows one signal, at -18.6 ppm (referenced to D_3PO_4). The addition of excess phosphine produces one additional peak at -60.9 ppm corresponding to free trimethylphosphine.

§ 2.3 Conclusions

(Diphenylamido)titanium complexes have demonstrated a variety of reactivities and have proven to be potential olefin polymerization catalysts. Complex **(2)** serves as the starting material for complexes **(3) - (10).** Complex **(4)** is a rare example of a *tris*(amido) titanium methyl. It has been well characterized and the associated reactivities have been studied thoroughly. The abstraction of the methyl moiety from

complex **(4)** demonstrates the ability of the amido ligands on the $[(Ar_2N)_3\text{-}Ti]$ moiety to stabilize the developing cation character. The phosphinomethanide complex, **(6)**, however does not show the same reactivity, alluding to the fact that complex **(4)** is coordinatively unsaturated while complex **(6)** is coordinatively saturated. Complexes **(2)**, **(4)**, **(5)**, and **(7)** possess the necessary requirements to be a possible olefin polymerization catalyst. Those requirements are: 1) coordinatively unsaturated, 2) steric bulk for stabilization for chain grown and 3) highly Lewis acid metal center. Three of these four complexes also possess the necessary M-alkyl bond necessary for olefin insertion and chain grown. Complex **(7)** does not have the final requirement, but does show the ability to bind simple π-donor ligands and even olefins, much like Lewis acids used for alkene transformation like hydroboration or oxymercuration reactions.

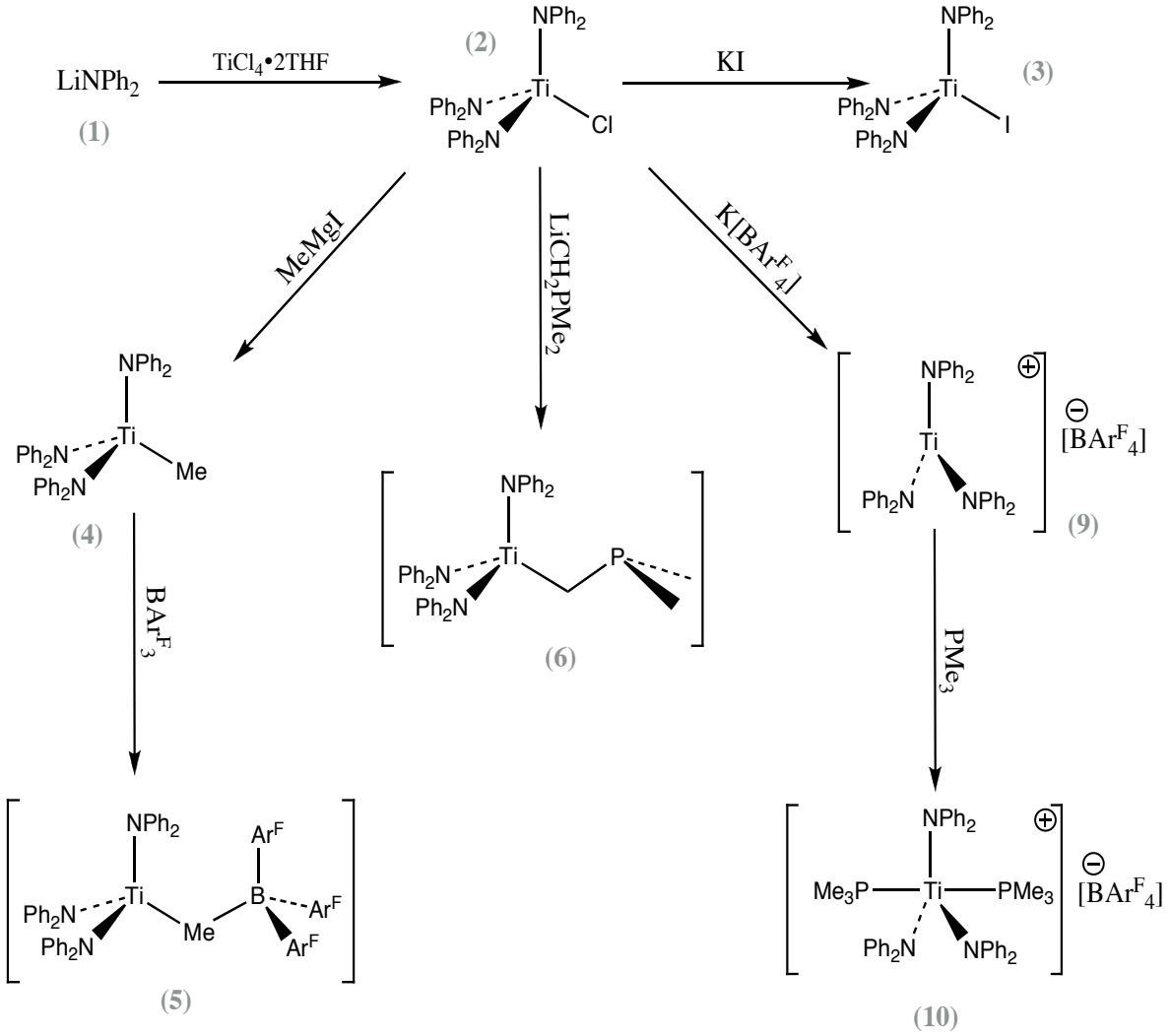

Figure 2.20: Full synthetic scheme for complexes (1)-(6), (9) and (10).

§ CHAPTER 3 Polymerization studies of *tris(*diphenylamido)titanium (IV) catalysts.

The work presented in this chapter is the subject of a US patent, Serial No. 60/919,964. The full details of the patent are given in Appendix II.

§ 3.1 Introduction

This chapter presents the experimental evaluation of systems based on the $[(Ph_2N)_3Ti]$ moiety as propylene polymerization catalysts. These systems are, at first sight, related to post-metallocene Ziegler-Natta catalysts, although the cationic *tetrakis* (perfluorotetraphenyl)borate system, which is highly active, must proceed *via* a novel mechanism. Mechanistic discussions are reserved until chapter 4.

§ 3.2 General polymerization procedures

All polymerization studies were conducted at sub-ambient pressures and temperatures in order to characterize rates of reaction. Most industrial catalysis setups utilize pressures greater than atmospheric, from 5 atm to 100 atm, and temperatures from 0 ºC to nearly 150 ºC in order to increase those rates.[99, 100] The concentration of catalyst used in all cases was extremely low ($1.5 \bullet 10^{-5}$ mol Ti) so that detection of deactivation was possible.

A volume-calibrated high-vacuum line (Figure 3.1), outfitted with a MKS Baratron Pressure Transducer (model number 750B13TGA2GC) was used in order to monitor the pressure of a known volume of gas added to the catalyst. Solid catalyst and activator were added to an ampoule fitted with a high-vacuum adaptor (approximately

150 mL volume) in the dry box. The ampoule was attached to the line and ~25 mL of toluene (standing over K_3Na) was vacuum transferred into the polymerization flask. Dry monomer was expanded from the source tank into the volume of line, approximately 940 mL. The polymerization vessel was cooled to 0.0 ºC in an ice bath, and the vessel was then opened to the monomer feed. Time recording was begun with the opening of the vessel. The baratron was monitored every 30 seconds for the rate of monomer consumption. Polymerization reactions were complete after 20 minutes.

Upon completion of the polymerizations, a 1:1 methanol: conc. HCl mixture was added to the vessel to neutralize any residual active catalyst. All solvent was removed under reduced pressure, yielding the polymer. In the case of dry polymer, the product was slurried in methanol:HCl and filtered to remove any catalyst byproducts. Liquid products were washed with methanol:HCl, filtered and all excess solvent was removed under reduced pressure. Characterization of the polymers produced was made by ^1H NMR. Molecular weight analysis were carried out by Tom Malgram of the Polymer Characterization Lab at the University of Tennessee *via* Gel Permeation

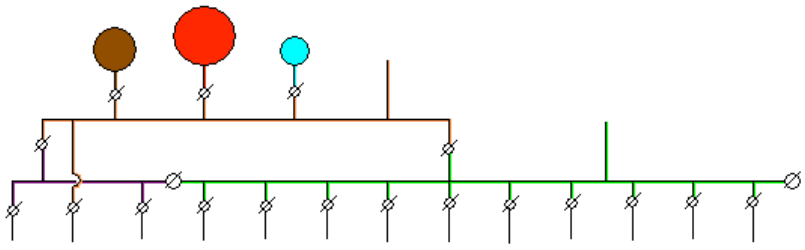

Figure 3.1: Schematic of the high vacuum line used for polymerization reactions

Chromatography, on a PolymerLabs GPC 120 with three light scattering detectors: PD2040, PD2000DLS (PD = Precision Detector) and a Viscotek 220. As a secondary method for characterization the GPC 120 is also outfitted with a PolymerLabs refractometer.

§ 3.3 Polymerizations using $(Ph_2N)_3TiCl$/ MAO

Tris(diphenylamido)titanium(IV) chloride has been reported to act as an olefin polymerization catalyst when heterogenized on solid magnesium dihalide substrates. Initial attempts at showing homogenous reactivity therefore relied on reacting solutions of $(Ph_2N)_3TiCl$ with the standard industrial activator, MAO.

$(Ph_2N)_3TiCl$ has many of the properties that an olefin polymerization catalyst should possess: The coordination sphere around the metal center must have vacancies for addition and chain growth, and the metal center must be Lewis acidic enough to drive the polymerization reaction. Complex **(2)** also contains a chloride ligand, which can be reacted to form a cationic 12-electron titanium center, at first sight analogous to the metallocene catalysts. Traditional activation *via* MAO yields an extremely active yet often uncharacterizable catalyst.

In a representative polymerization reaction, *tris*(diphenylamido)titanium(IV) chloride (8.82 mg, $1.5 \bullet 10^{-5}$ mol, 1 eq) was added to a heavy walled ampoule, and dry MAO (21.8 mg, $3.75 \bullet 10^{-4}$ mol, 25 eq) was added on top of the catalyst in the dry box. The ampoule was evacuated ($\sim 10^{-6}$ mbar), and 21.2 g (24.5 mL) of toluene was vacuum distilled into the ampoule, 45.4 mmol of propylene, without purification, was expanded

into 940 mL at a pressure of 883.3 Torr. The frozen solution was allowed to thaw and warm to 0.0 ºC. The color of the activated titanium catalyst in solution is a translucent blood-red, and on deactivation the color changes to a light green. The gas was expanded into the ampoule, and the temperature was kept at 0.0 ºC during the experiment. On opening the ampoule to the monomer the pressure drops roughly 100 Torr as the monomer expands into the ampoule and begins to polymerize. The rate settles to a constant decrease of 0.667 (Torr/sec) for 6 minutes as the monomer is consumed. After about 7 minutes the rate diminishes as the catalyst deactivates and the solution turns green.

Table 3.1: Propylene (wet) polymerization data from the reaction with $(Ph_2N)_3TiCl$ and MAO.

$(Ph_2N)_3TiCl$/ MAO with Propylene			
Time (/sec)	**Pressure (/Torr)**	**Time (/sec)**	**Pressure (/Torr)**
0	794.6	630	486.3
30	699.4	660	485.2
60	676.2	690	484.9
90	656.6	720	484.9
120	629.7	750	484.6
150	596.7	780	484.6
180	565.1	810	484.6
210	543.7	840	484.7
240	527.1	870	484.8
270	518.4	900	485
300	512.3	930	485
330	507.1	960	485
360	502.4	990	485
390	498.5	1020	485
420	495.6	1050	485
450	493.6	1080	485
480	492.4	1110	485
510	489.7	1140	485
540	488.4	1170	485
570	487.4	1200	485
600	487.5		

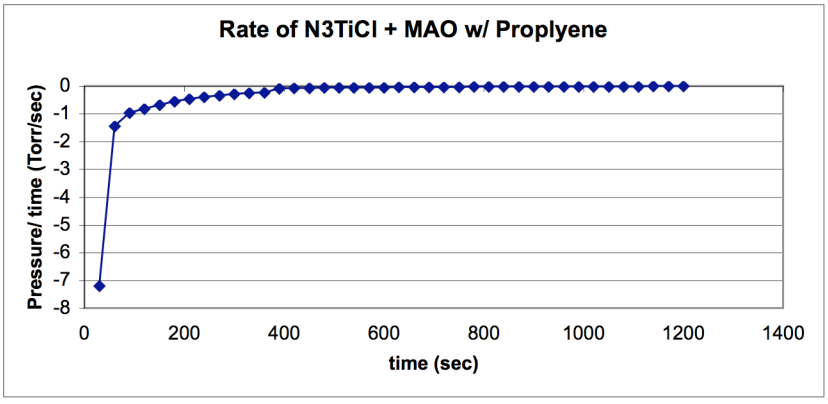

Figure 3.2: Rate of propylene (wet) polymerization with $(Ph_2N)_3TiCl$ and MAO.

Early deactivation of the catalyst prompted several attempts to lengthen the catalyst's activity. The propylene stock was vacuum distilled into an ampoule with potassium mirror condensed on the interior wall, and allowed to stand over the mirror for twenty minutes. After twenty minutes, the gas was expanded back into the line and the standard polymerization continued. Predrying the monomer gas lengthened the catalyst's active time by almost ten minutes.

The addition of excess MAO was also attempted. If the amount of MAO was increased to 35 equivalents, the activity time roughly doubled. This method is preferred over the condensation into the potassium-mirrored ampoule due to ease of preparation. Unfortunately the use of excess MAO to dry the monomer stock is only useful for this system, as it is the only one that utilizes MAO as an activator. Both the $[(Ph_2N)_3Ti{\bullet\bullet\bullet}Me{\bullet\bullet\bullet}BAr^F{}_3]$ the $[(Ph_2N)_3Ti][BAr^F{}_4]$ systems used monomer dried over a potassium mirror.

A second polymerization reaction was prepared and run just as before, except the amount of MAO used was increased to 35 equivalents. The addition of extra MAO increased the activity time of the catalyst to the full twenty minutes of monitored time. The rate begins at the same rate as the first trial with wet propylene, but does not diminish nearly as quickly. For the final 2.5 minutes of the reaction, the rate diminished to 0.01 Torr/sec.

After work-up of the polymerization reaction approximately 70 mg of polypropylene was recovered. The ^1H NMR (d_8-toluene) showed three unresolved multiplets at 4.93, 1.31 and 0.87 ppm (assumed to be CH, CH_2 and CH_3 respectively).

Table 3.2: Propylene (dry) polymerization data from reaction with $(Ph_2N)_3TiCl$ and MAO

$(Ph_2N)_3TiCl$/ MAO with Propylene			
Time (/sec)	**Pressure (/Torr)**	**Time (/sec)**	**Pressure (/Torr)**
0	885.3	630	459.7
30	669.1	660	458.6
60	625.8	690	457.7
90	596.7	720	456.8
120	571.9	750	455.8
150	551.7	780	455.1
180	535	810	454.3
210	521.3	840	453.7
240	509.8	870	453.1
270	499.4	900	452.7
300	490.6	930	452.2
330	483.1	960	451.9
360	476.4	990	451.4
390	473.6	1020	451.1
420	471.2	1050	450.8
450	469	1080	450.5
480	467.2	1110	450.2
510	465.5	1140	450
540	463.9	1170	449.8
570	462.4	1200	449.7
600	461		

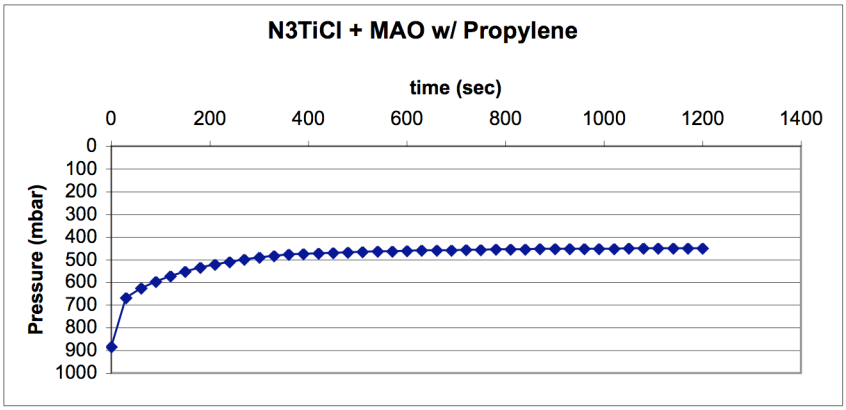

Figure 3.3: Rate of propylene (dry) polymerization with $(Ph_2N)_3TiCl$ and MAO

Solubility of the polymer product was extremely low in benzene, CH_2Cl_2, bromobenzene and 1-chloronaphthalene, all of which are typically used in the analysis of polypropylene. The low solubility of the polymer limits the ability that NMR could provide for analysis, such as tacticity of the product; visibility of any signals in ^{13}C NMR was minimal.

Molecular weight determinations were conducted in 1,3,5-trichlorobenzene at 218 ºC. The average molecular weight of the polypropylene produced was determined to be $8.143 \bullet 10^5$ Daltons, with a $M_W/M_N = 3.986$. Propylene analysis standards have average molecular weights near $6.515 \bullet 10^5$ Daltons, with a $M_W/M_N = 2.775$. Addition of α-olefins results in approximately 26.6 Kg of polymer/ mol of catalyst. Industrial zirconocene systems produce approximately 100 Kg of polymer/ mol of catalyst, but at high temperature and much higher pressures.

§ 3.4 Polymerizations using $[(Ph_2N)_3Ti \bullet\bullet\bullet Me \bullet\bullet\bullet BAr^F_3]$

After demonstrating the activity of the $(Ph_2N)_3TiCl$ /MAO system, Marks' activation method using BAr^F_3 was investigated, using $(Ph_2N)_3TiMe$ as the Ti source, in attempt to form a single-site, highly active polymerization system. As the Ti-Me bond is presumably the first product in the activation with MAO,[45] and abstraction of the methyl with the Lewis acidic MAO residue produces the active catalyst (§ 1.4.2), the activation process should be able to be recreated by abstracting the methyl group from the complex **(4)**. As described in § 2.2.5, complex **(5)** is synthesised in quantitative yields and can be isolated. *In situ* preparation of the complex is also suitable as there are no side products in the reaction between $(Ph_2N)_3TiMe$ and BAr^F_3. Activation with BAr^F_3 clearly only

requires only one molar equivalent, unlike activation with MAO, which requires an excess of 15 equivalents or greater for the activation to be maximized.

Unfortunately, since excess MAO also dries the system and reactivates any deactivated catalyst, without the excess activator the rate diminishes extremely quickly as the catalyst is 'chemically unprotected' from adventitious water and oxygen. In order to keep the catalyst active for extended times, the monomer must first be dried. For this reason the monomer was condensed onto a potassium mirror and then expanded back in to the vacuum line before polymerization, as described in § 3.2.

In a representative reaction, *tris*(diphenylamido)titanium (IV) methyl (8.51 mg, $1.5 \bullet 10^{-5}$ mol, 1 eq) was added to a heavy walled ampoule, and *tris*(pentafluorophenyl)boron (7.68 mg, $1.5 \bullet 10^{-5}$ mol, 1 eq) was added on top of the catalyst in the dry box. The ampoule was evacuated ($\sim 10^{-6}$ mbar) and 23.7 g (27.3 mL) of toluene was vacuum distilled into the ampoule, 43.2 mmol of propylene, was expanded from the potassium mirror, into 940 mL at a pressure of 905.7 Torr. The frozen solution was allowed to thaw and warm to 0.0 ºC. The color of the activated titanium catalyst in solution is a deep blood-red, and upon deactivation the color changes to a light green and eventually all color diminishes. The gas was expanded into the ampoule, and the temperature was kept at 0.0 ºC during the experiment. Upon opening the ampoule to the monomer the pressure drops roughly 100 Torr as the monomer expands into the ampoule and begins to polymerize.

Table 3.3: Propylene (dry) polymerization data from the reaction with $(Ph_2N)_3TiMe$ and $BAr^F{}_3$

$(Ph_2N)_3TiMe/ BAr^F{}_3$ with Propylene			
Time (/sec)	**Pressure (/Torr)**	**Time (/sec)**	**Pressure (/Torr)**
0	905.7	600	391.8
30	763.7	630	391.8
60	621.7	660	391.7
90	539.8	690	391.4
120	490.3	720	391.4
150	458.4	750	391.3
180	438.9	780	391.3
210	424.7	810	391.4
240	414.2	840	391.4
270	407.1	870	391.3
300	402.4	900	391
330	398.8	930	391
360	396.6	960	390.8
390	395	990	390.5
420	393.9	1020	390.5
450	393.2	1050	390.5
480	392.6	1080	390.5
510	392.1	1110	390.7
540	391.9	1140	390.8
570	391.9	1170	391

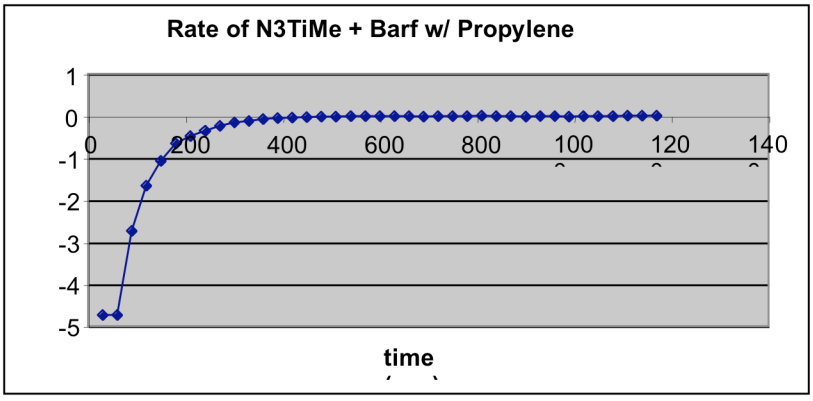

Figure 3.4: Rate of propylene (dry) polymerization with $(Ph_2N)_3TiMe$ and $BAr^F{}_3$

The initial minute of polymerization is very similar to $(Ph_2N)_3TiCl$/ MAO system, but unlike the MAO system, the BAr^F_3 system stays extremely active for five minutes. The rate decreases rapidly after eleven minutes and becomes completely inactive at eighteen minutes. The color of the solution depends greatly on the concentration of water in the flask. As the polymerization continues, the monomer, although dried, still contains trace amounts of water, and slowly deactivates the catalyst. The polymerization can be monitored *via* the change in color of the solution. Before monomer addition, the solution is deep blood-red; after three minutes there is a noticeable lightening in the color. After five minutes the color has changed to a translucent orange, and after eleven minutes the solution has changed completely to a light green. Between eleven and eighteen minutes, the rate is nearly zero, but slight activity is still identified.

In both the $(Ph_2N)_3TiCl$/ MAO and $(Ph_2N)_3TiMe$/ BAr^F_3 systems the active species is assumed to be a cationic titanium center with a methyl-Lewis acid adduct as the counter anion. It is assumed that in both of these systems there is a moderately strong interaction between the anion and cation, and the methyl moiety is still partially bound to the titanium center. The weak Ti-Me bond increases the Lewis acidity of the titanium center, and provides the M-R bound required for insertion. The methyl signal of complex **(9)** in the ^1H NMR appears at 0.45 ppm compared to 1.189 ppm and 0.759 ppm for $[(Ph_2N)_3\bullet\bullet\bullet Me\bullet\bullet\bullet BAr^F_3]$ and $LiMeBAr^F_3$ respectively. The adduct resonance at 1.189 ppm signifies the delocalization of charge between the B-Me-Ti, species (b) in Figure 3.5. If the methyl were fully bonded to the boron moiety, the methyl should exhibit the upfield resonance of the species $[MeBAr^F_3]^-$ (c).

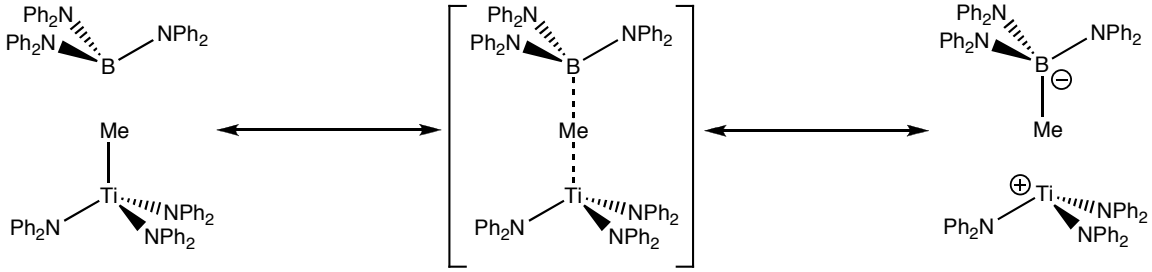

	Complex	^{1}H NMR chemical shift for methyl
(a)	$(Ph_2N)_3TiMe$	0.45 ppm
(b)	$[(Ph_2N)_3$•••Me•••$BAr^F_3]$	1.189 ppm
(c)	$LiMeBAr^F_3$	0.759 ppm

Figure 3.5: Possible equilibrium between Ti-Me-B species, and ^{1}H NMR chemical shifts for those methyl species

There is a direct competition for the methyl group, or growing alkyl chain, between the two Lewis Acids. It is this competition that keeps the active site continuously ready for the next monomer coordination and insertion. For the Cp_2ZrMe_2/ BAr^F_3 system, Marks *et al* states the most probable mechanism involves the Zr-Me bond that is not associated with the BAr^F_3. The abstracted methyl has two functions: to increase Lewis Acidity of the Zr center and to, open a vacancy in the coordination sphere. The non-abstracted methyl serves as the insertion point for incoming olefin and as the start of the growing polymer chain. In the $[(Ph_2N)_3{\bullet\bullet\bullet}Me{\bullet\bullet\bullet}BAr^F_3]$ system, there is only one methyl to be abstracted which serves as the M-R for insertion.

§ 3.5 Polymerizations using $[(Ph_2N)_3Ti][BAr^F_4]$

Complex **(5)** demonstrates interesting results as an olefin polymerization catalyst. Its activity suggests that an alkyl-free cationic titanium center is partially if not entirely responsible for the polymerization. With that in mind, the alkyl-free $[(Ph_2N)_3Ti][BAr^F_4]$ was tested as an olefin polymerization catalyst. If the fully cationic titanium catalyst is active as a catalyst, the traditional Ziegler-Natta mechanism cannot be used, and a new mechanism must be responsible.

In a representative polymerization reaction *tris*(diphenylamido)titanium (IV) chloride (8.81 mg, $1.5{\bullet}10^{-5}$ mol, 1 eq) was added to a heavy walled ampoule and potassium *tetrakis*(pentafluorophenyl)borate (10.77 mg, $1.5{\bullet}10^{-5}$ mol, 1 eq) was added on top of the catalyst in the dry box. The ampoule was evacuated (~10^{-6} mbar) and 20.3 g (23.4 mL) of toluene was vacuum distilled into the ampoule, 41.3 mmol of propylene,

was expanded from the potassium mirror into 940 mL at a pressure of 900.2 Torr. The frozen toluene was allowed to thaw and warmed to 0.0 ºC. The color of the activated titanium catalyst in solution is a deep blood-red (same color as complex **(5)**), upon deactivation the color changes to a light green and eventually no color remains. The gas was expanded into the ampoule and temperature was kept at 0.0 ºC during the experiment. Upon opening the ampoule to the monomer the pressure drops roughly 100 Torr as the monomer expands into the ampoule and begins to polymerize.

The reaction begins similarily as the other catalysts, with an initial large drop in pressure that leads a constant decrease in rate until the catalyst is completely deactivated. This catalyst is the least active of three, with complete deactivation by seventeen minutes. One remarkable feature of this catalyst is that while the rate decrease rapidly, there is always a short dip in the rate followed by a slight increase in rate for nearly one minute. This anomaly occurs around 200 seconds and can be seen in Figure3.6. Similarly to the $(Ph_2N)_3TiMe/\ BAr^F_3$ system, the color is indicative of reactivity. The $[BAr^F_4]^-$ catalyst begins as a deep blood-red solution, and after 5 minutes the color has faded slightly to a translucent red. By nine minutes the solution is orange and by twelve minutes the solution has changed completely to the 'deactivated green.'

Complex **(9)** is unique in that it polymerizes α-olefins although it contains no M-R bond. Obviously the $[(Ph_2N)_3Ti]^+$ is extremely Lewis acidic, and binding of any π-type ligands is possible, even benzene. It is possible for coordination of a single olefin to the titanium center, but insertion is impossible.

Table 3.4: Polymerization of propylene with [$(Ph_2N)_3Ti$][$BAr^F{}_4$]

[$(Ph_2N)_3Ti$][$BAr^F{}_4$] with Propylene			
Time (/sec)	**Pressure (/Torr)**	**Time (/sec)**	**Pressure (/Torr)**
0	900.4	630	548
30	753.3	660	544.6
60	715	690	542.1
90	682.3	720	540
120	658.7	750	539.7
150	640.2	780	538.9
180	628.2	810	538.1
210	619.1	840	537.8
240	603.8	870	537.6
270	596.8	900	537.6
300	589.8	930	537.6
330	584	960	537.7
360	578.4	990	537.8
390	574	1020	538.1
420	570.8	1050	538.1
450	565.4	1080	538
480	561.4	1110	538
510	557.1	1140	538
540	554.9	1170	538
570	551.6	1200	538
600	548	1230	538

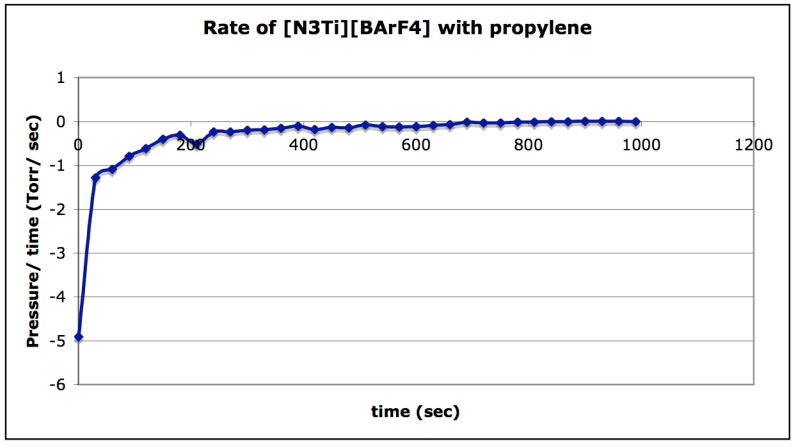

Figure 3.6: Polymerization of propylene with [$(Ph_2N)_3Ti$][$BAr^F{}_4$]

§ 3.6 Conclusions

Direct comparison of the three catalysts is difficult. While all three catalysts do produce polypropylene, they polymerize at different rates, and more than one mechanism is present. The $[(Ph_2N)_3Ti][BAr^F_4]$ catalyst shows with the highest activity but quickly deactivates. The $(Ph_2N)_3TiMe/\ BAr^F_3$ system is the most robust of the systems and stays active the longest. The traditional $(Ph_2N)_3TiCl/$ MAO catalyst, while not as active as the other two, is the easiest to use and keep active. Addition of excess MAO keeps the catalyst active longer and does not require the additional drying step. Also, *in situ* generation of the MAO system with $AlMe_3$ does produce an active catalyst. Using $AlMe_3$ does not produce the same rate as with MAO is used as the activator, implying the that the amount of water is not high enough to turn all of the $AlMe_3$ into MAO *in situ*, but rather a fraction, which decreases the rate. The small amount of water present in the monomer can be dried with excess MAO or with the potassium mirror.

The catalysts also polymerized other olefins. Ethylene was successfully polymerized by all three catalysts, although the rates were all lower than their propylene analogues. Propylene oxide was also polymerized by $[(Ph_2N)_3Ti][BAr^F_4]$ to an extremely viscous polyether with an extremely low vapor pressure. Attempts to polymerize other non-α-olefins were also attempted. Attempts with norbornylene and $[(Ph_2N)_3Ti][BAr^F_4]$ failed to produce polymer.

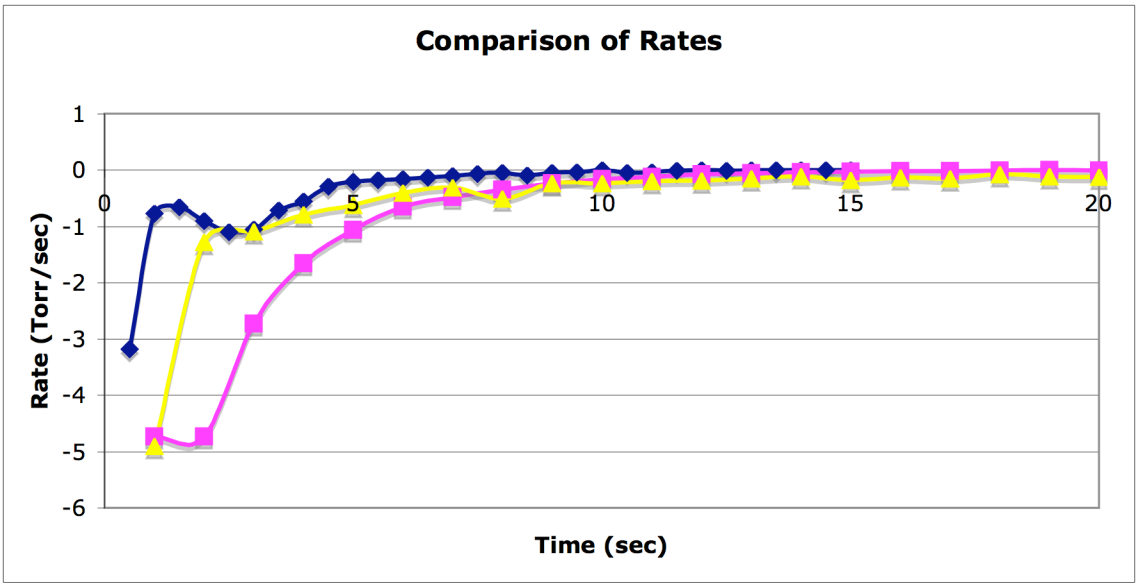

Figure 3.7: Comparison of reaction rates for the three catalysts.

blue diamonds: $(Ph_2N)_3TiCl$/ MAO, purple squares: $(Ph_2N)_3TiMe$/ BAr^F_3, yellow triangles: $[(Ph_2N)_3Ti][BAr^F_4]$. All three were treated usingthe same conditions, dried over a potassium mirror and studied at the same temperatures.

§ CHAPTER 4 Mechanistic aspects for polymerizations

§ 4.1 Introduction

The two currently accepted Ziegler-Natta mechanisms both require a transition metal alkyl bond, M-R, into which insertion can take place. The Cossee-Arlman mechanism uses a vacancy in the coordination sphere adjacent to a M-R bond for the insertion step in Ziegler-Natta polymerization. The modified Green-Rooney mechanism not only exploits the vacancy and M-R bond but also employs the hydrogens on the R residue to stabilize and regulate the stereochemistry.

The original α-$TiCl_3$-based catalysts are unable to polymerize olefins without activation. Activation in the context of Zielger-Natta catalysis involves both alkylation and abstraction. As discussed in §1.4.1, reaction with alkyl aluminum reagents or MAO alkylates and then abstracts the alkyl group to form the catalyst; the Cp_2ZrMe_2/ $BAr^F{}_3$ system requires similar abstraction steps to transform the inactive metallocene into a cationic catalyst complex.

Reaction of $(Ph_2N)_3TiCl$ with MAO and $(Ph_2N)_3TiMe$ with $BAr^F{}_3$ mimics these activation steps, by analogy with α-$TiCl_3$ and Cp_2ZrMe_2 systems. With respect to the activation processes, these reactions mirror conventional Ziegler-Natta protocols. However, the species generated by these reactions should be inactive with respect to Ziegler-Natta catalysis by conventional mechanisms, due to the absence of the M-R bond for insertion.

$[(Ph_2N)_3Ti][BAr^F{}_4]$ does not fit any conventional mechanistic model for Ziegler-Natta polymerization for the same reason, and moreover, there is no possible intermediacy of a Me group bound to any moiety in the system. However it does polymerize α-olefins with rates that are comparable to or exceed those of the traditional Ziegler-Natta systems. With no M-R bond for insertion to initiate polymerization, another mechanism must be active. This chapter outlines experiments designed to elucidate the new mechanism that must be responsible for the observed reactivity.

§ 4.2 General considerations

The most reasonable assumption for the first step is that an olefin binds to the cationic titanium center. Based on the fact that benzene was identified as being bound to the 'pocket' created by phenyl rings on the $[(Ph_2N)_3]$ cation, as detailed in § 2.2.8, this is a reasonable assumption.

$[(Ph_2N)_3Ti]^+$ is a 12 electron species and, in D_{3h} symmetry, the three L_π functions on the N atoms span A_2" + E". *d*-derived functions on the Ti center that can interact with the *E*" set, *via* linear combinations of d_{xz} and d_{yz}, but the only available function that can interact with the A_2" L_π function is the $4p_z$ on Ti. Overlap between this orbital and the A_2" L_π function on N will be reduced due to the energetic difference between the $4p_z$(Ti) and the $2p_z$(N). It is therefore likely that $[(Ph_2N)_3Ti]^+$ is less stabilized as a L_3X_4 system than the formal electron count or the MLX assessment suggests.

The approaching olefin would have to be bound *via* the olefin's π-bond to the titanium $d(z^2)$ orbital.

Lewis acid addition to an alkene is an extremely common scheme in organic chemistry. Examples of double bond functionalization that take place through coordination *via* a Lewis acid includes hydration, oxymercuration, halogenation and hydroboration, to name but a few. The regiochemistry is dictated by the stability of the developing carbocation and therefore the regiochemistry of addition follows the stability trend for carbocations. As most reagents that add to double bonds are less electropositive than hydrogen, Markovnikov's rule for addition is followed, which is a masked statement of the trends for carbocationic stability. Given that boron is more electropositive than either hydrogen or carbon, hydroboration, usually thought of as 'anti-Markovnikov' addition is actually Markovnikov, when the electronegativity of the electrophile is included in the formulation of the rule.

Given that a three coordinate titanium cation must be a very powerful Lewis acid and is only available through the use of $[BAr^F_4]$ as reactions with tetraphenylborate fail to yield tractable material, the analogy between reactions of more conventional electrophiles with alkenes is a useful starting point for the new mechanism.

As very rapid and efficient polymerization of propylene is observed with systems that either contain $[(Ph_2N)_3Ti]^+$ or species related to it, a series of experiments were performed to investigate the binding of alkenes to these types of cationic titanium centers.

§ 4.2.1 The interaction of $[(Ph_2N)_3Ti]^+$ with one equivalent of propylene

As described in §2.2.8, formation of $[(Ph_2N)_3Ti][BAr^F_4]$ is performed by halide abstraction of Cl using $KBAr^F_4$ and is essentially quantitative, with no other Ti-

containing species being observed.

In situ formation of $[(Ph_2N)_3Ti][BAr^F{}_4]$ was performed in d_8-toluene in an identical manner to preparative scale reactions. After initial spectra were recorded, 1 molar equivalent of propylene was introduced using high vacuum manometry and a series of spectra were recorded in order to elucidate the nature of the species present.

Free propylene in toluene is characterized by a quartet of doublet of doublets at 5.72 ppm ($CH_2C\mathbf{H}Me$), doublets of doublets at 4.88 and 4.97 ppm ($C\mathbf{H_2}CHMe$) and a pseudo-triplet of doublets at 1.72 ppm ($CH_2CH\mathbf{Me}$). This spectrum is shown in figure 4.1. The spectrum of $[(Ph_2N)_3Ti][BAr^F{}_4]$ contains triplets at 6.712, 6.793 and 7.012 and doublet at 6.944, and 7.313 ppm.

In the presence of 1 molar equivalent of propylene, no polymerization occurs and new resonances are observed. Excluding changes in the aromatic ligand region, the new, broad and unresolved signals are observed at 3.63, 3.28, 1.11 and 0.88 ppm, in addition to the well understood peaks that correspond to free propylene. As observed from the ^1H NMR, there are two sets of propylene peaks, one free and one bound to the titanium center. Excluding the aromatic ligand resonances the ^{13}C NMR displays only free propylene with peaks at 136.2, 115.9 and 18.7 ppm.

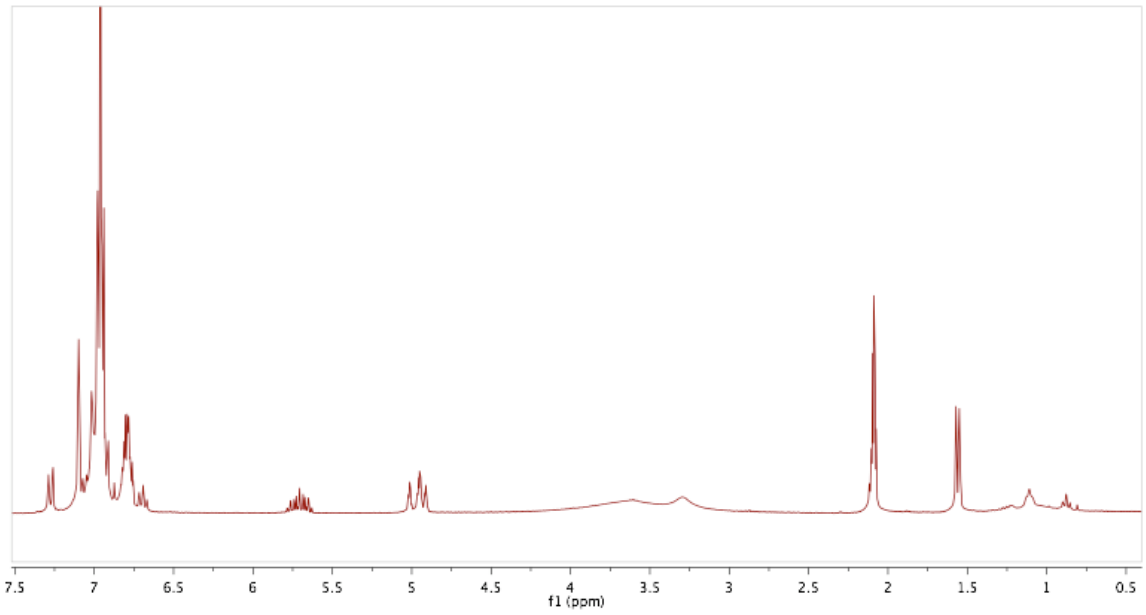

Figure 4.1: ^{1}H NMR of $[(Ph_2N)_3Ti][BAr^F{}_4]$ with 1 equivalent of propylene in d_8-toluene.

Given the broad nature of the room temperature ^{1}H spectrum and the absence of identifiable ^{13}C resonances, which is also observed in the preliminary ^{13}C spectrum for $(Ph_2N)_3TiMe$, a more detailed study using correlational techniques and variable temperature NMR spectroscopy was undertaken.

As seen in the gCOSY spectrum the resonances for the free and bound propylene do not correlate to one another, and assigning the peaks to the different species becomes clearer. The two broad peaks at 3.63 ($CH_2C\mathbf{H}Me$) and 3.28 ppm ($C\mathbf{H}_2CHMe$) correspond to the proton *gem* and *trans* to the methyl group on the bound propylene, and the more defined peaks at 1.11 ($CH_2CH\mathbf{Me}$) and 0.88 ($C\mathbf{H}_2CHMe$) correspond to the methyl and proton that is *cis* to it. Integration of the signals aids in assignment as the resonances are not baseline-resolved.

There is no correlation between the bound propylene and the aromatic rings. The

aromatic ligand region of the ^{1}H NMR is similar to complex **(9)**, but is less defined. The gCOSY spectrum is of no help for assignment of this region, due to the fact that the d_8-toluene used as the NMR solvent overlaps with most of the peaks.

The presence of through space-correlations was also examined *via* the NOESY pulse sequence; the NOESY spectrum matches the gCOSY spectra exactly, with no extra resonances being present. While the lack of cross-peaks in the NOESY does not definitely rule out through-space correlations, it signifies that any correlations that do exist are weak.

It is a reasonable assumption that the [N_3Ti] displays C_3 or *pseudo*- C_3 symmetry, which will necessarily force the *N*-phenyl rings to form a pocket, and the pocket thus created will display similar, related symmetry.

A possible model for the disposition of the propylene is shown in figure 4.2. When propylene is bound to the titanium center, the two *cis* hydrogens of the double bound will be sitting in the center of two of the rings. These two protons should be shielded by the ring currents of the phenyl rings, while the other proton and the methyl on the double bond should be far enough from the phenyl rings to not be shielded less. If the two protons are shielded sufficiently, they should also be locked into place *via* interaction with the π-electron in the phenyl rings. Even without the interactions between the *cis* protons and the phenyl rings, there is sufficient steric bulk created by the phenyl rings to restrict free rotation.

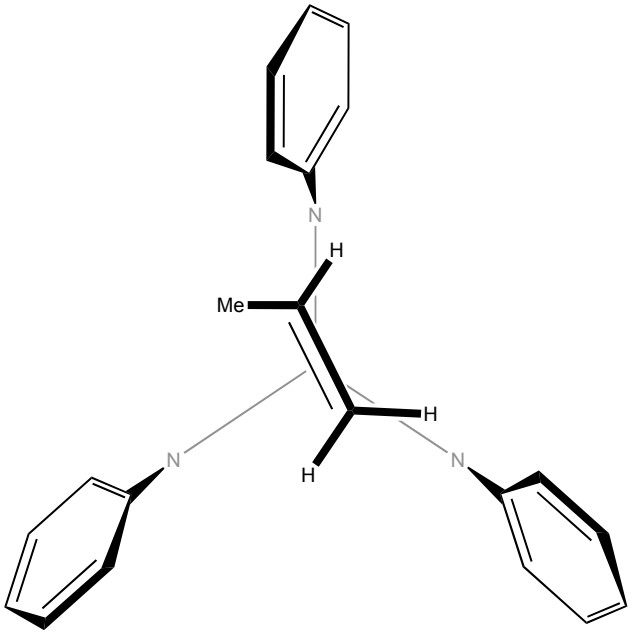

Figure 4.2: Propylene bound to the titanium center of [$(Ph_2N)_3Ti$][BAr^F_4]

Humphries *et al.* showed that when propylene is bound to [Nb{(η-$C_5H_4)_2CMe_2$}(N^tBu)][BAr^F_4], there is no coupling to the imido or Cp ligands.[116] They also noted that free rotation of propylene leads to extensive splitting (not seen in the spectra associated with [$(Ph_2N)_3Ti(\eta^2$-$CH_2CHCH_3)$][BAr^F_4]) in the aliphatic region. The bound propylene in the proton spectrum for Humphries' complex is shifted upfield from the free propylene resonances. The intense splitting of the free propylene is lost when bound to the niobium center, due to the fluxional behavior of the rotating propylene. The extensive splitting observed in Humphries' niobium complex does not exist in the [$(Ph_2N)_3Ti(\eta^2$-$CH_2CHCH_3)$][BAr^F_4] case, due the lack of free rotation around the titanium center.

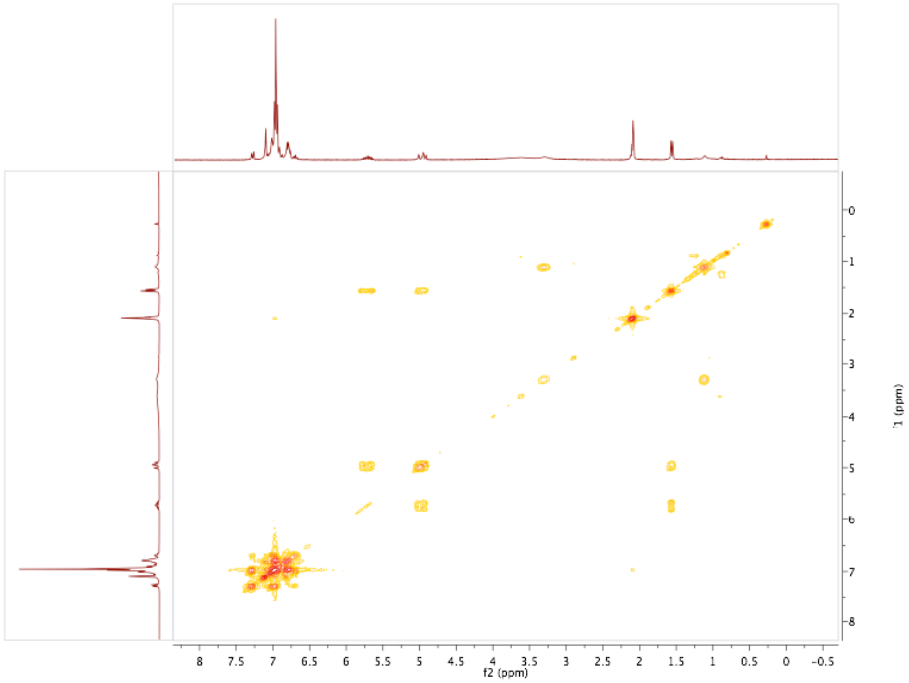

Figure 4.3: ^{1}H-^{1}H gCOSY of $[(Ph_2N)_3Ti][BAr^F{}_4]$ with 1 equivalent of propylene in d_8-toluene

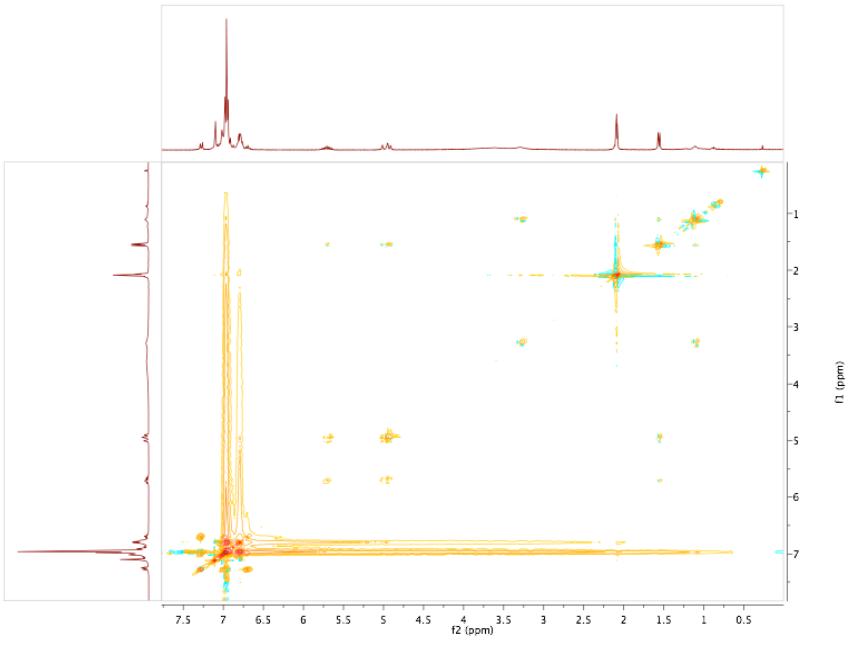

Figure 4.4: ^{1}H-^{1}H NOESY of $[(Ph_2N)_3Ti][BAr^F{}_4]$ with 1 equivalent of propylene in d_8-toluene

Due to the fluxional behavior of propylene, variable temperature ^{1}H NMR was employed to slow the motion in the pocket. When temperature is increased to 310 K the two broad resonances at 3.63 and 3.28 ppm spread slightly and become broader with increasing temperature. With decreasing temperature the broad resonances begin to converge. Near 275 K the two peaks coalesce into one broad peak; this new peak is much sharper than either of the two that converged to create it. Below 275 K, the peaks separate again and begin to show some splitting, although it remains unresolved. At the higher temperatures the two broad peaks represent the average state of the protons. At lower temperatures the peaks are still separate but much sharper, representing the approach to the slow exchange limit.

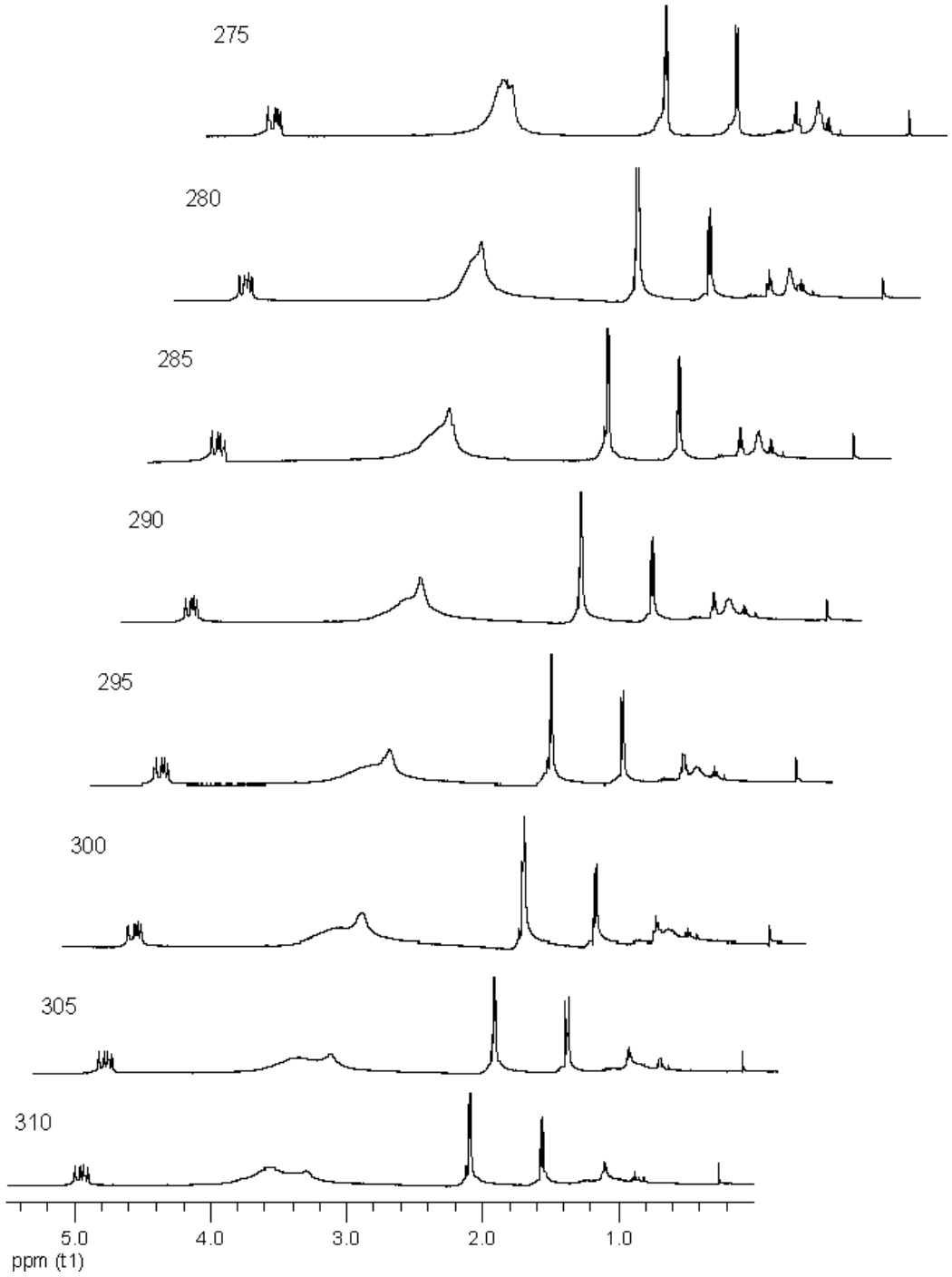

Figure 4.5: Variable Temperature 1H NMR spectra of [$(Ph_2N)_3Ti$][$BAr^F{}_4$] with 1 equivalent of propylene in d_8-toluene, upper range.

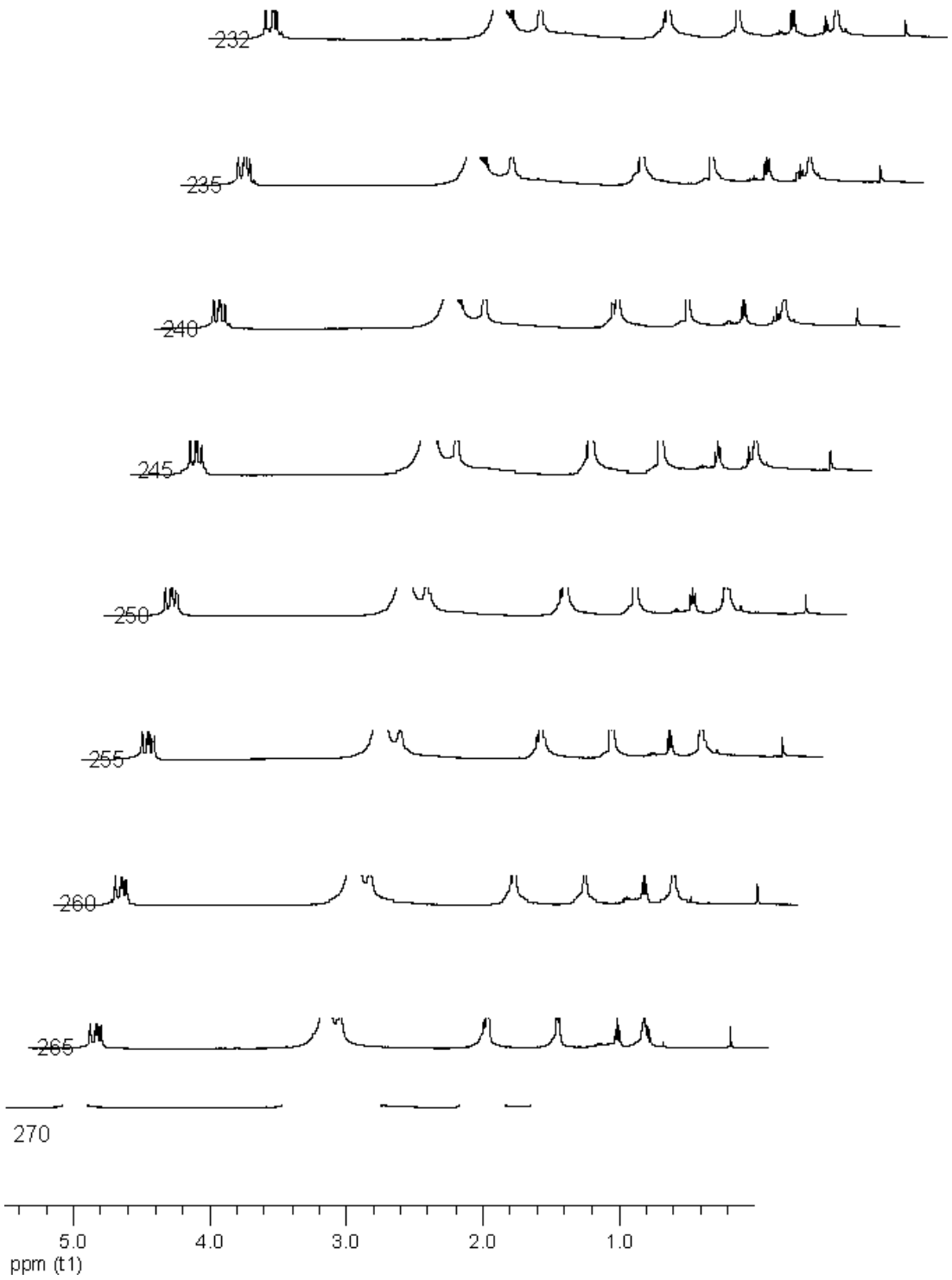

Figure 4.6: Variable Temperature 1H NMR spectra of [$(Ph_2N)_3Ti$][BAr^F_4] with 1 equivalent of propylene in d_8-toluene, lower range.

§ 4.2.2 The interaction of $[(Ph_2N)_3Ti]^+$ with two equivalents of propylene

A second molar equivalent of propylene was added to the NMR tube in hopes of identifying the product formed in the beginning stages of polymerization. The J-Youngs valve fitted NMR tube from the first experiment was attached to the high vacuum line and sequentially frozen from bottom to top, in order to trap the bound and free propylene within the tube. Once frozen, as close to the tap as possible, a second molar equivalent of propylene was condensed into the tube. The tube was thawed and allowed to react by gentle shaking.

Free propylene observed in the first experiment was no longer present in the ^1H NMR spectrum, and an additional, broad signal apeared at 3.32 ppm. Given that free propylene is observed in equilibrium with bound propylene when a single equivalent of the olefin is present, a simple successive addition to the species formed in the first experiment is inconsistent with these results. Any species that is initially formed when two equivalents of propylene are present clearly must then react to lower the concentration of free propylene below observable levels. Further experimental data are required to identify the final product in this experiment, and any assignment of a chemical structure is speculation in the absence of such data.

However, it is clear that successive addition of propylene to the titanium cation results in clean formation of products, leading to the possibility that $[(Ph_2N)_3Ti][BAr^F_4]$ is a genuine single site, living olefin polymerization catalyst. Further experimental work is required to confirm this hypothesis.

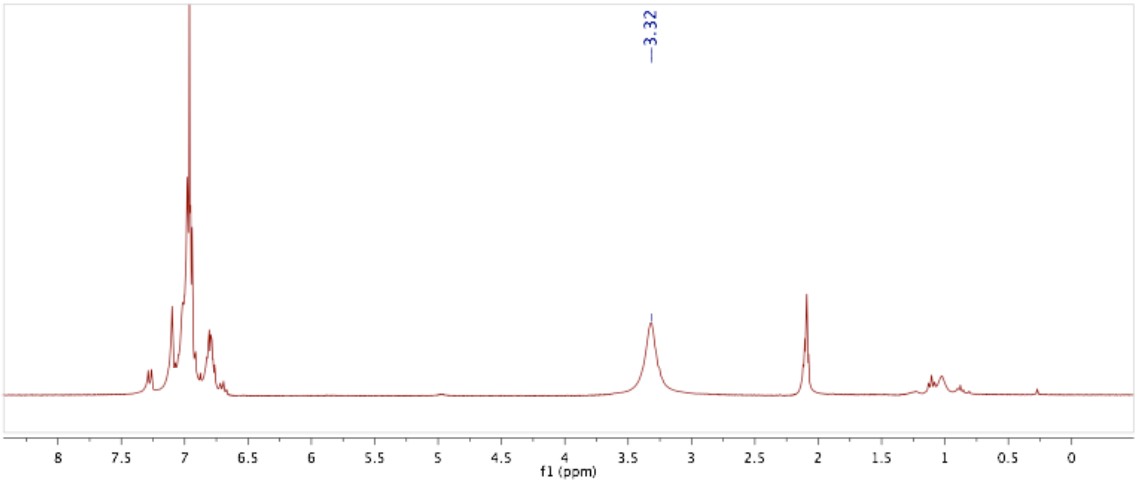

Figure 4.7: ^1H NMR of $[(Ph_2N)_3Ti][BAr^F{}_4]$ with 2 equivalent of propylene in d_8-toluene.

§ 4.2.3 $(Ph_2N)_3TiMe$ plus propylene

Further evidence that the mechanism of propylene polymerization in these systems differs in principle from the normal Ziegler-Natta mechanisms arises from the reaction of propylene with $(Ph_2N)_3TiMe$. As this complex possesses a Ti-Me bond, if insertion is possible in this chemical context a reaction should be observed.

1.03 equivalents of dry propylene were condensed into a J-Youngs valve fitted NMR tube containing 42 mg of freshly prepared $(Ph_2N)_3TiMe$ in d_6-benzene. The sample was thawed and allowed to react for twelve hours before analysis was under taken. The ^1H NMR spectrum displays the standard resonances for complex **(4)** plus resonances that are diagnostic for free propylene in solution. At room temperature, no propylene was observed to be bound to the titanium metal center or inserted into the Ti-Me bond. The tube was heated to 80 ºC for twelve hours to force the insertion. After twelve hours the ^1H NMR displayed the same spectrum as before, complex **(4)** plus free propylene.

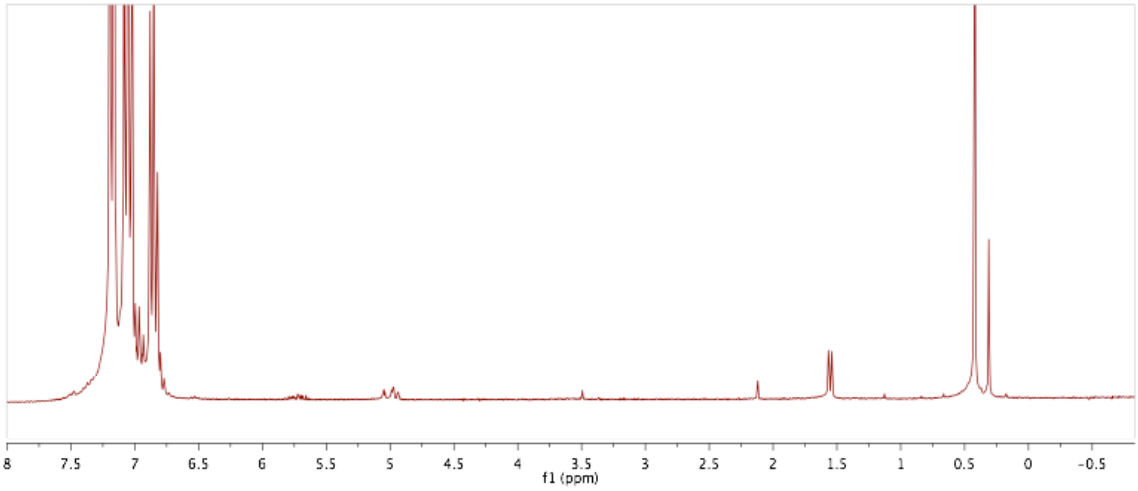

Figure 4.8: $(Ph_2N)_3TiMe$ and free propylene in d_6-benzene.

§ 4.2.4 $(Ph_2N)_3Ti•••Me•••BAr^F_3$ plus propylene

In order to raise the Lewis acidity of the titanium center and also to investigate the known catalytic reactivity of the $(Ph_2N)_3Ti—Me--BAr^F_3$ system., a solution of $(Ph_2N)_3Ti—Me--BAr^F_3$ was prepared *in situ* and treated with a single equivalent of propylene.

No bound propylene was identified; instead a small amount of polypropylene was produced, with broad singlet at 3.18 ppm (upfield slightly from polypropylene in toluene). The methyl signal associated with the Ti-Me-B is still present at 1.1983 ppm.

Clearly the catalyst is so active that binding a single molecule of propylene to the titanium is not observable, with insertion and chain grown occurring too rapidly to identify the first coordination. This is typical for Ziegler-Natta catalysts; the rate of chain-growth step is faster than that of initial coordination or hydride elimination and termination.[82]

§ 4.2.5 The interaction of $[(Ph_2N)_3Ti][BAr^F_4]$ with bicyclo-[2,2,1]-2-heptene

Bicyclo-[2,2,1]-2-heptene or norbornylene represents a substrate that should bind to but not polymerize with a Ziegler-Natta type catalyst. Indeed, polymerization of norbornylene is usually only observed in ring opening metathesis polymerization. In this respect, is should serve as a useful probe for the spectroscopic properties of a bound alkene, without complications from potential bond making or bond breaking processes.

One molar equivalent of norbornylene was placed in an NMR tube, together with one mole equivalent of both $(Ph_2N)_3TiCl$ and $KBAr^F_4$, so as to form *in situ* a solution of $[(Ph_2N)_3Ti][BAr^F_4]$ (norbornylene). A series of one and two dimensional NMR spectra were acquired, augmented by data collected at variable temperature.

The symmetry properties of norbornylene and propylene are similar in that neither has any symmetry elements when forced into a C_3 or *pseudo*-C_3 symmetry environment through coordination.

The ^1H spectra at room temperature and at 200 K show signals consistent with both free and bound norbornylene. A broad resonance consistent with **H**C=C**H** protons residing in a shielded environment is observed, which at 200 K resolves somewhat into two broad and overlapping resonances. This is consistent with the alkene residing in a highly asymmetric environment, similar to that observed for propylene bound to the same titanium center. The change in chemical shift from free to bound norbornylene is similar to that observed for the change in shift for the olefinic protons in free propylene and propylene bound to the same cation.

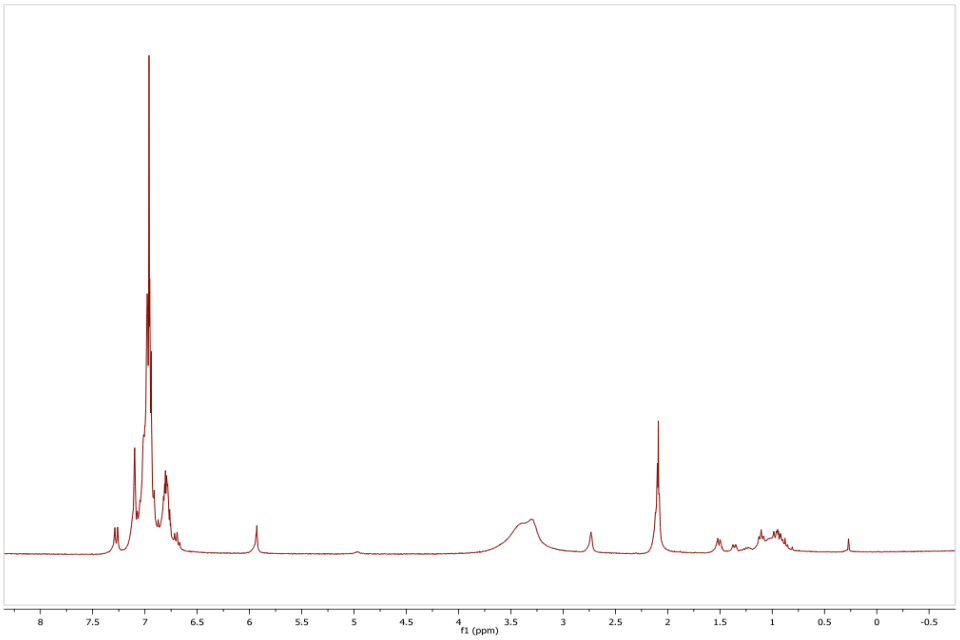

Figure 4.9: ^{1}H NMR of $[(Ph_2N)_3Ti][BAr^F{}_4]$ with norbornylene in d_8-toluene

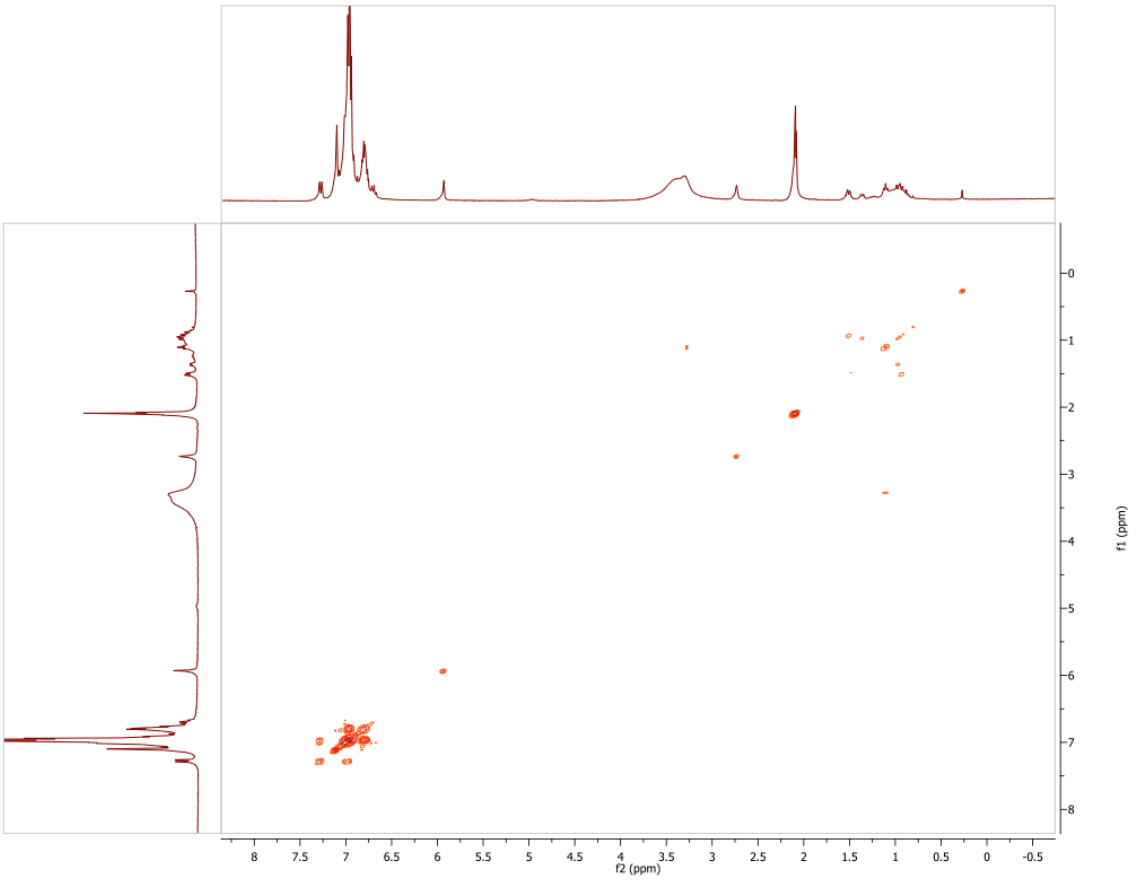

Figure 4.10: gCOSY of $[(Ph_2N)_3Ti][BAr^F{}_4]$ with norbornylene in d_8-toluene

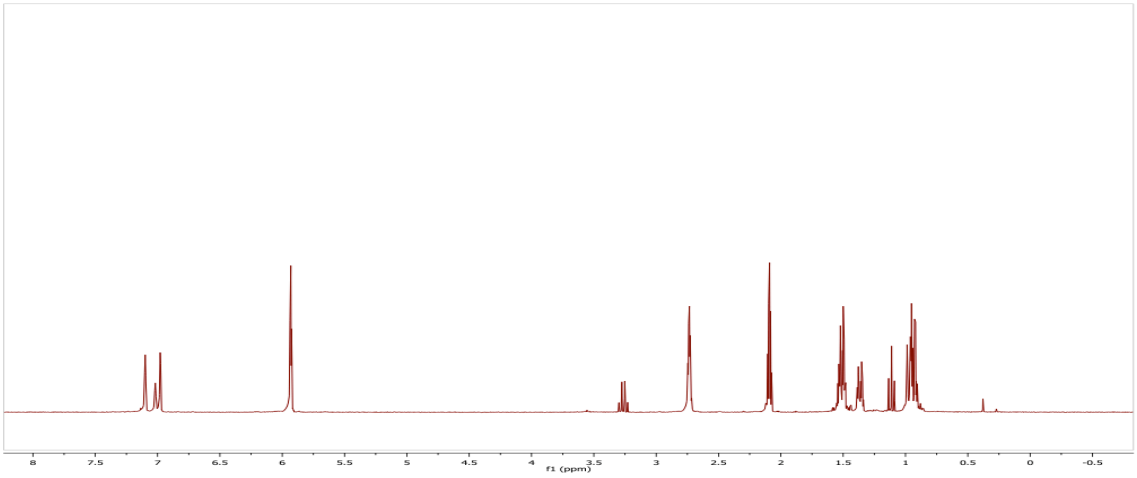

Figure 4.11: ^1H NMR of norbornylene in d_8-toluene

§ 4.3 Discussion

Preparation of $(Ph_2N)_3TiMe$ and $[(Ph_2N)_3Ti][BAr^F{}_4]$ provides a functional separation of the two important structural features for olefin polymerization in general, and Ziegler-Natta catalysis in particular. However, in contrast to the conventional mechanisms of Ziegler-Natta catalysis, a reversed reactivity is observed in these systems. A pure Lewis acidic transition metal center should not polymerize in the absence of an M-C bond for insertion, and great lengths have taken in order to generate transition metal hydrocarbyl cations for this type of transformation.

In contrast to other systems, $[(Ph_2N)_3Ti][BAr^F{}_4]$ rapidly polymerizes propylene, whereas the 12 electron $(Ph_2N)_3TiMe$ does not. That the latter species is unreactive with propylene at room temperature or above may be due to reduced Lewis acidity, although this is surprising in a 12 electron system. It is interesting to speculate whether heavier congeners of $(Ph_2N)_3TiMe$ would be sufficiently Lewis acidic to act as olefin polymerization catalysts in the absence of a Lewis acid activator.

The observation of through-space correlations between the methyl hydrogens and the *ortho* hydrogens on the ligands certainly speaks to the steric congestion at the possible active site.

Discrimination between intrinsically low Lewis acidity due to electronic effects and low Lewis acidity due to steric reasons is not possible with the data in hand, and given that $(Ph_2N)_3TiMe$ is inactive under the conditions studied, further speculation as to the cause of the lack of reactivity is probably specious.

The stoichiometric reaction between $[(Ph_2N)_3Ti][BAr^F{}_4]$ and propylene affords an identifiable adduct in equilibrium with free propylene, showing that $[(Ph_2N)_3Ti(\eta^2$-

$CH_2CHCH_3)][BAr^F_4]$ is not the catalytically active species. Treatment of $[(Ph_2N)_3Ti][BAr^F_4]$ with two equivalents of propylene cannot afford oligomerization that is related to the initial formation of $[(Ph_2N)_3Ti(\eta^2\text{-}CH_2CHCH_3)][BAr^F_4]$, as the latter species is observed to be present in equilibrium with free propylene. A second, intermediate species must be formed prior to the product of reaction with two equivalents of propylene. The identity of this product is unknown and will require more experimental investigation.

That several successive species are formed prior to the establishment of the catalytic species is also consistent with the observed slower period of initiation when this system is used catalytically, as shown in § 3.4. In contrast to the more rapid initiations with MAO-activated $(Ph_2N)_3TiCl$ or $(Ph_2N)_3TiMe$- BAr^F_3, there is a significant lag before the consumption of the monomer. However, the coexistence of free propylene with $[(Ph_2N)_3Ti(\eta^2\text{-}CH_2CHCH_3)][BAr^F_4]$ shows that systems based on $[(Ph_2N)_3Ti][BAr^F_4]$ may be able to act as a living system, i.e. a system that is stable in the absence of substrate.

§ CHAPTER 5 Synthetic Procedures

§ 5.1 General synthetic procedures

Unless otherwise stated, all solvents used in synthetic experiments were pre-dried over 4A molecular sieves, prior to distillation from $K_{(l)}$, (tetrahydrofuran, hexane), $K_3Na_{(l)}$ (diethyl ether, pentane), or $Na_{(l)}$ (toluene, 1,4-dioxane). Solvents for NMR spectroscopy were dried twice through reflux over CaH_2 or K prior to storage over a potassium mirror or the appropriate drying agent where potassium proves reactive with the solvent. All manipulations of solutions were conducted using Schlenk techniques under an argon atmosphere, using flamed-dried 316 stainless steel cannulæ and flame-dried Schlenk flasks or in an argon-filled glovebox, using standard techniques; solids were transferred in an argon-filled glove box. In both cases, the concentrations of O_2 and H_2O in the argon atmosphere were less than 5 ppm. Recrystallizations were preformed either through storage of solutions at -21°C, or between -65 and -85°C or by layering the solution with a solvent in which the solute is insoluble.

Diphenylamine was purchased from commercial sources as a brown to black solid. It was recrystallized once in air from 1:1 toluene xylenes, with at least two successive recrystallizations from toluene under an argon atmosphere. The resultant white crystalline material was then vacuum distilled at ~10^{-3} mbar and ~120 °C, with the white, amorphous solid being collected at liquid nitrogen temperatures. $TiCl_4 \cdot (THF)_2$ was prepared by treating a solution of doubly distilled $TiCl_4$ in dichloromethane with a solution of tetrahydrofuran in the same solvent at -80 °C; the resultant yellow precipitate

was filtered cold and dried.[117] TiI_4 was prepared from the elements in benzene and purified by Soxhlet extraction in pentane or sublimation. All other reagents were bought commercially and used as received. KI, NaI and LiI were dried at 100 °C at 10^{-3} mbar for 24 hours.

^{1}H NMR spectra were collected at 300 or 400 MHz on either a Bruker INOVA (400 MHz) or Varian Mercury (300 MHz), and were referenced to TMS *via* residual proton resonances in the deuterated solvent. ^{13}C NMR spectra were collected at 75 or 100 MHz on the same spectrometers, and were referenced to TMS *via* the ^{13}C resonances of the solvent. Elemental analysis was carried out at Galbraith Laboratories, Inc., in Knoxville, TN.

§ 5.2 Synthesis of Complexes

Synthesis of $LiNPh_2$, (1). 20g (0.118 mol, 1 eq) of diphenylamine was dissolved in 300 mL of hexane. 83.4 mL (0.142 mol, 1.2 eq) of 1.7 M ^{t}butyl lithium in hexane (Aldrich) was added drop-wise over a period of twenty minutes. A white precipitate immediately formed and this suspension was allowed to stir at room temperature for twelve hours, after which it was filtered. The resulting white solid was washed with 3 x 20 mL portions of pentane and dried under reduced pressure. ^{1}H NMR (d_8-THF): δ 6.130 (t, 1 H, *p*-$C_6\mathbf{H}_5$, ^3J= 7.8 Hz), 6.681 (d, 2 H, *o*-$C_6\mathbf{H}_5$, ^3J = 7.8 Hz), 6.787 (t, 2H, *m*-$C_6\mathbf{H}_5$-meta, ^3J = 7.8 Hz). Yield: 19.6g/ 94.7%.

Synthesis $(Ph_2N)_3TiCl$, (2). 10.0 g (0.057 mol, 3 eq) of **(1)** was dissolved in 150 mL of toluene and added drop-wise to a slurry of 6.354 g (0.019 mol, 1 eq) $TiCl_4 \cdot 2THF$ in 150 mL of toluene over a period of twenty-five minutes. The color changed to blood red within the first minute. This solution was left to stir at room temperature for a period of twelve hours, at which time the solution was cooled to -40 °C to allow the salt to settle. The deep red solution was filtered and the resulting salt was washed with 3 x 50 mL portions of hexane. All filtrates were combined, and the solvent was removed under reduced pressure. The wet product was recrystallized from pentane. Yield: 9.869g/ 88.20% ^{1}H NMR (d_8-THF): δ 6.8167 (d of t, 2 H, *o*-$C_6\mathbf{H}_5$), 6.978 (t of t, 1 H, *p*-$C_6\mathbf{H}_5$), 7.114 (t of t, 2 H, *m*-$C_6\mathbf{H}_5$). ^{1}H-^{1}H Coupling constants: $^4J_{o\text{-}p}$ = 1.2 Hz, $^3J_{p\text{-}m}$ = 5.4 Hz, $^3J_{o\text{-}m}$ = 6.0 Hz. Anal. Calcd: C, 73.54; H, 5.14; Cl, 6.03; N, 7.15; Ti, 8.14. Found C, 71.94; H, 5.28; N, 6.97.

Synthesis $(Ph_2N)_3TiI$, (3). 5.0 g (8.5mmol, 1 eq) of **(2)** was refluxed in 150 mL of THF with 22.75 g (0.17mol, 20 eq) of dry KI with *ca* ~ 0.5 eq. of LiI for seventy-two hours, at which time, 100 mL of pentane was added. The deep orange/ red solution was filtered and solvent removed under reduced pressure, yielding a dark orange/ red powder. Yield: 4.45g/ 89% The product was recrystallized from pentane. NMR ^{13}C NMR (d_8-THF): δ 129.7, 123.7, 120.7, and 118.08.

Synthesis $(Ph_2N)_3TiMe$, (4). 3.0 g (5.1 mmol, 1 eq) of **(2)** was dissolved in 100 mL of toluene. Freshly prepared MeMgI (6.1mmol, 1.2 eq) in dry diethyl ether was

added to the first solution over a period of 20 minutes. The resulting solution was allowed to stir at room temperature for one hour, at which time 1.079 g (0.0122 mol, 2.4 eq) of 1,4 dioxane was added drop-wise for twenty minutes. An appreciable amount of precipitate forms within the first few drops and grows for a *ca* minute after the addition is complete. This solution was allowed to stir for thirty minutes and then allowed to settle. The solution was filtered and left at -80°C for twelve hours, in which time an orange precipitate formed. The mother solution was filtered from the precipitate, concentrated and placed back into the -80 °C freezer for further precipitation. ^{1}H NMR (d_8-THF): δ 0.045 (s, 3 H, C**H**$_3$), 6.9375 (d, 12H, *o*-C$_6$**H**$_5$), 7.7009 (t, 12H, *m*-C$_6$**H**$_5$), and 7.194 (t, 6H, *p*-C$_6$**H**$_5$). ^{1}H-^{1}H Coupling constants: $^{3}J_{o\text{-}m}$ = 7.5 Hz, $^{3}J_{\text{m-p}}$ = 7.0 Hz. ^{13}C NMR (d_8-THF): δ 65.684, 124.532, 125.361, 130.442, and 148.656. ^{1}H NMR (C_6D_6): δ 0.424 (d, 3H, C**H**$_3$), 6.843 (t of t, 6H, *p*-C$_6$**H**$_5$), 7.043 (t of t, 12 H, *m*-C$_6$**H**$_5$), and 7.166 (d of t, 12 H, *o*-C$_6$**H**$_5$). ^{1}H-^{1}H Coupling constants: $^{3}J_{o\text{-}m}$ = 7.44 Hz, $^{3}J_{o\text{-}p}$ = 1.13 Hz, and $^{3}J_{p\text{-}m}$ = 7.9 Hz ^{13}C NMR (C_6D_6) δ 65.509 (**C**H$_3$), 124.023 (*m*-**C**$_6$H$_5$), 124.866 (*p*-**C**$_6$H$_5$), 129.953 (*o*-**C**$_6$H$_5$), and 148.006 (*i*-**C**$_6$H$_5$). $^{1}J_{\text{C-H}}$ (CH$_3$) = 131.8 Hz Anal. Calcd: C, 78.30; H, 5.86; N, 7.40; Ti, 8.43. Found: C, 73.02; H, 5.69; N, 6.92.

Synthesis of (Ph$_2$N)$_3$Ti-Me-B(C$_6$F$_5$)$_3$ (5). 0.450g (0.88 mmol, 1 eq) of B(C_6F_5)$_3$ dissolved in 50 mL of hexane was added drop wise over thirty minutes to 0.50 g (8.8 mmol, 1 eq) of **(4)** in 200 mL of hexane with 10 mL of benzene for solubility. Not all of **(4)** was dissolved before the reaction; upon completion of the reaction there was no visible solid in the flask. The solution changed from orange to a deep purple/red with the

addition of the first few drops. The reaction was left to react for three hours and at that time all solvent was removed and the purple/red solid was washed with 3 x 10 mL portions of pentane. Yield: 0.7714 g/ 83% yield. Anal. Calcd: C, 61.19; H, 3.08; B, 1.00; F, 26.40; N, 3.89; Ti, 4.43. Found: C, 59.25; H, 3.39; N, 3.385; B, 0.893.

Synthesis of $(Ph_2N)_3TiCH_2PMe_2$ (6). 5.00g of **(2)** (8.50 mmol, 1 eq) dissolved in 300 mL of toluene. 0.70 g of $LiCH_2PMe_2$ (8.50 mmol, 1 eq) dissolved in 150 mL of toluene and 10 mL of THF, added for solubility, was added to the first solution drop wise over a period of 30 minutes. Addition of the phosphine changed the color to a deeper red. The reaction mixture was allowed to react for six hours, at which time 100 mL of hexane was added and the solution was filtered. The solvent was removed under reduced pressure to yield 4.46g/ 83.61% ^{1}H NMR (d_6-benzene): ∂ 7.317 (t, J =7.87), 7.08, 6.982 (t, J = 3.77), 6.84 (broad), 6.71 (t, J 7.30), 1.73, 1.25, (t, J =6.94), amd 0.44 (broad) ^{13}C NMR (d_6-benzene): 151.86, 150.56, 144.29, 129.81, 124.87, 124.02, 123.06, 122.77, 118.79, 34.77, 23.05 and 14.62. ^{31}P NMR (d_3-phosphoric acid): -39.18 (-CH_2**P**Me_2). Anal. Calcd: C, 74.64; H, 6.10; N, 6.70; P, 4.94; Ti, 7.63. Found: C, 72.47; H, 5.76; N, 5.91; P, 4.79.

Synthesis of $[(Ph_2N)_3Ti][B(C_6F_5)_4]$ (9). 0.50 g (0.736 mmol, 1 eq) of $K[B(C_6F_5)_4]$ dissolved in 50 mL of benzene was added drop wise over thirty minutes to 0.430 g (0.736 mmol, 1 eq) of **(2)** in 200 mL of benzene. The solution changed to a deeper purple/red color with the addition of the first few drops. The reaction was left to

react for three hours and at that time 200 mL of hexane was added to precipitate the KCl out of solution. The precipitate was filtered from the solution. The solvent was removed and the purple/red solid was washed with 4 x 10 mL portions of pentane. Yield: 0.8622 g (95.1% yield). ^{1}H NMR (d_8-benzene): δ 0.89 (unresolved multiplet), 0.89 (broad singlet), 3.24 (broad singlet), 6.712 (t, $^{3}J_{H\text{-}H}$ 7.86 Hz), 6.793 (t, $^{3}J_{H\text{-}H}$ 7.15 Hz), 6.944 (d, $^{3}J_{H\text{-}H}$ 8.33 Hz), 7.012 (t, $^{3}J_{H\text{-}H}$ 8.68 Hz), and 7.313 (d, $^{3}J_{H\text{-}H}$ 7.86). ^{13}C NMR (d_6-benzene): δ 118.82, 122.77, 123.74, 125.91, 129.75 and 150.31. Anal. Calcd: C, 58.52; H, 2.46; B, 0.88; F, 30.85; N, 3.41; Ti, 3.89. Found: C, 56.14; H, 2.80; N, 3.23; B, 0.807

Synthesis of $((C_6H_5)_2N)_3Ti(PMe_3)_2^{+}$ $^{-}B(C_6F_5)_4$ (10). 0.040g of **(7)** was dissolved in 2.00 mL of d_6-benzene in a J-Youngs Tap NMR tube. The sample was frozen and the head-space was evacuated. Two equivalents of dry PMe_3 was transferred *via* vapor pressure condensation. The tube was allowed to warm to room temperature and react for one hour before analysis. No color changed occurred with the addition of phosphine.

§ 5.3 Synthesis of Reactants

Synthesis of PMe_3. A solution of triphenylphospshite in di-^{n}butyl ether (0.672 mol, 208.5g, 175.96 mL, 1 eq in 0.5 L) was slowly added to freshly prepared MeMgI (2.15 mol, 3.2 eq) in dry di-^{n}butyl (1.5 L) ether over a period of two hours. The reaction temperature was kept at 0.0 ºC throughout the addition. After the addition, the system was allowed to continue to react for another three hours, after which time, the product was distilled from the reaction mixture in a receiving flask held at -80 ºC. The product

was then distilled again, and 53.4 mL of the product was collected in 86 % yield. ^{1}H NMR (d_6-benzene): δ = 0.801 ppm, (d, $^{2}J_{H\text{-}P}$ = 2.4 Hz), ^{13}C NMR (d_6-benzene): δ = 13.4 ppm, (d, $^{1}J_{C\text{-}P}$ = 13.4 Hz), ^{31}P NMR (d_3-phosphoric acid): δ = -60.9 ppm

Synthesis of $LiCH_2PMe_2$ Trimethylphosphine (0.891 mol, 50.0 mL 1 eq) diluted in 300 mL of hexane was cooled to 0 ºC and ^{t}BuLi (1.7 M, 1.1583 mol, 681 mL, 1.3 eq) in hexane was added drop wise over a period of forty-five minutes. After a minute, the white powder precipitated out. After addition, the reaction mixture was kept cool and allowed to continue t react for another four hours, at which time the solution was filtered leaving the phosphinomethanide product behind. The white precipitate was washed twice with 20 mL portions of toluene and three times with 20 mL portions of pentane, and dried under vacuum. The white-to off white solid was collected in 93% yield. Lithium dimethylphosphinomethanide is extremely pyrophoric and must be handled with care. ^{1}H NMR (d_8-THF): δ = 0.756 ppm (d, 6 H, $CH_2P\mathbf{Me_2}$, $^{2}J_{H\text{-}P}$ = 0.9 Hz), -0.918 ppm (d, 2H, $C\mathbf{H_2}PMe_2$), ^{13}C NMR (d_8-THF): δ = 23.989 ppm (d, $CH_2P\mathbf{Me_2}$, $^{1}J_{C\text{-}P}$ = 18.3 Hz), 9.576 ppm (d, $\mathbf{CH_2}PMe_2$, $^{1}J_{C\text{-}P}$ = 36.7 Hz), ^{31}P NMR (d_3-phosphoric acid): δ = -40.9 ppm

Synthesis of $KB(C_6F_5)_4$. Fresh $BrMgC_6F_5$ was prepared from 10.0 g (0.040 mol, 5.047 mL, 1 eq) of BrC_6F_5 was added to 1.181g (0.0485 mol, 1.2 eq) of activated Mg in 150 mL diethyl ether. The halide was added to the magnesium over a period of one hour and the resulting Grignard was allowed to stir for two hours before use. The freshly prepared Grignard was added drop wise to a slurry of 1.2745 g KBF_4 (0.0101 mol, .25

eq) in 150 mL of diethyl ether. This solution was allowed to react for twenty-four hours, at which time, 100 mL of hexane was added to the flask and cooled to -35 ºC to enhance precipitation. The solution was filtered cold and the remaining salt was washed with 2 x 15 mL portions of hexane. The solvent was removed under reduced pressure producing an oily solid, which was washed with 3 x 20 mL of pentane to give an off-white powder. Yield: 6.87g (94.5% yield). Anal. Calcd: C, 40.14; B, 1.51; F, 52.91; K, 5.44 found C, 39.22; B, 1.32.

Synthesis of Methylaluminoxane MAO:[118] 24 g (0.086 mol, 6 eq) of $FeSO_4 \bullet 7H_2O$ was dissolved in 250 mL of toluene in a three-liter round-bottom Schlenk flask and placed in a 0.0 ºC bath. 50 mL (0.52 mol, 37.6g 1 eq) of neat $AlMe_3$ was diluted with 100 mL of toluene in a large Schlenk flask. The $AlMe_3$ solution was added drop-wise to the $FeSO_4$ solution, stirring vigorously, over a period of one hour. Upon the addition of the first drop of $AlMe_3$, the flask became cloudy and hissed with every drop. After addition was complete the flask was kept cool for an additional two hours, after which time the reaction was stirred at room temperature for twelve hours. After the twelve hours, the solution was filtered into a large Schlenk flask, the residue was washed 4 x 30 mL of dry toluene, and the solvent was removed under reduced vacuum. Once all of the solvent had been removed, a sticky, pink solid remained; it was washed 3 x 15 mL pentane to remove residual toluene. The product was dried for twenty-four hours on the high-vacuum line and the yield was 23.2 g of a slightly pink, waxy solid. Percent yield = 76.95%

Synthesis of $LiMeB(C_6F_5)_3$. 1.7 mg of dry MeLi (7.812 mmol, 1 eq) was added to a J-Young valve fitted NMR tube and 40 mg of BAr^F_3 was added to it. D_8-toluene was vacuum distilled into the tube. The tube was thawed and allowed to react for 1 hour at which time analysis was conducted. While the complex is partially soluble in benzene, it is extremely soluble in toluene. No ethereal or donating polar solvents can be used, as they will alter the H_3C-Bond. Special care must be taken when handling the complex free from polar solvents, $LiMeB(C_6F_5)_3$ is explosive when dry. ^1H NMR (d_8-toluene): δ 0.759 ppm.

§ References

1. Wilkinson, G., The Iron Sandwich. A Recollection of the First Four Months. *Journal of Organometallic Chemistry* **1975,** 100, 273-278.

2. Wilkinson, G., *Bis*-Cyclopentadienyl Derivativies of Some Transition Elements. *Journal of the American Chemical Society* **1953**, (75), 1011.

3. Breslow, D. S.; Newburg, N. R., *Bis*-(cyclopentadienyl)-titanium Dichloride-Alkylaluminum Complexes as Soluble Catalysts for the Polymerization of Ethylene. *Journal of the American Chemical Society* **1959,** 81, 81.

4. Arlman, E. J.; Cossee, P., Ziegler-Natta Catalysis III. Stereospecific Polymerization of Propene with the Catalyst System TiCl3-AlEt3. *Journal of Catalysis* **1964**, 1964.

5. Ewen, J. A., Mechanism of Stereochemical Control in Propylene Polymerizations with Soluble Group 4B Metallocene/ Methylalumoxane Catalysts. *Journal of the American Chemical Society* **1984,** 106, 6355-6364.

6. Kaminsky, W.; Kulper, K.; Brintzinger, H. H.; Wild, F., R. W. P., Polymrization of Propene and Butene with Chira Zirconocene and Methylalumoxane as Cocatalyst. *Angewandte Chemie Int. Ed. Engl* **1985,** 24, (6), 507-508.

7. Bochmann, M.; Wilson, L. M., Synthesis and Insertion Reactions of Ctaionic Alkyl*bis*(cyclopentadienyl)titanium Complexes *Journal of the Chemical Societ, Chemical Communications* **1986**, 1610.

8. Jordan, R. F.; Bajgur, C. S.; Willett, R.; Scott, B., Ethylene Polymerization by a Cationic Dicyclopentadienylzirconium (IV) Alkyl Complex. *Journal of the American*

Chemical Society **1986,** 108, 7410-7411.

9. Ewen, J. A.; Jones, R. L.; Razavi, A., Syndiospecific Propylene Polymerization with Group 4 Metallocenes. *Journal of the American Chemical Society* **1988,** 110, 6255-6256.

10. Friedrich, P.; Marvel, C. S., *Journal of the American Chemical Society* **1930,** 52, 376.

11. Ziegler, K., Aluminum organics and their importance to olefin chemistry. *Chimica e l'Industria* **1954,** 34, 520-7.

12. Ziegler, K.; Krupp, F.; Schneider, J., Aluminum in orgaic chemistry. VI A simple synthesis of primary alcohols from olefins. *Angewandte Chemie* **1955,** 67, (425).

13. Natta, G.; Pino, P.; Mazzanti, G.; Giannini, U., A Crystallizable Organometallic Complex containing Titanium and Aluminum *Journal of the American Chemical Society* **1957**, (75), 1011.

14. Proffit, M., *The Oxford English Dictionary*. Oxford Press: London, 2005.

15. Gaylord, N. G.; Mark, H. F., *Linear and Stereoregular Addition Polymers*. Wiley (interscience): New York, 1959.

16. Breslow, D. S.; Newburg, N. R., *Bis*-(cyclopentadienyl)-titanium dichloride-alkylaluminum complexes as catalysts for the polymerization of ethylene. *Journal of the American Chemical Society* **1957**, 5072-5073.

17. Hays, M. L.; Hanusa, T. P., Subsituent effects as probes of structure and bonding in molecular metallocenes. *Advances in Organometallic Chemistry* **1996,** 40, 117.

18. Halterman, R. L., Synthesis and Applications if Chiral Cyclopentadienylmetal Complexes. *Chemical Reviews* **1992,** 92, 965-994.

19. Green, J. C., Bent metallocenes revisited. *Chemical Society Reviews* **1998,** 27, 263-271.

20. Long, W. P.; Breslow, D. S., Effect of water on the catalytic activity of *bis*(cyclopentadienyl)titanium dichloride-dimethylaluminum chloride for the polymerization of ethylene. *Justus Liebigs Annalen der Chemie* **1975,** 3, 463-9.

21. Andresen, A.; Cordes, H.-G.; Herwig, J.; Kaminsky, W.; Merck, A.; Pein, J.; Sinn, H.; Vollmer, H.-J., Halogen-Free Soluble Ziegler Catalysts for the Polymerization of Ethylene. Control of Molecular Weight by Choice of Temperature. *Angewandte Chemie International Ed.* **1976,** 15, 630.

22. Bochmann, M.; Wilson, L. M., Cationic Alkyl*bis*(cyclopentadienyl)titanium Complexes. Synthesis, Reactions with CO and ^{t}BuNC, and the Structure of [$Cp_2Ti\{\eta^2$-C(Me)N-^{t}Bu}(CN-^{t}Bu)]BPh_4MeCN. *Organometallics* **1987,** 6, 2556-2563.

23. Jordan, R. F.; LaPointe, R. E.; Bajgur, C. S.; Echols, S. F.; Willett, R., Chemistry of Cationic Zirconium Benzyl Complexes. One-Electron Oxidation of d^0 Organometallics. *Journal of the American Chemical Society* **1987,** 109, (13), 4111.

24. Yang, X.; Stern, C. L.; Marks, T. J., Models for Organometallic Molecular-Support Complexes. Very Large Counterion Modulation of Cationic Actinide Alkyl Reactivity. *Organometallics* **1991,** 10, 840.

25. Yang, X.; Stern, C. L.; Marks, T. J., Cationic Zirconocene Olefin Polymerization Catalysts Based on the Organo-Lewis Acid *Tris*(pentafluorphenyl)borane. A synthetic Structural, Solution Dynamic, ad Polymerization Catalytic Study. *Journal of the American Chemical Society* **1994,** 116, 10015-10031.

26. Zuccaccia, C.; Stahl, N. G.; Macchioni, A.; Chen, M.-C.; Roberts, J., A.; Marks, T. J., NOE and PGSE NMR Spectroscopic Studies of Solution Structure and Aggregation in Metallocenium Ion-Pairs. *Journal of the American Chemical Society* **2004,** 126, 1148-1464.

27. Doring, S.; Kotov, V. V.; Erker, G.; Kehr, G.; Bergander, K.; Kataeva, O.; Frohlich, R., Synthesis and Dynamic Features of (chloro)zirconocene Cations Stabilized by Pendant (Diarylphosphanyl)alkyl and (Dimethylamino)alkyl Substituents at Their Cyclopentadienyl Ring Systems. *European Journal of Inorganic Chemistry* **2003**, 1599-1607.

28. Wu, F.; Jordan, R. F., *Organometallics* **1988,** 24, 2688.

29. Spaleck, W.; Kuber, F.; Winter, A.; Rohrmann, J.; Bachmann, B.; Antberg, M.; Dolle, V.; Paulus, E. F., The Influence of Aromatic substituents on the Polymerization Behavior of Bridged Zirconocene Catalysts. *Organometallics* **1994,** 13, 954-963.

30. Butin, K. P.; Beloglazkina, E. K.; Zyk, N. V., Metal complexes with non-innocent ligands. *Russian Chemical Reviews* **2005,** 74, (6), 531-553.

31. Brintzinger, H. H.; Fischer, D.; Mulhaupt, R.; Reiger, B.; Waymouth, R. M., Stereospecific Olefin Polymerization with Chiral Metallocene Catalysts. *Angewandte Chemie International Ed.* **1995,** 34, 1143-1170.

32. McDaniel, M., *Supported Chromium Catalysis for Ethylene Polymerization*. Academic Press Inc.: New York, 1985; Vol. 33.

33. Miesserov, K. C., Mechanism of polymerization of alpha-olefins on oxide catalysts. *Journal of Polymer Science, Polymer Chemistry Edition* **1966,** 4, (12), 3047-3054.

34. Krauss, H. L., New Results with Phillips Systems: Surface Compounds of Transition Metals, Part XXXII. *Journal of Molecular Catalysis* **1988,** 46, 97-108.

35. Theopold, K. H., Understanding chromium-based olefin polymerization catalysts. *Chemtech* **1997,** 10, 26-32.

36. Theopold, K. H., Homogeneous Chromium Catalysis for Olefin Polymerization. *European Journal of Inorganic Chemistry* **1998**, 15-24.

37. Elschenbroich, C., *Organometallics: Third, Completely Revised and Extended Edition*. Wiley-VCH: Weinheim, Germany, 2005.

38. Rix, F. C.; Brookhart, M., Energentics of Migratory Insertion Reactions In Pd(II) Acyl Ethylene, Alkyl Ethylene, and Alkyl Carbonyl Complexes. *Journal of the American Chemical Society* **1995,** 117, 1137-1138.

39. Peuckert, M.; Keim, W., A New Nickel Complex for the Oligomerization of Ethylene. *Organometallics* **1983,** 2, 594-597.

40. Keim, W., Nickel: An Element with Wide Application in Industrial Homogeneous Catalysis. *Angewandte Chemie Int. Ed. Engl* **1990,** 29, (3), 235-244.

41. Johnson, L. K.; Killian, C. M.; Brookhart, M., New Pd(II)- and Ni(II)-based Catalysts for Polymerization of Ethylene and alpha-Olefins. *Journal of the American Chemical Society* **1995,** 117, 6414-6415.

42. Wang, C.; Friedrich, S.; Younkin, T. R.; Li, R. T.; Grubbs, R. H.; Bansleben, D. A.; Day, M. W., Neutral Nickel(II)-Based Catalysts for Ethylene Polymerization *Organometallics* **1998,** 17, 3149-3151.

43. Small, B. L.; Brookhart, M., Iron-Based Catalysts with Exceptionally High Activities and Selectivities for Oligomerization of Ethylene to Linear alpha-Olefins.

Journal of the American Chemical Society **1998,** 120, 7143-7144.

44. Marks, T. J.; Chen, E. Y.-X., Cocatalysts for Metal-Catalyzed Olefin Polymerization: Activators, Activation Process, and Structure-Activity Relationships. *Chemical Reviews* **2000**, (100), 1391-1434.

45. Bochmann, M., Cationic Group 4 metallocene complexes and their role in polymerization catalysis: the chemistry of well defined Ziegler catalysts. *Journal of the Chemical Societ, Dalton Transactions* **1996**, 255-270.

46. Erker, G., *Tris*(pentafluorophenyl)borane: a specieal boron Lewis acid for special reactions. *Journal of the Chemical Society, Dalton Transactions* **2005**, 1883.

47. Ingo Krossing, P.-D. D.; Ines raabe, D.-C., Non-coordinating Anions - Fact or Fiction? A Survey of Likely Candidates. *Angewandte Chemie International Ed.* **2004,** 43, (16), 2066-2090.

48. Ziegler, K.; Gellert, H. G.; Martin, H.; Nagel, K.; Schneider, J., Organoalkali compounds XIX. Reactions of the aluminum-hydrogen linkage with olefins. *Ann* **1954,** 589, 91-121.

49. Ziegler, K.; Holzkamp, E.; Breil, H.; Martin, H., Aluminum in organic chemistry VII. Polymerization of ethylene and other olefins. *Angewandte Chemie* **1955,** 67, 541.

50. Long, W. P.; Breslow, D. S., Polymerization of Ethylene with Bis-(cyclopentadienyl)-titanium Dichloride and Diethylaluminum Chloride. *Journal of the American Chemical Society* **1960**, 1953-1957.

51. Chien, J. C. W., Kinetics of Ethylene Polymerization Catalyzed by Bis-(cyclopentadienyl)-titanium Dichloride-Dimethylaluminum Chloride. *Journal of the American Chemical Society* **1959**, 86-92.

52. Dyachovskii, F. S.; Shilov, A. E.; Shilova, A. K., Role of free ions in reactions of olefins with soluble complex catalysts. *Journal of Polymer Science* **1967**.

53. Babkina, O. N.; Grigoryan, E. A.; D'yachkovskii, F. S.; Shilov, A. E.; Shuvalova, N. I., Kinetics of the interaction of active *bis*cyclopentadinylmethyltitanium(IV) cations with decene. *Zhurnal Fizicheskoi Khimii* **1969,** 43.

54. Pasynkiewicz, S., Alumoxanes: Synthesis, Structures, Complexes and Reactions. *Polyhedron* **1990**, 429.

55. Harlan, C. J.; Bott, S. G.; Barron, A. R., Three-Coordinate Aluminum Is Not a Prerequisite for Catalytic Activity in the Zirconocene-Alumoxane Polymerization of Ethylene. *Journal of the American Chemical Society* **1995,** 117, 6465.

56. Mason, M. R.; M., S. J.; Bott, S. G.; Barron, A. R., Hydrolysis of Tri-*tert*-butylaluminum: The First Structural Characterization of Alkylalumoxanes [(R2Al)2O]n and (RAlO)n. *Journal of the American Chemical Society* **1993,** 115, 4971.

57. Barron, A. R., New Methods for the Determination of Trialkylaluminum content in Alumoxanes. *Organometallics* **1995,** 14, 3581.

58. Imhoff, D. W.; Simeral, L. S.; Blevin, D. R.; Beard, W. R., *Determination of Trimethylaluminum and characterization of methylaluminoxanes Using Proton NMR*. Oxford University Press: 2000.

59. Rosenthal, M. R., The Myth of the Non-Coordinating Anion. *The Journal of Chemical Education* **1973,** 5, 331.

60. Straus, S. H., The search for Larger and More Weakly Coordinating Anions. *Chemical Reviews* **1993,** 93, 927-942.

61. Bochmann, M.; Wilson, L. M.; Hursthouse, M. B.; Short, R. L., Cationic

alkyl*bis*(cyclopentadienyl)titanium complexes. Synthesis, reactions with carbon monoxide and ter-butyl isocyanide and the structure of[Cp_2Ti-[η^2-C(Me)NBu-*tert*](CNBu-*tert*)]BPh_4.MeCN. *Organometallics* **1987,** 6, 2556-63.

62. Winter, J. C.; Zhou, X. X.; Heeg, M. J., *Journal of Inorganic Chemistry* **1992,** 31, 1808.

63. Gorrell, I. B.; Parkin, G., *Inorganic Chemistry* **1990,** 29, 2452.

64. Chattaraj, P. K.; Lee, H.; Parr, R. G., HSAB Principle. *Journal of the American Chemical Society* **1991,** 113, 1855-1856.

65. March, J.; Smith, M. B., *March's Advanced Organic Chemistry: Reactions, Mechanisms, ad Structure*. Wiley-Interscience 2001.

66. Christe, K. O.; Dixon, D. A.; McLemore, D.; W., W. W.; Sheehy, J. A.; Boatz, J. A., On a quantitative scale for Lewis acidity and recent progress in polynitrogen chemistry. *Journal of Fluorine Chemistry* **2000,** 101, 151-153.

67. Massey, A. G.; Park, A. J., Perfluorophenyl derivatives of the elements. VII. Further studies on *tris*(pentafluorophenyl)boron. *Journal of Organometallic Chemistry* **1966,** 5, (3), 218-225.

68. Piers, W. E.; Chivers, T., Pentafluorophenylboranes: from obscurity to applications *Chemical Society Reviews* **1997,** 26, 345.

69. Chambers, R. D.; Chivers, T., Pentafluorophenyl-metal compounds. *Organometallic Chemistry Reviews* **1966,** 1, (3), 279-304.

70. Chambers, R. D.; Chivers, T., Polyfluoroaryl Organimetallic Compounds. Part II: Pentafluorophenylboron Halides and some derived compounds. *Journal of the Chemical*

Society **1965**, 3933.

71. Massey, A. G.; Park, A. J., Perfluorophenyl derivatives of the elements I. *Tris*(pentafluorophenyl)boron. *Journal of Organometallic Chemistry* **1964,** 2, (3), 245-250.

72. Fenton, D. E.; Park, A. J.; Shaw, D.; Massey, A. G., Perfluorophenyl Derviatives of the elements II (pentafluorophenyl)lithium, A source of 2-substituted nonafluorobiphenyls. *Journal of Organometallic Chemistry* **1964,** 2, (6), 437-446.

73. Brookhart, M.; Grant, B.; Volpe, A. F. J., [(3,5-(CF3)2C6H3)4B]-[HOEt2)2]+: A Convenient Reagent for Generation and Stabilization of Cationic, Highly Electrophilic Organometallic Complexes. *Organometallics* **1992,** 11, 3920-3922.

74. Nishida, H.; Takada, N.; Yoshimura, M.; Sonoda, T.; Kobayashi, H., *Bull. Chem. Soc. Jpn* **1984,** 57, 2600.

75. Grubbs, R. H.; Coates, G. W., alpha-Agostic Interactions and Olefin Insertion in Metallocene Polymerization Catalysts. *Accounts of Chemical Research* **1996,** 29, 85-93.

76. Erker, G.; Kehr, G.; Frohlich, R., Some selected chapters from the (butadiene)zirconocene story. *Journal of Organometallic Chemistry* **2004,** 689, 4305-4318.

77. Natta, G., Stereospecific polymerization by means of coordinated anionic catalysis. *Journal of Inorganic and Nuclear Chemistry* **1958,** 8, 589.

78. Natta, G.; Pasquon, I., Kinetics of the stereospecific polymerization of alpha-olefins. *Advances in Catalysis and Related Subjects* **1959,** 11, 1-66.

79. Patat, F.; H., S., The course of low-pressure polymerization of alpha olefins I. Complex polymerizations. *Angewandte Chemie* **1958,** 70, 496.

80. Boor, J. J., Ziegler polymerization of olefins II. Nature of the catalytic sites. *Journal of Polymer Science* **1963,** 56, 161.

81. Ewen, J. A., Symmetry rules and reaction mechanisms of Ziegler-Natta catalysts. *Journal of Molecular Catalysis A: Chemical* **1998,** 128, 103-109.

82. Keii, T., *Kinetics of Ziegler-Natta Polymerizations*. Chapman and Hall Limited: London, 1972.

83. Cossee, P., *The Mechanism of Ziegler-Natta Polymerization. II. Quantum-Chemical and Crystal-Chemical Aspects*. Marcel Decker, Inc: New York, New York, 1967; Vol. 1.

84. Sobota, P., *Journal of the Chemical Society, Dalton Transactions* **2001**, 1379.

85. Brookhart, M.; Green, M. L. H., Carbon-Hydrogen-Transition Metal Bonds. *Journal of Organometallic Chemistry* **1983**, (250), 395-408.

86. Brookhart, M.; Green, M. L. H.; Wong, L.-L., Carbon-Hydrogen-Transition Metal Bonds. *Progress in Inorganic Chemistry* **1988,** 36, 1-124.

87. Dawoodi, Z.; Green, M. L. H.; Mtetwa, V. S. B.; Prout, K., Evidence for a Direct Bonding Interaction between Titanium nd Beta-C-H Moiety in a Titanium-Ethyl Compound; X-ray Crystal Structure of [Ti(Me2PCH2CH2PMe2)EtCl3]. *Journal of the Chemical Societ, Chemical Communications* **1982**, 802.

88. Dawoodi, Z.; Green, M. L. H.; Mtetwa, V. S. B.; Prout, K.; Schultz, A. J.; Williams, J. M.; Koetzle, T. F., Evidence for Carbon-Hydrogen-Titanium Interactions: Synthesis and Crystal Structures of the Agostic Alkyls [TiCl3(Me2PCH2CH2PMe2)R](R= Et or Me). *Journal of the Chemical Society, Dalton Transactions* **1986**, 1629.

89. Cotton, F. A.; Frenz, B. A.; Hunter, D. L., Structure of (2,4-Pentanedionato)(triphenylphosphine)ethylnickel(II). *Journal of the American Chemical Society* **1974**, (96), 4820.

90. Calligaris, M.; Mitchelli, D.; Nardin, G.; L., R., Crystal and Molecular Structure of NN'-Ethylene*bis*(salicylideneimnato)ethylcobalt (III). *Journal of the Chemical Society, A Inorganic, Physical, and Theoretical* **1971**, 2720.

91. Moseley, P. T.; Shearer, H. M. M., Alkylzinc compounds. Part I. Crystal Structure of Ethylzinc Iodide. *Journal of the Chemical Society, Dalton Transactions* **1973**, 64.

92. Green, M. L. H., A new approach to the formal classification of covalent compounds of the elements. *The Journal of Organometallic Chemistry* **1995,** 500, 127-148.

93. Calvert, R. B.; Shapley, J. R., $HOs_3(CO)_{10}CH3$: NMR Evidence for a C-H-Os Interaction. *Journal of the American Chemical Society* **1978**, (7726).

94. Calvert, R. B.; Shapley, J. R.; Schultz, A. J.; Williams, J. M.; Suib, S. L.; Stucky, G. D., Equilibrium Isotope Effect on Hydrogen Distribution between Carbon- and Metal-Bound Sites. A Neutron Diffraction Study of Partially Deuterated Decacarbonyldihydriodomethylenetriosium. *Journal of the American Chemical Society* **1978,** 100, (19), 6240.

95. Piers, W. E.; Bercaw, J. E., alpha 'Agostic' Assistance in Ziegler-Natta Polymerization of Olefins. Deuterium Isotopic Perturbation of Stereochemistry Indicating Coordination of an alpha C-H Bond in Chain Propagation. *Journal of the American Chemical Society* **1990,** 112, 9406-9407.

96. Jenkins, A. D.; Lappert, M. F.; Srivastava, R. C., The Initiation of Polymerization

by Organometallic Compounds-II. *European Polymer Journal* **1971,** 7, 289-302.

97. Bradley, D. C.; Copperthwaite, R. G., Three-co-ordinated Compounds of Titanium (III) an Vanadium (III). *Chemical Communications* **1971**, 764.

98. Yoshida, T.; Yuguchi, S. Catalysts for Ethylene Polymerization. 1963.

99. Adrien, N.; Joseph, A. Compositions catalytiques de polymerisation d'alpha-olefins. 1963.

100. Giannini, U.; Longi, P.; Deluca, D.; Pivotto, B. Olefin Polymerization Catalysts. 1970.

101. Hefner, J. G. Transition metal amides as catalysts for the polymerization of olefins. 1989.

102. Laplaza, C. E.; Johnson, M. J. A.; Peters, J., C.; Odom, A. L.; Kim, E.; Cummins, C. C.; George, G. N.; Pickering, I. J., Dinitrogen Cleavage by Three-Coordinate Molybdenum (III) Complexes: Mechanistic and Structural Data. *Journal of the American Chemical Society* **1996,** 118, 8623-8638.

103. Laplaza, C. E.; Odom, A. L.; Davis, W. M.; Cummins, C. C., Cleavage of the Nirtous Oxide NN Bond by a Three-Coordinate Molybdenum (III) Complex. *Journal of the American Chemical Society* **1995,** 117, 4999-5000.

104. Curley, J. J.; Sceats, E. L.; Cummins, C. C., A cycle for Organic Nitrile Syntesis via Dinitrgen Cleavage. *Journal of the American Chemical Society* **2006,** 128, 14036-14037.

105. Yandulov, D. V.; Schrock, R. R., Reduction of Dinitrogen to Ammonia at a Well -Protected Reaction Site in a Molybdenum Triamidoamine Complex. *Journal of the American Chemical Society* **2002,** 124, 6252-6253.

106. Yandulov, D. V.; Schrock, R. R., Catalytic Reduction of Dinitrogen to ammonia at a single Molybdenum Center. *Science* **2003,** 301, 76-78.

107. Shi, J.; Ciszewski, J. T.; Odom, A. L., Ti(NMe2)4 as a Precatalyst for Hydroamination of Alkynes with Primary Amines. *Organometallics* **2001,** 19, (17), 3967-3969.

108. Cummins, C. C.; Baxter, S. M.; Wolczanski, P. T., Methane and Benzene Activation via Transient (*t*-Bu3SiNH)2Zr=NSi-*t*-Bu3. *Journal of the American Chemical Society* **1998,** 110, 8731-873.

109. Schaller, C. P.; Cummins, C. C.; Wolczanski, P. T., Hydrocarbon Activation via Reversible 1,2-RH_Elimination from $(^{t}Bu_3SiNH)_3ZrR$: Synthetic, Structural, and Mechanistic Investigations. *Journal of the American Chemical Society* **1996,** 118, 591-611.

110. Jordan, R. F.; Dasher, W. E.; Echols, S. F., Reactive Cationic Dicyclpentadienylzirconium (IV) Complexes. *Journal of the American Chemical Society* **1986,** 108, 1718-1719.

111. Yang, X.; Stern, C. L.; Marks, T. J., "Cation-like" Homogeneous Olefin Polymerization Catalysts Based upon Zirconocene Alkyls and Tris(pentafluorophenyl)borane. *Journal of the American Chemical Society* **1991,** 113, 3623-3625.

112. Klamo, S. B.; Wendt, O. F.; Henling, L. M.; Day, M. W.; Bercaw, J. E., Dialkyl and Methyl-Alkyl Zirconocenes: Synthesis and Characterization of Zirconocene-Alkyls That Model the Polymeryl Chain in Alkene Polymerizations. *Organometallics C* **2006**.

113. Claridge, T. D. W., *High-Resolution NMR Techniques in Organic Chemisry*.

Pergamon: Oxford, 1999; Vol. 19.

114. Quarberg, R. P. On the nature of the dimethylphosphinomethanide ligand in organometallic chemistry. University of Tennessee, Knoxville, 2003.

115. Pretsch, E.; Buhlmann, P.; Affolter, C., *Structure Determination of Organic Compounds*. third ed.; Springer: Berlin, 2000.

116. Humphries, M. J. Studies in niobium imido chemistry. University of Oxford, Oxford, 1999.

117. Gomez-Ramirez, R., Personal communication. In.

118. Resconi, L.; Bossi, S.; Abis, L., Study on the role methylaluminoxane in homogeneous olefin polymerization *Macromolecules* **1990,** 23, (20), 4489-4491.

Appendix I

DRAFT CLAIMS FOR
"CATIONIC PERAMIDO TITANIUM POLYMERIZATION CATALYSTS"

What is claimed is:

1. A method of polymerizing a monomer, the method comprising:
providing a transition metal complex, the complex having a structure of Formula (I):

X-M-(L)3 (I)

wherein:
X is selected from the group consisting of halo, alkyl, aryl, aryloxy, alkoxyl, silyl, and BH4;
M is a transition metal; and
each L is independently a monodentate diarylamino group;
providing an activator, wherein the activator is selected from the group consisting of an alumoxane, a tetraarylboron compound, a triarylboron compound and a combination thereof;
providing a monomer, wherein the monomer is selected from an olefin, propylene oxide, and a combination thereof;
contacting the transition metal complex with the activator to form an activated catalyst species; and
contacting the activated catalyst species with the monomer at a pre-determined pressure and at a pre-determined temperature for a period of time, thereby polymerizing the monomer to form a polymer.

2. The method of claim 1, wherein each L has a structure of Formula (II):

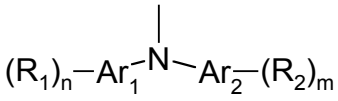

(II)

wherein:
Ar1 and Ar2 are independently C6-C26 aryl groups;
n and m are each independently an integer from 5 to 17; and
each R1 and R2 is independently selected from the group consisting of H, alkyl, halo, nitro, cyano, alkoxyl, acyl, acyloxy, aryl, aryloxy, aralkyl, aralkyoxy, and dialkylamino; or
an R1 and an R2 together are a direct bond; or
an R1 and an R2 together are alkylene.

3. The method of claim 2, wherein one or more L has a structure of Formula (III):

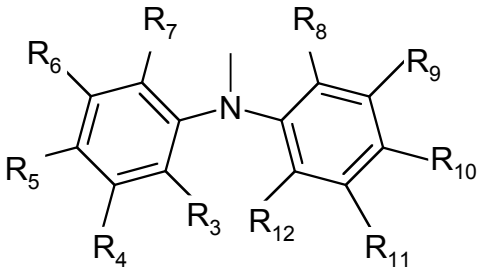

(III)

wherein:

each of R3, R4, R5, R6, R7, R8, R9, R10, R11, and R12 is independently selected from the group consisting of H, alkyl, halo, nitro, cyano, alkoxyl, acyl, acyloxy, aryl, aryloxy, aralkyl, aralkyoxy, and dialkylamino; or

R3 and R12 together are a direct bond; or

R3 and R12 together are C1-C2 alkylene.

The method of claim 3, wherein each of R3, R4, R5, R6, R7, R8, R9, R10, R11, and R12 is H and one or more L has the structure:

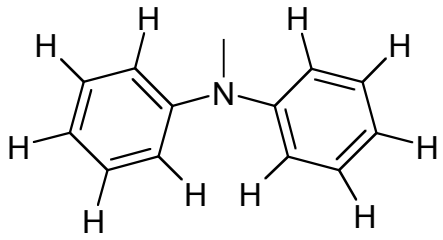

.

5. The method of claim 3, wherein R3 and R12 together are a direct bond and one or more L has a structure of Formula (IV):

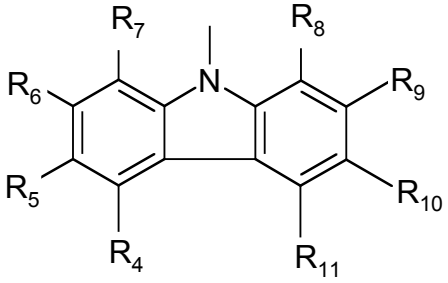

(IV) .

.

6. The method of claim 3, wherein R3 and R12 together are alkylene, and one or more L has a structure of Formula (V):

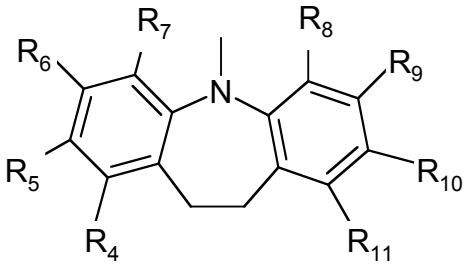

(V) .

.

7. The method of claim 1, wherein X is chloro.

8. The method of claim 1, wherein X is methyl.

9. The method of claim 1, wherein M is selected from the group consisting of titanium, zirconium, and halfnium.

The method of claim 9, wherein M is titanium.

11. The method of claim 1, wherein the activator is selected from the group consisting of methyl alumoxane (MAO), tris(pentafluorophenyl)borane, and potassium tetrakis(pentafluorophenyl)borate.

12. The method of claim 1, wherein the monomer is selected from the group consisting of propylene, ethylene, propylene oxide and combinations thereof.

13. The method of claim 12, wherein the monomer is propylene.

14. The method of claim 13, wherein the polymer is atactic polypropylene.

15. The method of claim 1, wherein the polymer has an average molecular weight (Mw) of about 10,000 or more.
[[Dr. Turner: Please feel free to suggest other potential average molecular weight ranges or polydispersity indexes based on the polymers that have been made thus far or that would be useful or unique for polypropylene. Are there any other polymer characteristics that could be the subject of claims: tensile strength, melting point, polymer density, etc. ?]]

16. The method of claim 15, wherein the average molecular weight is about 100,000 or more.

17. The method of claim 16, wherein the average molecular weight is 500,000 or more.

18. The method of claim 1, wherein the polymer has a polydispersity index ranging between 0.9 and 1.1.

19. The method of claim 18, wherein the polydispersity index ranges between 0.95 and 1.05.

20. The method of claim 1, wherein contacting the transition metal complex and the activator takes place in a solvent selected from the group comprising … [[Dr. Turner: Please provide a list of suitable solvents.]]

21. The method of claim 1, wherein contacting the transition metal complex and the activator comprises contacting the transition metal complex with a molar excess of the activator.

22. The method of claim 21, wherein contacting the transition metal complex and the activator comprises contacting the transition metal complex with 25 molar equivalents of the activator.

23. The method of claim 1, wherein the temperature ranges between about -20°C and about 50°C.

24. The method of claim 23, wherein the temperature ranges between about -5°C and about 30°C.

25. The method of claim 24, wherein the temperature ranges between about 20°C and about 25°C.

26. The method of claim 1, wherein the pressure is about 1 atm or less.

27. The method of claim 26, wherein the pressure ranges between about 1 atm and about 0.5 atm.

28. The method of claim 1, wherein the period of time is less than about 25 minutes.

29. The method of claim 28, wherein the period of time is less than about 30 minutes.

30. The method of claim 29, wherein the period of time is less than about 10 minutes.

31. The method of claim 1, wherein contacting the activated catalyst species with the monomer provides at least 20 kg of polymer per mole of catalyst species.

32. The method of claim 31, wherein contacting the activated catalyst species with the monomer provides 26.6 kg of polymer per mole of catalyst species.

33. An activated catalyst species, wherein the catalyst species has a structure of

Formula (VI):

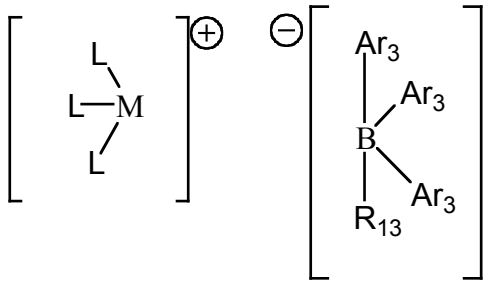

(VI)

wherein:

M is a transition metal;

each L is a monodentate diarylamine;

each Ar3 is aryl or substituted aryl; and

R13 is alkyl, aryl, or substituted aryl.

34. The catalyst species of claim 33, wherein each Ar3 is pentafluorophenyl and R13 is selected from the group consisting of methyl and pentafluorophenyl.

The catalyst species of claim 33, wherein each L has a structure of Formula (III):

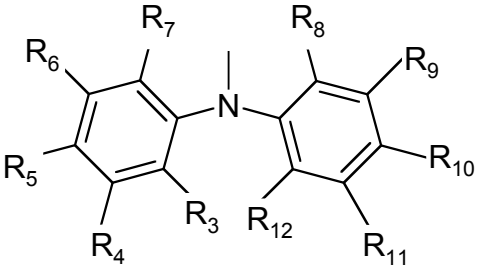

(III)

wherein:

each of R3, R4, R5, R6, R7, R8, R9, R10, R11, and R12 is independently selected from the group consisting of H, alkyl, halo, nitro, cyano, alkoxyl, acyl, acyloxy, aryl, aryloxy, aralkyl, aralkyoxy, and dialkylamino; or

R3 and R12 together are a direct bond; or

R3 and R12 together are C1-C2 alkylene.

36. The activated catalyst species of claim 35, wherein each L is selected from the group consisting of:

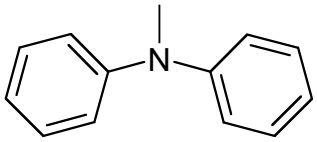

;

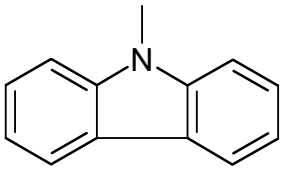

; and

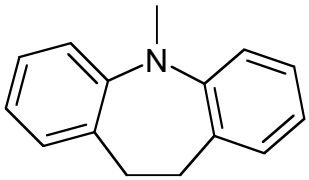

.

37. The activated catalyst species of claim 33, having an activity of 20 kg of polymer per mole of catalyst or more.

VITA

Michael A. Blanchard was born in Bolingbrook, IL – a suburb of Chicago. He graduated from Bolingbrook High School in the spring of 1999. Mike began college in the following fall at Ohio University in Athens, OH. He graduated from OU in the spring of 2003 with a Bachelor of Science degree in Forensic Chemistry. While at OU, Mike conducted undergraduate research with Professor Jared A. Butcher; the research involved the separation of isomers for the 'construction of exotic molecules.'

Mike began his studies at the University of Tennessee in the fall of 2003. While at UT, Mike concerned himself with mainly organic based classes. He joined the Turner group in the same fall and began working in organometallic synthesis. After four years at UT, Mike will graduate in August of 2007.